This material has been copied
under licence from CANCOPY.
Resale or further copying of this material is
strictly prohibited.

Le présent document a été reproduit
avec l'autorisation de CANCOPY.
La revente ou la reproduction ultérieure
en sont strictement interdites.

PROCEEDINGS SERIES

EXPONENTIAL AND CRITICAL EXPERIMENTS

PROCEEDINGS OF THE SYMPOSIUM ON
EXPONENTIAL AND CRITICAL EXPERIMENTS
HELD BY THE
INTERNATIONAL ATOMIC ENERGY AGENCY
IN AMSTERDAM, NETHERLANDS,
2-6 SEPTEMBER 1963

In three volumes

VOL. II

INTERNATIONAL ATOMIC ENERGY AGENCY
VIENNA, 1964

CONTENTS OF VOL. II

IV. SUBCRITICAL WATER ASSEMBLIES (H_2O or D_2O)

Experience at Brookhaven in the measurement of cell parameters (SM-42/27) 3
G. A. Price
Discussion 18
Some problems in the interpretation of exponential experiments (SM-42/28) 21
R. L. Hellens and E. Andersen
Discussion 41
Subcritical reactivity measurement by pulsed-neutron source method (SM-42/2) 43
S. Ogura, K. Hayata, M. Sugeno, T. Kondo, M. Mukae and T. Naganuma
Discussion 55
MINOR, a subcritical facility for heavy-water lattice studies (SM-42/55) 59
R. W. Meier, H. R. Lutz and E. Utzinger
Discussion 82
Two-region, heavy-water, natural-uranium lattice studies in the subcritical assembly MINOR (SM-42/56) 85
H. R. Lutz, T. Auerbach, W. Heer and R. W. Meier
Discussion 107
Massachusetts Institute of Technology exponential assembly studies of low-enrichment, heavy-water lattices (SM-42/31) 109
I. Kaplan, D. D. Lanning, A. E. Profio and T. J. Thompson
Measurement of the ratio of fissions in U^{238} to fissions in U^{235} using 1.60 MeV gamma rays of the fission product La^{140} (SM-42/46) 147
J. R. Wolberg, T. J. Thompson and I. Kaplan
Discussion 158
Methods for the determination of ρ_{28} and δ^{28} based on chemical separation of Np^{239} and Mo^{99} from uranium and fission products (SM-42/75) 161
S. O. Larvin, D. C. Perricos, J. A. Thomassen and H. H. Windsor
Discussion 178
Interaction du flux macroscopique et de la structure fine dans les réacteurs hétérogènes (SM-42/66) 181
P. Benoist et P. F. Palmedo
Discussion 194

V. WATER ASSEMBLIES (H_2O AND/OR D_2O)

Работа критического стенда ВВР-М (SM-42/84) 197
Д. М. Каминкер, К. А. Коноплев, Ю. В. Петров, Р. Г. Пикулик
Discussion 207
The role of experimental reactor physics in General Electric core design philosophy (SM-42/40) 209
G. T. Petersen, P. G. Aline and R. J. McWhorter
Discussion 230
The critical facility KRITO (SM-42/58) 233
J. Coehoorn, J. G. Ackers, M. Bustraan, A. Tas, W. L. Zijp, M. Nuysken, W. W. Nijs, R. J. Heyboer and F. Luidinga
Discussion 255
Role of critical, exponential and small lattice experiments in the design of the spectral shift control reactor (SM-42/41) 257
T. C. Engelder, L. G. Barrett, R. H. Clark and N. L. Snidow
Discussion 289

Measurements of void effects in the zero-power critical facility NORA (SM-42/73) 291
K. Bryhn-Ingebrigtsen, V. O. Eriksen, J. Schatvet, A. Ukkestad, J. I. Wood and K. Øfjord
Discussion 311
Mesures d'indices de spectres dans les assemblages homogènes nus modérés à l'eau (SM-42/65) 313
C. Clouet d'Orval, J. G. Bruna, M. Cadilhac et J. Moret-Bailly
Discussion 337
Thermal neutron spectral and spatial distributions in light-water-moderated uranium lattices (SM-42/35) 339
J. Hardy, J. J. Volpe, D. Klein, E. Schmidt and E. Gelbard
Discussion 359
Cálculos nucleares de reactores moderados por agua ligera y correlación experimental (SM-42/25) 361
R. Solanilla
Comparison of Knolls Atomic Power Laboratory clean critical and sub-critical experiments with calculations (SM-42/29) 391
D. R. Bach, J. A. Bistline, S. I. Bunch, R. J. Cerbone, F. Feiner, W. Skolnik, R. E. Slovacek and S. Weinstein
Discussion 444

VI. D_2O ASSEMBLIES

The role of critical experiments in the Chalk River Power Programme (SM-42/24) 449
A. G. Ward
Discussion 454
Lattice parameter measurements in ZED-2 (SM-42/23) 457
R. E. Green and C. B. Bigham
Discussion 476
Comparison of the worth of critical and exponential measurements for heavy-water-moderated reactors (SM-42/42) 479
W. E. Graves and E. J. Hennelly
Discussion 506
Determination of D_2O - 2% enriched uranium lattice parameters by means of a critical system (SM-42/4) 509
N. Raišić, S. Takač, H. Marković and T. Boševski
Discussion 526
Void reactivity effects in the second charge of the Halden Boiling Water Reactor (SM-42/69) 527
J. E. Lunde
Discussion 559
Effectiveness of a large number of control rods in the second charge of the Halden Boiling Water Reactor (SM-42/70) 561
H. Smidt Olsen
Discussion 572
Pulsed-neutron measurements on a heavy-water reactor at zero energy (SM-42/6) 575
M. Küchle
Discussion 585
Flux-flattening experiments on a heavy-water critical facility (SM-42/83) 587
F. Accinni and G. B. Zorzoli
Discussion 605

List of Chairmen of Sessions and Secretariat of the Symposium 607

THE ROLE OF CRITICAL EXPERIMENTS IN THE CHALK RIVER POWER PROGRAMME

A.G. WARD
ATOMIC ENERGY OF CANADA LIMITED,
CHALK RIVER, ONTARIO, CANADA

Abstract — Résumé — Аннотация — Resumen

THE ROLE OF CRITICAL EXPERIMENTS IN THE CHALK RIVER POWER PROGRAMME. Critical experiments have formed a considerable part of the reactor physics programme at Chalk River. The ZEEP reactor has been used since 1951 for measurements of buckling, fine structure of the neutron flux distribution, and other related studies. In 1960 the ZED-2 reactor was commissioned for an expanded programme of lattice experiments to support the Canadian effort on the development of heavy-water-moderated power reactors.

These measurements provide a basis for optimum-power reactor design. Current interest is in the use of boiling H_2O or fog as an alternative to D_2O coolant with oxide-fuel assemblies, and in the use of organic coolant with uranium-carbide fuel. Precise measurements are being made to determine the neutron balance. They complement the buckling measurements and are important in the development of accurate lattice recipes.

Critical experiments during start-up of large reactors have provided additional information and check the validity of the design data. Problems for future study include the lattice parameters for large fuel clusters, accurate measurements relating to power and void coefficients of reactivity, and the use of plutonium to simulate irradiated fuel for lattice experiments.

RÔLE DES EXPÉRIENCES CRITIQUES DANS LE PROGRAMME CANADIEN DE RÉACTEURS DE PUISSANCE. Les expériences critiques tiennent une grande place dans le programme de la physique des réacteurs, à Chalk River. Depuis 1951, on utilise le réacteur ZEEP pour des mesures du laplacien et de la structure fine de la répartition du flux de neutrons et pour d'autres études connexes. En 1960, on a mis en service le réacteur ZED-2 en vue d'exécuter un programme étendu d'expériences de réseaux, dans le cadre du programme plus vaste de développement de réacteurs de puissance à l'eau lourde.

Ces mesures fournissent une base pour l'optimisation des réacteurs de puissance. A l'heure actuelle, on s'intéresse à l'utilisation d'eau bouillante au lieu de D_2O comme fluide de refroidissement avec les assemblages à l'oxyde d'uranium, et à l'utilisation d'un fluide organique avec le carbure d'uranium. Des mesures précises sont faites pour déterminer l'économie des neutrons. Elles complètent les mesures sur le laplacien et sont importantes pour la mise au point de formules de réseau.

Des expériences critiques faites pendant le démarrage de grands réacteurs ont fourni des informations supplémentaires et ont permis de vérifier l'exactitude des caractéristiques. Pour l'avenir, le programme des travaux comporte l'étude des paramètres de réseau pour les grappes d'éléments de combustible de grande dimension, des mesures précises relatives au coefficient de température et au coefficient cavitaire, et l'utilisation du plutonium pour simuler le combustible irradié dans les expériences de réseau.

РОЛЬ КРИТИЧЕСКИХ ЭКСПЕРИМЕНТОВ В ПРОГРАММЕ ПО ЭНЕРГЕТИКЕ В ЧОК-РИВЕР. Критические эксперименты составляют значительную часть программы по физике реакторов в Чок-Ривер. Реактор ZEEP с 1951 года используется для измерения лапласиана, тонкой структуры распределения потока нейтронов и проведения других смежных исследований. В 1960 году реактор ZED-2 был передан для осуществления расширенной программы опытов с решетками в целях поддержки усилий, предпринимаемых в Канаде по разработке энергетических реакторов с тяжеловодным замедлителем.

Эти измерения обеспечивают основу для разработки оптимальной конструкции энергетического реактора. В настоящее время проявляется не ослабевающий интерес к вопросу использования кипящей воды или пара в качестве альтернативы тяжеловодному теплоносителю с топливными сборками из окиси урана и при использовании органического теплоносителя с топливом в виде карбида урана. Точные измерения проводятся в настоящее время с целью определения баланса нейтронов. Они являются дополнением к работам по измерению лапласианов и представляют важное значение для разработки точных методов с применением решеток.

В результате проведения критических опытов во время пуска больших реакторов получена дополнительная информация и осуществлена проверка пригодности проектных данных. В число проблем для исследований в будущем входят изучение параметров решеток для больших сборок топливных элементов, проведение точных измерений мощности и пустотных коэффициентов реактивности и применение плутония в целях имитирования облученного топлива для опытов с решетками.

FUNCIÓN DE LOS EXPERIMENTOS CRÍTICOS EN EL PROGRAMA DE REACTORES DE POTENCIA DE CHALK RIVER. Los experimentos críticos constituyen una parte importante del programa de física de reactores llevado a la práctica en Chalk River. El reactor ZEEP se viene utilizando desde 1951 para medición de los laplacianos, determinación de la estructura fina del flujo neutrónico y otros estudios conexos. En 1960 se puso en servicio el reactor ZED-2 a fin de efectuar un programa ampliado de experimentos sobre reticulados, con objeto de impulsar los trabajos que se realizan en el Canadá con miras al perfeccionamiento de los reactores de potencia moderados por agua pesada.

Estas mediciones sirven de base para proyectar los reactores de potencia en condiciones óptimas. Actualmente se estudia el empleo de H_2O hirviente o pulverizada para reemplazar al D_2O utilizada como refrigerante de los conjuntos combustibles de óxido de uranio, así como el empleo de refrigerante orgánico con combustible de carburo de uranio. Se están efectuando mediciones precisas para determinar el balance neutrónico. Sirven de complemento a la medición de laplacianos y facilitan el establecimiento de fórmulas exactas para cálculo de reticulados.

Los experimentos críticos efectuados durante la puesta en servicio de reactores de elevada potencia proporcionan información suplementaria y sirven para comprobar la validez de los datos utilizados en el proyecto. Entre los problemas que se estudiarán en lo futuro, figuran los parámetros del reticulado en el caso de grandes haces de barras de combustible, mediciones precisas relativas a los coeficientes de reactividad de potencia y de vacío y el empleo de plutonio para simular combustible irradiado con objeto de efectuar experimentos sobre el reticulado.

Critical experiments have formed a considerable part of the reactor-physics programme at Chalk River. The necessity for such experiments and their value seem obvious to those who want to carry out the experimental programme. The only problem is to put on paper convincing reasons to justify the expenditure of effort and money. In this paper we discuss the motivation for our current programme of critical experiments, the development of the experimental programme and where we think further work is needed.

Chalk River experience and interest is in heavy-water-moderated reactors. We have three large reactors at or near Chalk River, NRX which went critical in 1947, NRU which started in 1957 and NPD which went critical in 1962. In addition, the construction of the CANDU reactor to produce 200 MW of electrical power is well advanced and a new test reactor WR-1 is just being constructed. NRX is cooled with light water, NRU, NPD and CANDU are cooled with D_2O and WR-1 will use organic coolant in many channels.

Exponential experiments were used in 1943 at the Montreal Laboratory to verify the lattice design of NRX. In addition the ZEEP reactor was designed as a versatile lattice test facility and it first went critical in 1945. The ZEEP reactor was used for a hectic series of experiments, including only one lattice experiment, during 1946 and 1947. Then the heavy water was removed from ZEEP to be used in the start-up of the NRX reactor. Critical experiments with the ZEEP reactor were restarted in 1951, to assist in the choice of a lattice for the NRU reactor. These experiments were carried out with mock-ups of the proposed NRU rod design. The choice had to be made between experiments using a complete lattice of rods and

perturbation experiments using fewer rod assemblies. The following extract is from an unpublished report written in 1953.

"There are three main reasons for performing a core experiment rather than one with a complete lattice of rods;

(a) A full lattice may not react in the experimental system available in this case (ZEEP).

(b) The lattice information is needed in the early stages of the reactor design so that the time spent awaiting the fabrication of a full set of rods is costly.

(c) In the case where several rod designs are to be tested, it would be uneconomical in material and workshop time to fabricate a full set of each type."

It is interesting that much the same type of argument for core experiments is advanced today, with equal validity. Nevertheless for a variety of reasons we at Chalk River have normally used 55 or more rods for buckling experiments, a number which can hardly be classed as a core experiment.

By 1954 it became clear that Chalk River would work towards the development of power reactors. The programme soon concentrated on D_2O moderated and cooled reactors, using UO_2 fuel. More recently other coolants, steam, boiling D_2O, organic and fog, have been seriously considered.

With this background, it is natural that our lattice experiments have been concentrated on D_2O-moderated natural-uranium-fuelled reactors and the studies have been directed at obtaining more detailed and accurate knowledge of the neutron behaviour in such lattices.

The programme of lattice experiments which started in ZEEP in 1951 has been a continuing one. By 1957 buckling measurements as a function of spacing had been carried out on ZEEP rods, NRX rods, NRU rods, 19-element metal rods, hollow metal rods and 19-element oxide rods. The measurements on hollow metal rods were carried out as a part of a joint programme with the U.K.A.E.A. in 1952. The measurements on the 19-element metal rods were carried out before we had realized the advantages of oxide for water-cooled power-reactor rod assemblies.

In 1958 we decided to build a second lattice testing facility, ZED-2, which first went critical in 1960. The reasons for building this facility were as follows: we felt we could usefully employ both ZEEP and the second reactor ZED-2 on lattice physics experiments. The early studies of power reactors of the pressure tube design indicated some advantage for designs with relatively large fuel cross-section areas, of the order of 50 cm^2 or even more and correspondingly large spacings. The ZEEP reactor was not large enough for critical experiments with such lattices. Further, the minimum value of buckling which we can measure with a complete lattice in ZEEP is of the order of 5 m^{-2}. On the other hand, this is close to the maximum value which we can get with oxide lattices. We wanted to be able to make measurements with spacings less than and greater than the optimum to check the validity of lattice recipes. Finally, considerations of optimum power-reactor designs lead to problems of flattened flux distributions, optimum reflector thicknesses, etc. and ZEEP is not really suitable for such experiments.

These were the reasons which led us to build ZED-2. We have subsequently used it for most of the experiments for which it was built, except for measurements on large rod assemblies. Fortunately there exists a set

of measurements from Savannah River on large assemblies; however we hope soon to include a set of measurements on large rod assemblies in the ZED-2 programme.

The experimental programme on ZED-2 has differed somewhat from our expectations. We have attempted to make complete sets of measurements for the lattices being studied. Current studies are on 19-element oxide rods very similar to CANDU fuel, but we are using D_2O, air and organic in the coolant channels. Previous studies were on 7-element oxide rods. Included in the measurements are experiments to determine the fast fission factor, initial conversion ratio, fine structure of the neutron density in the lattice cell, and values of the buckling. We also make measurements of the neutron temperature as a function of position in the lattice cell and values of the epithermal neutron density are measured. Recent reviews of these measurements have been given by GREEN et al. [1] and by BIGHAM and GREEN in a paper at this Symposium [2].

Although such measurements require a great deal of time and effort, we think they are worthwhile. They provide a much better test of lattice recipes and most important of all, they show clearly which components of the recipes are in error when calculated and measured bucklings do not agree.

Up to now I have reviewed briefly the history of lattice experiments at Chalk River. Perhaps we should look at the usefulness of such experiments. We make use of our results when we study the design of a power reactor. Immediately we are faced with questions of optimum design, choice of rod size and lattice pitch, prediction of power and temperature coefficients of reactivity, the fuel burn-up life time, the pattern of power distribution, fuel and control rod management, safety analysis, control and stability and a host of other problems.

The information from the clean cold critical experiments provides direct answers to some of these problems. One aim of reactor-physics experiments is to be able to answer design problems accurately and quickly. The required accuracy is sometimes difficult to judge. For instance, the choice of fuel design and lattice pitch are vital to the choice of an optimum design. However the uncertainties inherent in lattice recipes, and the resulting errors in prediction of fuel burn-up, may be small compared with errors in estimating the difference in the production cost of different fuel designs.

Lattice of natural uranium oxide and metal rods, moderated and cooled by heavy water, have been extensively studied in many laboratories. In fact, the only gaps in this information relate to details of neutron behaviour in the lattices of rods with large cross-sectional areas. Generally speaking, this lattice physics information is adequate for a reactor design. When the coolant is changed to boiling light water, steam, fog, or organic coolant, there are many gaps in the required information. This is partly because the positive coolant void coefficients of reactivity need to be accurately known for control and safety studies. Lattices of the type proposed for the U.K.A.E.A. reactor SGHW are extreme designs which demand critical experiments as well as a prototype reactor. Thus in the field of heavy-water-moderated lattices, it is easy to be complacent about the state of knowledge of the physics of some particular type of lattice; it is equally easy to be

asked an important question on the merits of some particular reactor design for which the answer is unknown.

Our future experimental programme at Chalk River is not rigidly planned. I hope to see a complete set of measurements on large cross-sectional area UO_2 rods similar to the current set for 19-element oxide fuel. We have planned a few measurements on rod assemblies containing carbide fuel and organic coolant. We are investigating the procurement of some rod assemblies containing uranium carbide. Some measurements of moderator and fuel temperature coefficients of reactivity and coolant void coefficients are being considered. We would like to see some lattice experiments with depleted uranium mixed with plutonium.

Critical experiments during the start-up of a new reactor are always interesting and instructive. An extensive series of measurements on the NRX reactor were reported at the 1955 Geneva Conference [3]. A corresponding set of measurements was made on NRU and is partially documented [4]. The start-up experiments on the NPD reactor have been described by WHITTIER [5]. In this latter case, cadium dissolved in the coolant was used to calibrate the reactivity versus moderator level and the moderator and coolant temperature coefficients were measured. There was some juggling with the loading of the depleted fuel, used to absorb the excess reactivity of a fresh fuel load, as a result of the initial critical height measurement near half tank. This measurement was of the order of 10 mk less reactive than predicted; on the other hand the full tank reactivity was close to the predicted value. Subsequent analysis has attributed the 10 mk discrepancy in the initial critical height prediction to differences in fuel loading assumed in the calculation and that used in the reactor, and approximations in the use of a two-dimensional analysis as applied to a relatively complicated three-dimensional reactor. Another interesting result from NPD was the loss of reactivity due to degradation in the D_2O moderator in a fuelling incident, and the corresponding large alteration of the moderator temperature coefficient of reactivity.

One important product of critical experiments is trained reactor physicists. Each reactor which contains new features in the design may have problems due to simple oversights on the part of the designers. The detection of power modulation of NRX due to waves on the surface of the moderator came as a surprise and equally unexpectedly we discovered power modulation of NRU due to flutter of the control rods. In the latter case this caused some difficulties with rate trip settings. It is to be hoped that such oversights remain of minor importance for the operation of large reactors. Well-trained reactor physicists are a partial guarantee of this hope.

Finally, I would like to comment on lattice recipes. We at Chalk River have made good use of the familiar two-group calculations and the old four-factor formulae. Such recipes are badly strained by the current wide range of accurate experimental data. Since experimental lattice work is readily available to lattice designers only when condensed into recipes we have been forced to look for newer and better methods of correlating the experimental data. It is tempting to look towards the powerful models developed for H_2O reactor calculations and a correspondingly painstaking problem to check such recipes against the wealth of experimental data.

Although one may hope for the day when the reactor-physics calculations are confidently based on computer programmes, with no recourse to experimental or critical facilities, it seems likely this happy time will only arrive when new reactor designs are no longer of interest.

REFERENCES

[1] GREEN, R.E. et al., Highlights of Chalk River work on the physics of heavy water lattices since the 1959 IAEA Panel, Heavy Water Lattices: Second Panel Report, Technical Reports Series No.20, IAEA, Vienna (1963) 51.

[2] BIGHAM, C.B. and GREEN, R.E., Lattice parameter measurements in ZED-2, these Proceedings.

[3] HURST, D.G. and WARD, A.G., Characteristics of the NRX Reactor, Proc. UN Int. Conf. PUAE 5 (1956) 111, 119.

[4] CRITOPH, E., Preliminary report on the NRU start-up experiments, AEC Rpt. RPI-30 (1958).

[5] WHITTIER, A.C., Nuclear performance of power reactor cores, Amer. Nucl. Soc. Meeting, San Francisco, 26-27 Sep. 1963.

DISCUSSION

C.G. CAMPBELL: The U.K.A.E.A. experiments at Winfrith in support of the steam-generating heavy-water reactor project (SGHW), to which the paper refers, have made extensive use of a heavy-water-moderated, light-water-cooled exponential assembly, together with a high-flux subcritical assembly fed by neutrons from the source reactor NESTOR. These assemblies have been used for studying uniform lattices and also to get bucklings and a wide range of reaction rates as a function of coolant density in a variety of lattice arrangements. The critical assembly DIMPLE has also been used for this work and for studying non-uniform lattice arrangements. I might mention that we in the United Kingdom have been moving away from simple two-group correlation techniques as a means of accounting for the sort of complicated physical processes going on in these dual moderator systems.

A. HITCHCOCK: In his paper, Dr. Ward attaches some importance to making measurements of reflector properties and flux distributions in systems with control rods etc. in the lattice, i.e. systems of somewhat larger than the minimum critical size available in a small facility. Does he feel that the results which can be obtained justify the additional cost of the larger critical facility needed for such measurements? These costs must be rather considerable, especially if heavy water is involved.

A.G. WARD: It is rather difficult to answer this question because thus far we have not done a great deal of experimental work along these lines. Studies which have been made of the effects of heavy-water reflectors in our power reactor designs show that we have been tending to over-estimate the benefits from them. If we can find answers to some of the questions involved, the cost of the heavy water needed in our experimental facility would be largely offset by the resultant savings in heavy-water costs for even one reactor.

P.F. PALMEDO: I should like to make a comment on the interesting results from Chalk River reported by Dr. Ward. We at Saclay have started

a rather extensive programme of detailed fine structure measurements on a variety of oxide clusters, both air-cooled and in D_2O. Our experiments may be of interest in relation to the Chalk River measurements, since we have studied a cluster very similar to the 19-element CANDU type, as well as a number of rather different configurations.

The first results from this series will soon be published, and I think it would be very profitable to compare in detail both the results obtained and the methods used in the two laboratories. As a general policy, I consider that an increase in such detailed inter-laboratory comparisons would be beneficial.

A.G. WARD: We shall certainly be interested in seeing the results of these Saclay measurements.

E. HELLSTRAND: You mention in the paper that you would like to see some lattice experiments done on depleted uranium mixed with plutonium. Does that mean that you have definite plans for doing such experiments and, if so, will you restrict yourself to this type of plutonium fuel?

A.G. WARD: We have plans for such measurements. At the present stage, they are based largely on hopes of persuading our friends in the United States to do measurements for us on depleted uranium-238 with plutonium mixed in. I can't say any more at present, because the arrangements are still somewhat tentative.

Y.E. GIRARD: On the subject of experiments with slightly enriched or Pu-alloyed fuels, I should like to mention a programme that has been started on AQUILON at Saclay, under a contract with EURATOM. In these experiments use is made of fuels slightly enriched or slightly depleted in U^{235} and fuels alloyed with plutonium (metallic bars, diameter 29.2 mm). The first measurements have been completed and are reported in IAEA Technical Reports Series No.20.* The measurements on the first Pu set (uranium metal, 0.05% Pu, low Pu^{240} content) are now under way. The two other sets which are planned involve the use of 0.2% U and 0.3% Pu with high and low contents of Pu^{240}.

The Spanish Atomic Energy Board is due to start measurements at Madrid on organically cooled carbide elements. Under an agreement with the French Atomic Energy Commission, the initial measurements were carried out on AQUILON at Saclay, in June 1963.

A.G. WARD: We should certainly be very interested in seeing the results of the EURATOM programme when they become available. Our lack of knowledge of the properties of plutonium in the neutron spectrum in the lattices is the big question mark in present-day reactor design, hence, the importance of experiments in which plutonium is used in the lattice.

---

* GIRARD, Y. et NAUDET, R., «Rapport d'ensemble sur l'expérimentation AQUILON» et «Description de quelques expériences récentes dans AQUILON», Heavy Water Lattices: Second Panel Report, IAEA, Vienna (1963) 93-145.

LATTICE PARAMETER MEASUREMENTS IN ZED-2

R.E. GREEN AND C.B. BIGHAM
ATOMIC ENERGY OF CANADA LTD, CHALK RIVER,
ONTARIO, CANADA

Abstract — Résumé — Аннотация — Resumen

LATTICE PARAMETER MEASUREMENTS IN ZED-2. This paper describes current experiments using the Chalk River lattice-testing reactor, ZED-2. The fuel assemblies closely resemble the fuel channels of the Canadian power reactors NPD and CANDU. The experimental fuel consists of 19-rod clusters of 1.42 cm diameter, zircaloy-clad UO_2 of density 10.4 g/cm³ which are housed in double-walled tube assemblies to simulate the pressure and calandria tubes of the power reactors.

Bucklings are determined from macroscopic flux distributions and reactivity measurements. Microscopic neutron activation distributions are also measured from which the thermal utilization f and thermal diffusion area L^2 are deduced. The Westcott epithermal neutron-spectrum parameter r and the effective neutron temperature T_n are determined using In, Mn and Lu detectors. Fast-fission ratios and initial conversion ratios are also measured; these results yield values for the fast-fission factor ϵ and the resonance-escape probability p respectively. All of these parameters are determined in hexagonal lattices for several pitches in the range 18-36 cm. The measurements are being made with D_2O, air (i.e. void) or an organic liquid, HB-40, which has the chemical formula $C_{16}H_{22}$, filling the coolant spaces of the fuel assemblies. The moderator is in all cases D_2O.

Descriptions of the lattice arrangements and the measurement techniques are given as well as a summary of the results that have been obtained so far. These results for the 19-rod UO_2 fuel clusters are compared to the results of experiments that were done earlier with 7-rod clusters of 2.40 cm diameter UO_2 which are similar to some of the NPD fuel channels. The bucklings are also compared with the calculated values given by the latest Chalk River lattice recipes.

MESURES DE PARAMÈTRES DE RÉSEAU AU MOYEN DE ZED-2. Les auteurs décrivent des expériences courantes faites au moyen du réacteur d'essai de réseaux ZED-2 de Chalk River. Les cartouches de combustible ressemblent de très près aux canaux de combustible des réacteurs de puissance canadiens NPD et CANDU. Le combustible servant à l'expérience est formé de grappes de 19 barres gainées de Zircaloy de 1,42 cm de diamètre, en UO_2 d'une densité de 10,4 g/cm³; ces grappes sont logées dans des assemblages tubulaires à double paroi de manière à simuler les tubes de pression et ceux de la calandre de réacteurs de puissance.

Les auteurs déduisent les laplaciens de mesures des répartitions macroscopiques du flux et de la réactivité. Ils mesurent aussi les répartitions microscopiques de l'activation neutronique d'où ils déduisent l'utilisation thermique f et l'aire de diffusion thermique L^2. Ils déterminent le paramètre du spectre des neutrons épithermiques, r, dit de Westcott, et la température effective des neutrons T_n en utilisant des détecteurs à In, Mn et Lu. Ils mesurent également les taux de fission rapide et les taux de conversion initiaux; ces résultats donnent des valeurs pour le facteur de fission rapide ϵ et pour la probabilité d'échapper à la capture par résonance, p. Tous ces paramètres sont déterminés dans des réseaux hexagonaux pour des pas de réseau compris entre 18 et 36 cm. Les espaces destinés à recevoir le fluide de refroidissement sont remplis de D_2O, d'air (cavité) ou de $C_{16}H_{22}$. *Dans tous les cas, le ralentisseur est du D_2O.*

Les auteurs donnent une description des configurations de réseau et des méthodes de mesure ainsi qu'un bref aperçu des résultats obtenus jusqu'à présent. Ils comparent les résultats concernant les grappes de 19 barres d'UO_2 et ceux d'expériences faites antérieurement avec des grappes de sept barres de 2,40 cm de diamètre en UO_2, analogues à certains des canaux de combustible du réacteur NPD. Ils comparent aussi les laplaciens aux valeurs calculées d'après les dernières formules de réseau de Chalk River.

ИЗМЕРЕНИЯ ПАРАМЕТРОВ РЕШЕТОК РЕАКТОРА ZED-2. Дается описание текущих опытов на реакторе для испытания решеток ZED-2 в Чок-Ривер. Топливные сборки реакторов очень похожи на топливные каналы канадских энергетических реакторов NPD и CANDU. Экспериментальное топливо состоит из сборок, составленных из 19 стержней UO_2 диаметром 1,42 см в циркаллоевой оболочке плотностью 10,4 кг/см³, которые помещаются в трубках с

двойными стенками для имитирования давления и в трубках цилиндрической формы, используемых в энергетических реакторах.

Лапласины определяются по данным макроскопических распределений потоков и измерений реактивности, также измеряется микроскопическое распределение активации нейтронов, и из полученных данных выводятся величина использования тепловых нейтронов f и область термодиффузии L^2. С помощью детекторов из индиевой, марганцевой и лютециевой фольг определяются параметр спектра надтепловых нейтронов Весткота r и эффективная температура T_n. Измеряются также отношения интенсивностей деления быстрых нейтронов и начальные коэффициенты конверсии. Эти результаты приводят соответственно к величинам коэффициента деления быстрых нейтронов ε и к вероятности резонансной утечки p. Все эти параметры определяются в гексагональных решетках для нескольких значений постоянной решетки в диапазоне 18–36 см. Измерения проводятся с D_2O, воздухом (т.е. в вакууме) или с органической жидкостью HB-40, которая имеет химическую формулу $C_{18}H_{32}$ и заполняет пространство охлаждения в топливных сборках. Замедлителем во всех случаях служит D_2O.

Дается описание расположения решеток и методов измерения, а также обобщаются полученные результаты для сборок, составленных из 19 стержней с топливом в виде UO_2. Эти результаты сравниваются с результатами поставленных ранее опытов со сборками из 7 подобных стержней диаметром 2,40 см, которые похожи на некоторые из топливных каналов NPD. Значения лапласианов также сравниваются с расчетными величинами, полученными в результате применения в Чок-Ривер последних методов с использованием решеток.

MEDICIÓN DE PARÁMETROS DEL RETICULADO EN EL REACTOR ZED-2. Los autores describen los experimentos que se están realizando con ayuda del reactor de Chalk River para ensayo de reticulados, ZED-2. Los conjuntos combustibles son muy parecidos a los presentes en los canales de carga de los reactores de potencia NPD y CANDU del Canadá. El combustible experimental está formado por haces de 19 barras de 1,42 cm de diámetro, de UO_2 de 10,4 gm/cm³ de densidad, con revestimiento de zircaloy, que van alojadas en tubos de doble pared para simular la presión y los tubos de calandria de los reactores de potencia.

Los laplacianos se calculan en función de las distribuciones macroscópicas del flujo y en las mediciones de reactividad. También se miden las distribuciones microscópicas de activación neutrónica, de las cuales se deducen la utilización térmica, f, y el área de difusión térmica, L^2. El parámetro de Westcott para el espectro de neutrones epitérmicos, r, y la temperatura neutrónica efectiva, T_n, se determinan con ayuda de detectores de In, Mn y Lu. Asimismo, se determinan las razones de fisión por neutrones rápidos y las razones iniciales de conversión; estos resultados permiten deducir el valor del factor de fisión por los neutrones rápidos, ε, y la probabilidad de escape a la captura por resonancia, p, respectivamente. Todos estos parámetros se determinan en reticulados hexagonales para diferentes espaciamientos comprendidos entre 18 y 36 cm. Las mediciones se realizan utilizando como relleno de los circuitos de refrigeración de los elementos combustibles D_2O, aire (es decir, circuitos vacíos) o un líquido orgánico, HB-40, que responde a la fórmula química $C_{18}H_{32}$. En todos esos casos, el moderador consiste en D_2O.

Se describen las configuraciones del reticulado y las técnicas de medición y se facilita un resumen de los resultados obtenidos hasta ahora. Estos resultados, correspondientes a los haces de 19 barras de UO_2, se comparan con los de otros experimentos ejecutados anteriormente con haces de 7 barras de UO_2, de 2,40 cm de diámetro, que son parecidas al combustible introducido en algunos de los canales de carga del reactor NPD. Los laplacianos también se comparan con los valores calculados aplicando las fórmulas más recientes para cálculo de reticulados establecidas en Chalk River.

1. INTRODUCTION

The ZED-2 reactor [1] at Chalk River is a D_2O-moderated, zero-energy, critical facility in which experiments are done to determine the parameters of lattices of fuel assemblies which are possible contenders as fuel for nuclear power stations. In addition to obtaining information for a particular lattice arrangement of interest, measurements are made for various lattice arrangements, i.e. different lattice pitches and with different fuel conditions, e.g. different coolant materials, to provide a broad experimental background for the lattice recipes used by the designers of future power

reactors. Since ZED-2 first went into operation in September 1960 detailed lattice parameter measurements have been made for lattices of fuel assemblies which are similar to the fuel channels of the NPD and CANDU power reactors. Experimental results for lattices of NPD type 7-rod UO_2 fuel bundles were presented at the Second Panel Meeting on Heavy Water Lattices held by the IAEA [2]. This paper describes the results that have been obtained for lattices of CANDU type 19-rod UO_2 fuel bundles.

2. DESCRIPTION OF FUEL AND LATTICE ARRANGEMENTS

Fig. 1 is a cross-sectional view of one of the fuel assemblies used in the experiments. The fuel is in the form of bundles each consisting of 19 pencils of UO_2 having a diameter of 1.421 cm, and a density of 10.45 g/cm³. Each pencil was sheathed in 0.454-mm thick Zircaloy-2. More details of the fuel bundles are shown in Fig. 2. Each assembly contained six bundles. The main differences between the experimental fuel assemblies and the actual CANDU fuel channels are different bundle end-plates and the fact that the experimental pressure and calandria tubes were aluminium whereas in CANDU they are Zircaloy-2 and Zircaloy-4 respectively. However, the thickness of the aluminium pressure tube was chosen to give the same thermal neutron absorption as the actual pressure tube. Seven assemblies were also available having Zircaloy-2 pressure tubes (but Al calandria tubes) and these were used to determine the material bucklings of lattices of assemblies with Zircaloy pressure tubes. The physical details of the experimental fuel assemblies are listed in Table I. Note that the bundle end region is defined as that region lying between the UO_2 in adjacent bundles and extending radially to the inside surface of the pressure tube.

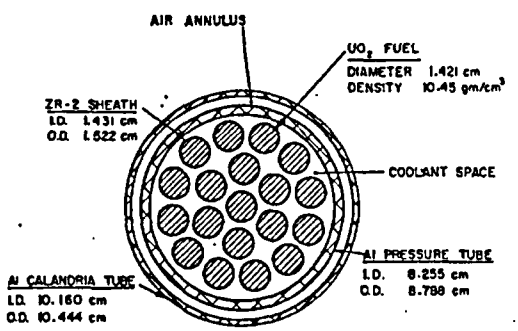

Fig. 1

Cross-section of 19-rod fuel assembly

Experiments have been done with three different materials in the coolant space, viz. D_2O of moderator purity, air (i.e. void) and an organic liquid, HB-40, which is a yellowish liquid having a formula of $C_{18}H_{22.0}$, a density of 1.00 g/cm³ at 25°C, and a temperature coefficient of density of -065% per deg C in the range 0°C to 300°C. In the D_2O-cooled lattices the D_2O entered

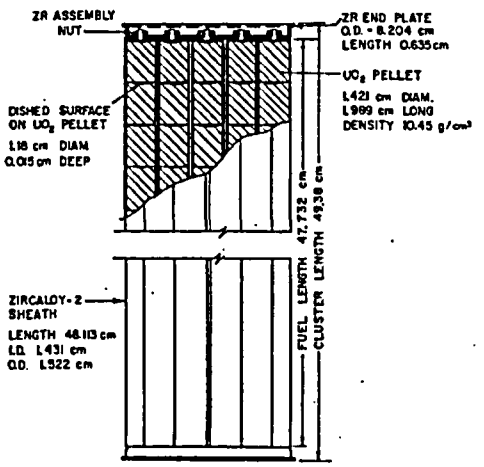

Fig. 2

Details of 19-rod fuel bundle

the coolant space from the moderator region through holes in the bottoms of the assemblies. The air-cooled lattices were obtained by excluding the D_2O coolant with helium gas; each assembly was made airtight and fitted at the top with plastic tubing which was connected via a manifold to a cylinder of helium gas located outside the reactor. The D_2O was forced from the coolant space into the moderator region. The organic HB-40 coolant was sealed inside the coolant space and thus isolated from the moderator.

Measurements were made in triangular lattices for a range of lattice pitches, 18-36 cm for the D_2O and air-cooled lattices and 18-28 cm for the organic-cooled lattices. All measurements were made in arrays of 55 assemblies. For the D_2O and air-cooled lattices at pitches greater than 21 cm only 55 fuel assemblies were required. Extra reactivity was required for all of the organic-cooled lattices and for the D_2O and air-cooled ones at 21 cm pitch and smaller. This was provided by adding six of the assemblies with Zircaloy pressure tubes and/or ZEEP rods [3] or NPD type 7-rod UO_2 cluster assemblies [1] around the outside of the core. A typical lattice arrangement is shown in Fig. 3, viz. the 21-cm D_2O-cooled lattice arrangement.

3. EXPERIMENTAL TECHNIQUES

The programme of measurements was aimed at the determination of the following lattice parameters for several different lattice pitches with each of the three coolants: the material buckling B^2, the microscopic neutron density distribution throughout the lattice cell, the initial conversion ratio γ_0, the fast fission ratio δ; and also the neutron spectrum parameters: the epithermal spectrum index r and the effective neutron temperature T_n. The experimental techniques used to determine them will now be described.

TABLE I

DETAILS OF ZED-2 EXPERIMENTAL FUEL ASSEMBLIES

Detail		7-rod Bundles [a]	19-rod bundles [b] Type 1	Type 2
Bundle length	(cm)	47.31	49.38	49.38
UO_2 Fuel:				
Length per bundle	(cm)	45.72	47.73	47.73
Diameter	(cm)	2.400	1.421	1.421
Density	(g/cm³)	10.20	10.45	10.45
Sheath spacing	(mm)	1.27	1.27	1.27
Fuel sheath:				
Material		Al	ZR-2 [c]	ZR-2
Inner diameter	(cm)	2.438	1.431	1.431
Wall thickness	(mm)	0.508	0.454	0.454
Pressure tube:				
Material		Al	Al	ZR-2
Inner diameter	(cm)	8.255	8.255	8.283
Wall Thickness	(mm)	0.89	2.67	4.28
Calandria tube:				
Material			Al	Al
Inner diameter	(cm)	-	10.160	10.160
Wall Thickness	(mm)	-	1.42	1.42
Bundle end region:				
Gap between UO_2	(cm)	1.59	1.65	1.65
Volume of sheath material	(cm³)	59.52	23.48	23.48
Volume of air	(cm³)	5.23	6.36	6.36
Volume of coolant	(cm³)	20.24	58.52	59.10

[a] The centres of the six outer rods lie on a 5.33-cm diameter circle
[b] The 19 rods are in a circular array; one rod on the axis, six on a 3.30-cm diameter circle and twelve on a 6.38-cm diameter circle
[c] ZR-2 = Zircaloy-2

3.1. *Bucklings*

The bucklings were determined from flux distribution measurements made with Mn(11% Ni) foils mounted in thin Al thimbles which were placed at cell boundary positions throughout the core. The resulting flux distributions well-removed from the core boundaries (the radial positions used in the analysis are shown in Fig. 3) were fitted by least squares to J_0 or I_0 Bessel and cosine functions to determine the radial and axial bucklings respectively. (The radial flux distribution was of the I_0 form in some low-buckling, tight lattices where a large driving region was used and there was a net flow of neutrons into the core from the driver region; in these cases the axial geometric buckling exceeds the material buckling.) Since the fuel is in the form of bundles, "flux peaking" at the elevations of the bundle ends was

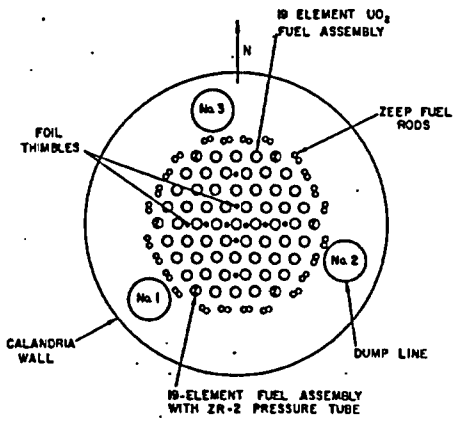

Fig. 3

21-cm D_2O-cooled UO_2 (19) lattice

observed particularly at tight spacings. The measured fluxes at the bundle end locations were omitted from the axial fitting.

Material bucklings were also obtained for lattices of D_2O-cooled assemblies having Zircaloy-2 pressure tubes by measuring the reactivity effect of replacing the central seven assemblies having Al pressure tubes with ones having Zircaloy pressure tubes. The procedure used was to measure the critical heights for three different reactor configurations:

(i) The normal unpertubed reactor containing a core of 55 fuel assemblies with Al pressure tubes;

(ii) The normal core ((i) above) but with a 2.54-mm diameter full-length Co wire located at the boundary of the central cell; and

(iii) The normal lattice with the seven central fuel assemblies of the core replaced by ones having Zircaloy-2 pressure tubes.

The changes in geometric buckling, ΔB^2, of the unperturbed lattice required to compensate for the perturbations were assumed to be given by

$$\Delta B^2 = F(h)\,\pi^2 \left[\frac{1}{(h+\Delta h)^2} - \frac{1}{h^2}\right], \tag{1}$$

where Δh is the change in height required to keep the reactor critical when the perturbation is made,

h is the extrapolated height of the unperturbed reactor, and

$F(h)$ is a factor which allows for the dependence of the radial leakage upon critical height. This is a reflector effect which depends upon the height h and the reflector properties and is known from other experiments to vary from 1.0 to 1.5 for the lattices studied here.

Using one-group statistical weight theory it can be shown that

$$B^2_{ZR} = B^2_{Al} + \frac{\Delta B^2_{ZR}}{\Delta B^2_{Co}} \frac{W_1}{W_7} \left(B^2_{Co} - B^2_{Al}\right), \tag{2}$$

where ΔB^2_{Co}, ΔB^2_{ZR} are the observed buckling changes for the Co wire and the seven-assembly fuel replacement respectively, obtained using Eq. (1),

B^2_{ZR} is the required material buckling of the lattice of fuel assemblies with Zircaloy-2 pressure tubes,

B^2_{Al} is the material buckling of the lattice of fuel assemblies with Al pressure tubes,

B^2_{Co} is the material buckling of a lattice of fuel assemblies with Al pressure tubes and also a full-length 2.54-mm diameter Co wire located at the boundary of each cell, and

W_1, W_7 are the statistical weights of the central cell and the central seven cells, respectively, of the unperturbed reactor.

$$\frac{W_1}{W_7} = \frac{\int_1 \phi^2 \, dV}{\int_7 \phi^2 \, dV} , \tag{3}$$

where $\int_1$, $\int_7$ are integrations over the central cell and central seven cells respectively, and ϕ is assumed to be given by

$$\phi = J_0 (\lambda r) \cos(\beta z) \tag{4}$$

where $\lambda^2 = B^2_{Al} - \beta^2$ and $\beta = \pi/h$.

Here only the radial dependence of ϕ is required since the perturbations are all full-length. All quantities in Eq. (2) except B^2_{Co} are known from measured flux distributions and critical heights. $(B^2_{Co} - B^2_{Al})$ was calculated using the known cross-section of Co, measured cell flux distributions and the flux depression factor for the Co wire which was measured separately. In making this calculation η and ϵ were assumed constant but the effect of the presence of the Co on all other parameters was included.

3.2. Microscopic neutron density distributions

Neutron activation distributions were measured throughout central lattice cells with ~ 0.10-mm thick Mn-Ni foils placed between fuel pellets and 0.51-mm diameter Mn-Ni wires located in holes drilled ultrasonically in the fuel pellets and at various positions in the coolant region and moderator. These measurements were made in a special short fuel assembly which replaced the normal central fuel assembly and which contained only three fuel bundles, the middle one of which was the experimental bundle. The measurements were made near the middle (axially) of this fuel bundle, well away from the end effects.

The total activities obtained were corrected for the macroscopic flux variation across the cell and for Mn resonance activation using the measured neutron spectrum parameters (see below) to arrive at the total neutron density distribution throughout the lattice cell. Since the total Mn activation is

proportional to

$$n\sigma_0 \left(G_t g + G_r s_0 r\sqrt{T_n/T_0}\right),$$

where n is the total neutron density,
σ_0 is the 2200 m/s cross-section of Mn,
G_t, G_r are the thermal and resonance self-shielding factors for the detectors,
$s_0 \equiv s\sqrt{T_0/T_n}$ and
g, r and s are the well-known parameters defined by WESTCOTT et al. [4].

The relative neutron density distribution is obtained by dividing the measured activities by the appropriate $(G_t g + G_r s_0 r\sqrt{T_n/T_0})$ factor using the measured values of $r\sqrt{T_n/T_0}$. G_t values were calculated, g was taken as 1.000 for Mn and $G_r s_0$ values were measured in separate Cd ratio experiments using thin Au foils as a standard. Graphical integration is used to determine average neutron densities in the various cell materials.

3.3. *Neutron spectrum parameters*

Measurements of the epithermal neutron spectrum parameter r, and the effective neutron temperature T_n (a measure of the spectral hardening) were made in the fuel at a cell boundary position in the moderator and on the outer surface of the calandria tube. The technique used has been described in detail by BIGHAM et al. [5]. Thin In-Al and Lu-Mn-Al foils were irradiated together at several positions inside the fuel cluster and in the moderator of the central cell and also at a reference position, either in the D_2O reflector outside the core or in the graphite reflector below the calandria floor. Once the specific activities of the In, Mn and Lu^{176} detectors have been determined, the values of r and T_n are deduced using the following expressions:

$$\frac{(A_{In}/A_{Mn})_x}{(A_{In}/A_{Mn})_0} = \left[\frac{(G_t g + (r\sqrt{T_n/T_0})_x G_r s_0)_{In}}{(G_t g + (r\sqrt{T_n/T_0})_x G_r s_0)_{Mn}}\right]\left[\frac{(G_t g + (r\sqrt{T_n/T_0})_0 G_r s_0)_{Mn}}{(G_t g + (r\sqrt{T_n/T_0})_0 G_r s_0)_{In}}\right] \quad (5)$$

$$\frac{(A_{Lu\text{-}176}/A_{Mn})_x}{(A_{Lu\text{-}176}/A_{Mn})_0} = \left[\frac{(G_t g_x + (r\sqrt{T_n/T_0})_x G_r s_0)_{Lu\text{-}176}}{(G_t g + (r\sqrt{T_n/T_0})_x G_r s_0)_{Mn}}\right]\left[\frac{(G_t g + (r\sqrt{T_n/T_0})_0 G_r s_0)_{Mn}}{(G_t g_0 + (r\sqrt{T_n/T_0})_0 G_r s_0)_{Lu\text{-}176}}\right], \quad (6)$$

where A is the specific activity, x refers to the position in the test cell, and 0 refers to the relector reference position.

The value of $(r\sqrt{T_n/T_0})_0$ is determined by measuring the Cd ratio for thin In-Al foils at this position; $(r\sqrt{T_n/T_0})_0$ is small so that the uncertainty in its measurement introduces a negligible error in the determination of $(r\sqrt{T_n/T_0})_x$. Values of $G_r s_0$ for the detectors are known from Cd ratio

measurements and are based on the value $s_0 = 18.8$ for In suggested by BIGHAM et al. [5]. G_t values are calculated and g values are taken from WESTCOTT [6]. Thus values of $r\sqrt{T_n/T_0}$ are derived from Eq. (5). These are used in Eq. (6) to deduce the effective neutron temperatures. The second square bracket in Eq. (6) is determined from the activity ratio in the reference position where the neutron temperature is assumed equal to the physical temperature. Thus values of g_x, which is a known function of T_n, are derived from Eq. (6) and hence T_n values are determined. Combining the values $r\sqrt{T_n/T_0}$ and T_n gives r.

3.4. *Fast fission ratios*

The fast fission ratio δ (the number of U^{238} fissions per U^{235} fission) was obtained by measuring the fission product gamma-ray activities in natural and depleted uranium metal foils. The foils were the same diameter as the fuel pellets and were irradiated in a representative cross-section of the central fuel assembly. The fission product gamma-counting rates, (above a threshold of 1.3 MeV) corrected for the U^{235} fission in the depleted foil and the U^{238} fissions in the natural foil, give the time dependent quantity

$$R_\gamma(t) = \left(\frac{U^{238}\text{ gamma-counting rate}}{U^{235}\text{ gamma-counting rate}}\right)_t . \tag{7}$$

The fast fission ratio is given by

$$\delta = P(t)\, R_\gamma(t). \tag{8}$$

The time dependent calibration factor P(t) was found by irradiating the same foils in a fast neutron facility, where the fast fission ratio δ' was known, and counting the gamma-ray activities to obtain $R'_\gamma(t)$ and hence $P(t) = \delta'/R'_\gamma(t)$. A back-to-back fission chamber containing natural uranium on one side and U^{235} on the other was used to obtain δ' by measuring the fission rate ratio, R', (natural U/U^{235}) with the chamber in the fast neutron facility and the corresponding ratio, R°, with it in a thermal flux ($\delta = 0$). Then, $\delta' = (R'/R°)-1$.

3.5. *Initial conversion ratios*

Values of the initial conversion ratio, γ_0 (the number of Pu^{239} atoms produced per U^{235} atom destroyed) were determined by comparing the relative neptunium and relative fission product activities induced in thin wafers of natural uranium oxide in a representative cross-section of the central fuel assembly and in a thermal neutron flux either in a tank of D_2O attached to the end of a thermal column in the NRX reactor or in the ZED-2 bottom graphite reflector. The neptunium was counted using a coincidence method which suppresses the fission product and natural background rates ten times more than the neptunium rate. The details of this technique have been described by TUNNICLIFFE et al. [7] and CHIDLEY et al. [8].

The conversion ratio is given in terms of the measured activity ratios by the following expression,

$$\gamma_0 = C\left[\frac{\Sigma_a^{28}}{\Sigma_a^{25}}\right]_{\text{thermal}} \left[\frac{(1+\alpha)_{\text{thermal}}}{(1+\alpha)_{\text{fuel}}}\right]_{U^{235}} \quad (9)$$

where Σ_a^{28}, Σ_a^{25} are the absorption cross-sections of U^{238} and U^{235} respectively, α is the ratio of capture to fission cross-sections of U^{235}, and

$$C = \frac{\left[\dfrac{Np^{239}\ \text{activity (fuel)}}{Np^{239}\ \text{activity (thermal)}}\right]}{\left[\dfrac{U^{235}\ \text{fission product activity (fuel)}}{U^{235}\ \text{fission product activity (thermal)}}\right]} \quad (10)$$

is the measured activity ratio corrected for U^{238} fission product activity. Hence the absolute value of the initial conversion ratio γ_0 is based on the value of $\left[\Sigma_a^{28}/\Sigma_a^{25}\right]_{\text{thermal}} = 0.562$ and values of $\frac{(1+\alpha)_{\text{thermal}}}{(1+\alpha)_{\text{fuel}}}$ obtained from reference [6] using the measured r-values and neutron temperatures. The correction for the U^{238} fission product activity in fuel was the time dependent quantity $R_\gamma(t)$ defined above, that is,

$$(U^{235}\ \text{fission product activity}) = \frac{(\text{Observed fission product activity})}{1+R_\gamma(t)}. \quad (11)$$

4. RESULTS AND DISCUSSION

The results of the buckling measurements are listed in Table II. The values given have been corrected for the loading effect of the experimental foils and thimbles and to the standard moderator conditions of 25°C and 99.63 at.% D_2O. The corrections were based on calculated temperature and purity coefficients obtained from POOOF, the latest version (due to PRIMEAU [9]) of the Chalk River lattice calculation programme. The errors quoted on the values of B_{Al}^2 are based on the error calculated from the counting statistics and assumed foil positioning uncertainties or that given by the goodness-of-fit of the measured flux distributions to the assumed functions, whichever was the greater. The values quoted are the means of at least two (in one case six) individual measurements. The values of B_{ZR}^2 have larger errors due to the uncertainty in the theory used to deduce

TABLE II

BUCKLINGS, FAST FISSION RATIOS AND INITIAL CONVERSION RATIOS

Coolant	Pitch (cm)	B^2_{Al} [a] (m^{-2})	B^2_{ZR} (m^{-2})	δ	γ_0
D_2O	18	1.407 ± 0.047	1.19 ± 0.07	0.0564	0.9653
	19	2.407 ± 0.028	-	-	-
	20	2.995 ± 0.034	-	-	-
	21	3.479 ± 0.029	3.30 ± 0.05	0.0543	0.8660
	22	3.804 ± 0.024	-	-	-
	24	4.065 ± 0.014	3.89 ± 0.05	0.0528	0.8037[b]
	26	4.078 ± 0.014	-	-	-
	28	3.952 ± 0.013	3.80 ± 0.03	0.0481	0.7454
	30	3.690 ± 0.020	-	-	-
	32	3.380 ± 0.010	-	-	-
	34	3.052 ± 0.007	-	-	-
	36	2.754 ± 0.012	2.64 ± 0.03	0.0475	0.7050
AR	18	0.718 ± 0.086	-	0.0659	0.9951
	20	2.768 ± 0.072	-	-	-
	21	3.351 ± 0.055	-	0.0623	0.8442
	22	3.717 ± 0.045	-	-	-
	24	4.115 ± 0.036	-	0.0565	0.7875
	26	4.174 ± 0.023	-	-	-
	28	4.070 ± 0.018	-	0.0549	0.7316
	30	3.861 ± 0.013	-	-	-
	32	3.576 ± 0.022	-	-	-
	34	3.277 ± 0.008	-	-	-
	36	2.970 ± 0.006	-	0.0532	0.6839
HB-40	18	-0.365 ± 0.062	-	0.0581	0.9163
	21	1.214 ± 0.035	-	0.0536	0.8266
	24	1.568 ± 0.019	-	0.0521	0.7839
	28	1.528 ± 0.012	-	0.0491	0.7575

[a] All buckling values correspond to moderator conditions of 25°C and 99.63 at.% D_2O
[b] Average of two measurements

(B^2_{Al} - B^2_{ZR}). B^2_{ZR} is ~0.2 m^{-2} less than B^2_{Al} at the lowest pitch but this difference decreases to ~0.1 m^{-2} at the widest lattice pitch studied. The differences observed are consistent with the differences in the cross-sections of Al and Zircaloy-2. The B^2_{Al} results are plotted in Fig. 4 as a function of lattice pitch. The curves shown in Fig. 4 are bucklings obtained with POOOF, the lattice calculation programme. As is evident from the graph, the calculations give bucklings lower than the measured values at large spacings and higher than the measured ones at small spacings. The programme attempts to allow for the bundle end effects by assuming that the cluster materials are full-length but with effective areas consistent with the total volume of each material.

It should be mentioned here that there is a possible systematic error in the buckling results. Recent work by HENDERSON [10], who has applied the microscopic-discrete theory [11] to the calculation of flux distributions in lattices similar to those studied here, suggests that the effect of the flux transient at the core-reflector (or core-driver region) interface is not negligible at the outer points used in the present analysis to determine the radial buckling. The results quoted here are derived using the five different radial positions shown in Fig. 3 to give the radial buckling; Henderson's analysis suggests that a more correct value is given by the three inner points. The effect is in a direction to give larger bucklings and is more pronounced at tighter lattices. At the widest lattices the effect appears to be ~0.05 m^{-2} in B^2 but could be much larger at the closest spacings. Investigation of this effect is continuing. The effect could account for (at least partially) the discrepancy between the experiments and calculations at the smaller pitches.

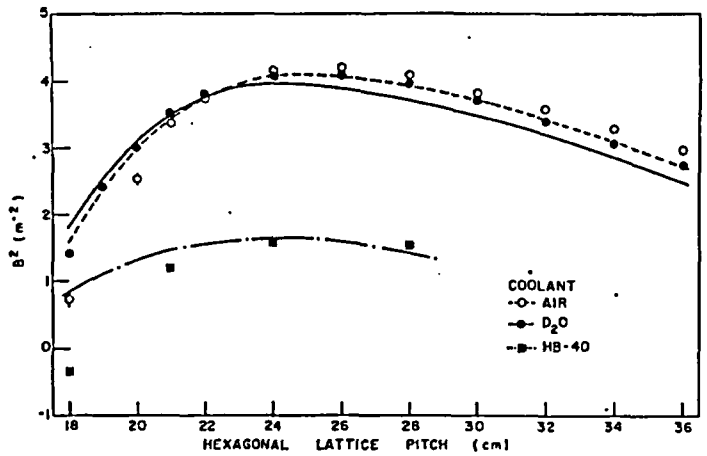

Fig. 4

Buckling versus lattice pitch for CANDU-type fuel assemblies

The results of the microscopic neutron density distributions are listed in Table III, normalized to 1.000 in the fuel. It is to be noted that these results apply to the mid-bundle region, well-removed from the flux peaking effect at the end of the bundles.

In the 21-cm D_2O-cooled lattice a measurement was made of the flux peaking caused by the gap between the fuel in adjacent bundles. The results are given at the bottom of Table III as "Flux peaking factors". The flux peaking factor for the ith material is defined as the factor by which the mid-bundle neutron density in the ith material must be multiplied to give the average (axial) neutron density in that material. It is assumed that the peaking factors are independent of lattice pitch and of type of coolant; the latter assumption is borne out by other experiments in lattices of 7-rod UO_2 bundles [2]. The errors in the relative neutron densities are thought to be ±2%. Throughout these measurements the moderator purity varied from 99.64 to 99.58 at.% and the temperature varied from 22 to 28°C; no corrections have been made for these effects.

TABLE III

RESULTS OF MICROSCOPIC NEUTRON DENSITY MEASUREMENTS

Coolant	Pitch (cm)	n_f*	n_s	n_c	n_{pt}	n_{ag}	n_{ct}	n_m
D_2O	18	1.000	1.033	1.162	1.431	1.440	1.452	1.685
	21	1.000	1.033	1.158	1.430	1.448	1.450	1.782
	24	1.000	1.021	1.147	1.427	1.454	1.467	1.856
	28	1.000	1.029	1.154	1.445	1.472	1.481	1.989
	32	1.000	1.032	1.147	1.452	1.479	1.489	2.087
	36	1.000	1.024	1.164	1.454	1.481	1.486	2.192
AIR	18	1.000	1.024	1.105	1.330	1.350	1.363	1.607
	21	1.000	1.023	1.090	1.330	1.350	1.358	1.713
	24	1.000	1.025	1.102	1.321	1.337	1.364	1.820
	28	1.000	1.033	1.110	1.333	1.363	1.409	1.946
	36	1.000	1.026	1.109	1.350	1.381	1.401	2.117
HB-40	18	1.000	1.048	1.195	1.650	1.701	1.713	1.863
	21	1.000	1.040	1.185	1.687	1.771	1.776	2.065
	24	1.000	1.034	1.195	1.763	1.796	1.806	2.109
	28	1.000	1.049	1.232	1.839	1.877	1.889	2.331
Flux peaking factors	21 (D_2O-cooled)	1.014	1.043	1.022	1.005	1.004	1.003	-

* Subscripts f, s, c, pt, ag, ct and m refer to fuel, sheath, coolant, pressure tube, air annulus, calandria tube and moderator, respectively

TABLE IV

NEUTRON SPECTRUM PARAMETERS

Coolant	Pitch (cm)	r_f [1]	r_m	r_s	ΔT_f [2] °C	ΔT_m °C	ΔT_s °C
D_2O	18	0.0886	0.0626	0.0694	86	37	51
	21	0.0658	0.0428	0.0507	72	23	39
	24	0.0487	0.0309	0.0368	59	15	30
	28	0.0376	0.0226	0.0283	51	9	24
	36	0.0230	0.0120	0.0176	44	3	19
AIR	18	0.1001	0.0698	0.0805	86	43	64
	21	0.0720	0.0480	0.0585	72	25	47
	24	0.0535	0.0322	0.0418	63	28[3]	40
	28	0.0402	0.0244	0.0316	58	14	32
	36	0.0247	0.0128	0.0197	49	3	25
HB-40	18	0.0687	0.0451	0.0473	80	26	32
	21	0.0537	0.0317	0.0353	72	18	26
	24	0.0436	0.0242	0.0282	62	9	19
	28	0.0339	0.0176	0.0208	53	6	10

1 Subscripts f, m, s refer to fuel average, a position in the moderator halfway between neighbouring rods, and the outer surface of the calandria tube, respectively

2 ΔT_x is the difference between the neutron temperature at position x and the physical moderator temperature

3 This value appears to be a flyer!

The measured values of r and T_n are given in Table IV. The temperatures are expressed as hardening values, ΔT, where ΔT_x is the difference between the neutron temperature at position x and the physical moderator temperature. We estimate the errors in r to be ±3% (mainly due to the uncertainty in the In resonance parameters; the relative values of r are felt to be good to ±1%) and in the ΔT values to be ±3°C. (We believe that ΔT_m for the 24-cm air-cooled lattice is a flyer!) The values of $r\sqrt{T_n/T_0}$ ΔT are plotted in Figs. 5 and 6 respectively against $V_{UO_2}/(V_{D_2O} + 3.753\ V_{HB\text{-}40})$ where V_{UO_2}, V_{D_2O} and $V_{HB\text{-}40}$ are volumes of UO_2, D_2O and HB-40 respectively per unit length of cell. The factor 3.753, equal to the ratio $(\xi\Sigma_s)_{HB\text{-}40}/(\xi\Sigma_s)_{D_2O}$ allows (at least nominally) for the greater moderating power of the HB-40. (V_{D_2O} includes both moderator and coolant in the D_2O-cooled cases.) The corresponding results for 7-element lattices are shown in Figs. 7 and 8. (Details of the 7-element fuel clusters are also listed in Table I.) In each figure the upper values are for the cluster average and the lower values are for the cell boundary position in the moderator. The calandria tube values for the 19-element clusters which are not plotted fall between the fuel and moderator values.

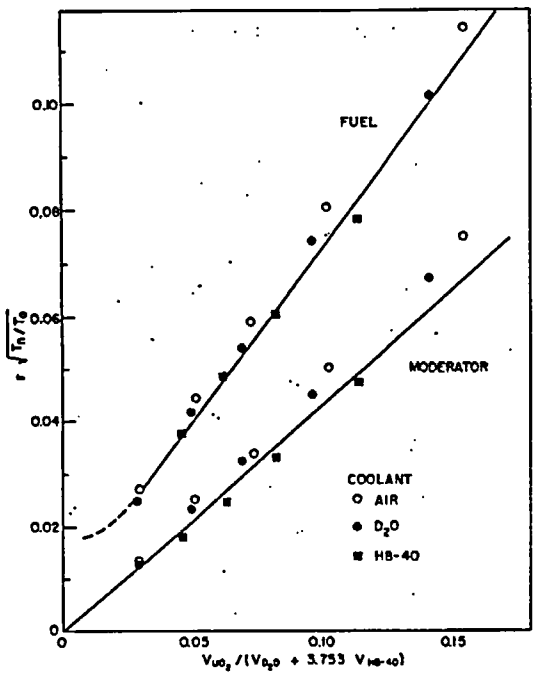

Fig. 5

$r\sqrt{T_n/T_0}$ values in 19-element lattices

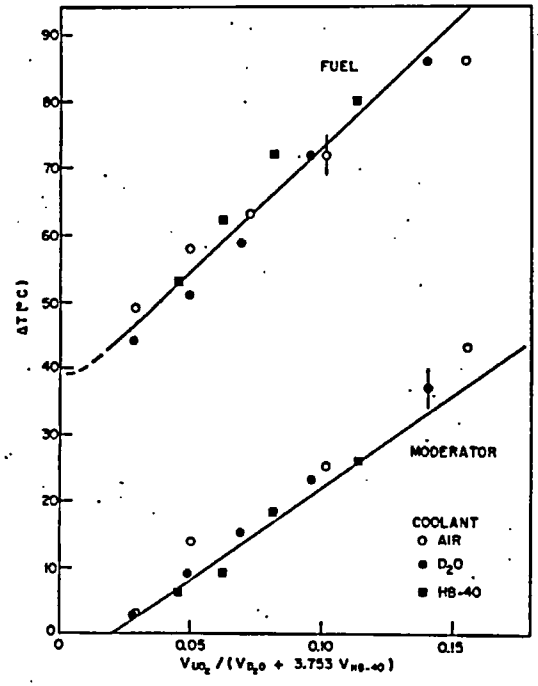

Fig. 6

ΔT_f and ΔT_m values in 19-element lattices

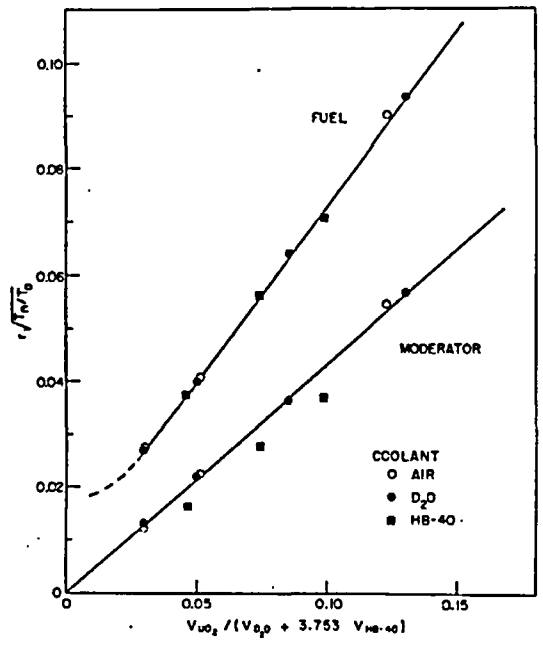

Fig. 7

$r\sqrt{T_n/T_0}$ values in 7-element lattices

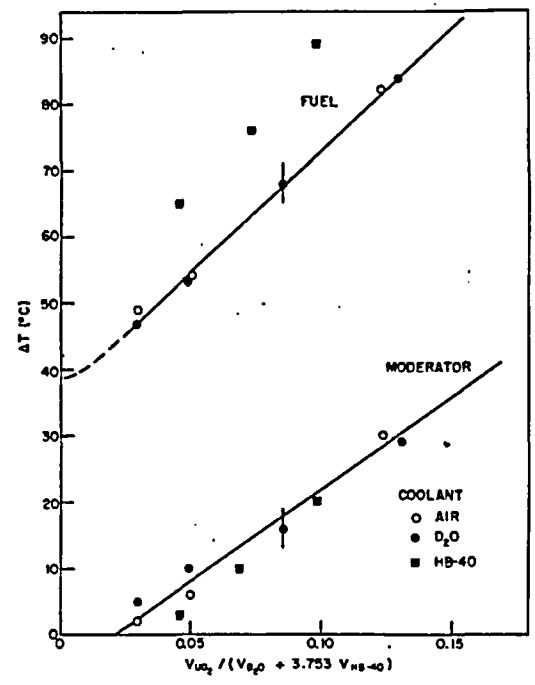

Fig. 8

ΔT_f and ΔT_m values in 7-element lattices

A linear dependence of $r\sqrt{T_n/T_0}$ and ΔT on $V_{UO_2}/(V_{D_2O} + 3.753\ V_{HB\text{-}40})$ is suggested and the straight lines shown as guides to the eye are the same in Figs. 5 and 7 and in Figs. 6 and 8. The cluster values of both $r\sqrt{T_n/T_0}$ and ΔT must approach a constant isolated rod value at wide spacings (small $V_{UO_2}/(V_{D_2O} + 3.753\ V_{HB\text{-}40})$) and this is suggested by the dashed extension of the lines although there is no indication of such curvature from the results. For the cell boundary results the lines through the $r\sqrt{T_n/T_0}$ values pass through the origin but the lines through the ΔT values have an intercept of about -6°C. This indicates a non-linearity at small values of ΔT or possibly an error in the assumption that the reference neutron temperature was equal to the moderator temperature.

These neutron spectrum parameters, when combined with the neutron density results listed in Table III, can be used to determine values of the thermal utilization f and thermal diffusion area L^2.

The experimental values of δ are listed in Table II and plotted in Fig. 9 against lattice pitch. Errors of ±2% are indicated. An increase in δ with decreasing pitch is clearly shown. The curves are of the form

$$\delta(d) = \delta(\infty)(1 + 6\ \exp[(d-2b)/\ell)], \qquad (12)$$

where $\delta(\infty)$ is the isolated cluster value, d is the lattice pitch, b = 1.5 cm is a constant, and ℓ = 4.6 cm is the relaxation length for fission neutrons (causing

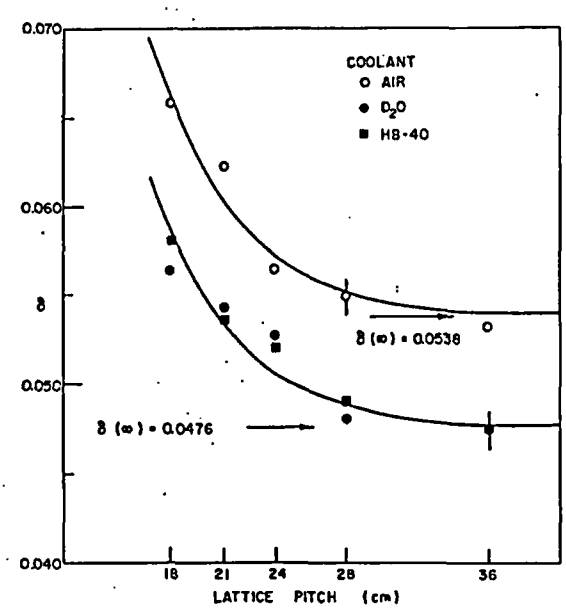

Fig. 9

Fast fission ratios in 19-element lattices

fast fission) in D_2O [12]. The exponential term is an approximation for the contribution from the six adjacent neighbours in the lattice. The values of $\delta(\infty) = 0.0476$ and 0.0538 for D_2O coolant and air coolant respectively are indicated. The HB-40 values indicate $\delta(\infty) = 0.0480$, not significantly higher than for D_2O.

The cluster average values of γ_0 are listed in Table II. The values for D_2O cooled lattices at spacings of 18, 21 and 28 cm are those given by CHIDLEY et al. [8] but increased a small amount due to a reduction in the correction for the small gap (~0.013 mm) between the wafer and the pellets. This correction (<0.5%) was remeasured and found to be somewhat smaller than that used by CHIDLEY et al. [8]. New measurements of γ_0 were made at 36 cm and 24 cm (two) and the values obtained are about 3% higher than those listed by CHIDLEY et al. [8]. The reason for this is not understood.

The values of γ_0 have been plotted against $V_{UO_2}/V_{D_2O} + 3.753\ V_{HB\text{-}40}$) in Fig. 10. An almost linear dependence, with an indication of curvature at large lattice spacings is suggested and curves have been drawn as guides to the eye.

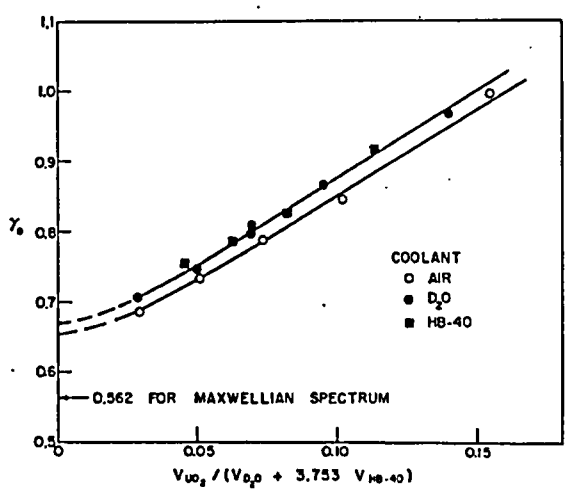

Fig. 10

Initial conversion ratios in 19-element lattices

The statistical counting errors, including uncertainties in the corrections, were in the range ±(0.3 - 0.5)%, that is, comparable with the size of the points in the figure. Measurements were made in all five elements across the cluster and consequently duplicate values of γ_0 were obtained for the outer and inner rings of elements. The differences between these duplicate values are a measure of the consistency of the measurements. The root mean square difference for 27 pairs of γ_0 values was 0.73% which corresponds to a 0.52% ($0.73/\sqrt{2}$) error for a single value. The corresponding average statistical error was about ±0.4%. The larger root mean square deviation indicates an additional error of about ±0.3%, perhaps due to misalignment of the wafers between pellets or misalignment of elements in the

cluster. There is also the systematic error of ±0.8% associated with the Maxwellian spectrum value (0.562) on which the results are based. More detailed discussion of the corrections and errors is given in references [7] and [8].

A comparison with the 7-element lattice values given by TUNNICLIFFE et al. [7] is made in Fig. 11 where the experimental points give the 7-element values and the curves the 19-element results. The trends are similar, with the 19-element values for each coolant about 3% higher than the 7-element values.

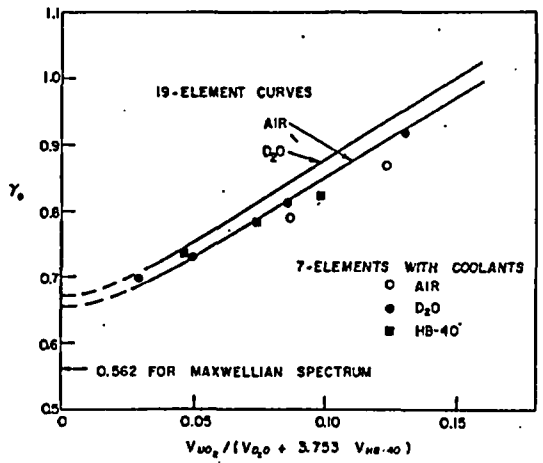

Fig. 11

Initial conversion ratios in 7 & 19 element lattices

The values of δ and γ_0 found here can be used in conjunction with the appropriate expressions to yield values for the fast fission factor ϵ, and the resonance escape probability p.

5. SUMMARY

Experiments done in the critical facility ZED-2 to determine parameters for lattices of fuel assemblies which are a close mock-up of the actual fuel channels of the power reactor CANDU (and also NPD) have been described.

The results of these measurements can now be compared with the same parameters obtained from the lattice recipes. The agreement between the measured and calculated parameters may then be useful as a guide to the development of better recipes. If the lattice recipes can predict correctly the results of clean, cold lattice experiments such as those described here, then some confidence can be felt in extrapolating them to the operating conditions appropriate to an actual power reactor.

ACKNOWLEDGEMENTS

The authors wish to acknowledge the help given by many people throughout the course of the work. In particular they would like to thank P. D. J. Ferrigan

who was in charge of reactor operations; E. Engel, T.J. Manuel and J.T.R. Young who performed most of the experiments and also assisted with the analysis of the results; Mrs. M.G. Cahill who ran the data reduction and least squares computer programmes an innumerable number of times; J.S. Rogers who helped with the analysis of the data and Miss E. Gehlert who typed the manuscript. D.B. Primeau kindly provided numerous POOOF† calculations for the ZED-2 experimental conditions. Helpful discussions were held with B.G. Chidley, E. Critoph, W.J. Henderson, D.G. Hurst and A.G. Ward.

REFERENCES

[1] BEER, G.A. and HONE, D.W., Lattice Measurements with 7-element UO_2 clusters in ZED-2, Part I: Bucklings Over a Range of Spacings with Three Coolants; AEC Rpt AECL-1505 (1962).

[2] GREEN, R.E. et al., Highlights of Chalk River Work on the Physics of Heavy Water Lattices Since the 1959 IAEA Panel Meeting; AEC Rpt. AECL-1684 (1962); Heavy Water Lattices; Second Panel Report, Technical Reports Series No.20, IAEA, Vienna (1963) 51.

[3] HONE, D.W. et al., Natural Uranium Heavy-Water Lattices, Experiment and Theory; Proc. 2nd.UN Int. Conf. PUAE 12 (1958) 351.

[4] WESTCOTT, C.H., WALKER, W.H. and ALEXANDER, T.K., Effective Cross Sections and Cd Ratios for the Neutron Spectra of Thermal Reactors; Proc. 2nd. UN Int.Conf. PUAE 16 (1958) 70.

[5] BIGHAM, C.B., CHIDLEY, B.G. and TURNER, R.B., Experimental Effective Cross Sections and Neutron Spectra in a Uranium Fuel Rod, Part II; CANDU-type Uranium Oxide Clusters, AEC Rpt. AECL-1350 (1961).

[6] WESTCOTT, C.H., Effective Cross Section Values for Well Moderated Thermal Reactor Spectra; AEC Rpt. AECL-1101 (1960).

[7] TUNNICLIFFE, P.R., SKILLINGS, D.J. and CHIDLEY, B.G., A Method For the Accurate Determination of Relative Initial Conversion Ratios, Nucl. Sci. Engng 15 (1963) 268.

[8] CHIDLEY, B.G., MANUEL, T.J. and TUNNICLIFFE, P.R., Initial Conversion Ratios and Fast Fission Factors in Heavy Water Natural Uranium Lattices Using 19-element UO_2 Fuel Rods. Nucl. Sci. Engng, in press.

[9] PRIMEAU, D.B., unpublished.

[10] HENDERSON, W.J., private communication.

[11] STEWART, J.D., A Microscopic-Discrete Theory of Thermal Neutron Piles, AEC Rpt. AECL-1470 (1962).

[12] BIGHAM, C.B. and CHIDLEY, B.G., AECL Progress Report PR-RRD-31 (1962) 70.

DISCUSSION

J. WOLBERG: I would first like to comment on your measurement of δ^{28}. I was surprised to see that you reached asymptotic values of δ^{28} at about 28 cm. This is much larger than the distance at which this effect was observed at the Massachusetts Institute of Technology for metallic, 2.5-cm natural uranium lattices. Even though your clusters are of larger diameter, it seems to me that the main factor influencing this distance is the fast neutron mean free path, and this was the same in both sets of lattices.

I would also like to comment on your buckling measurements. We have written a D_2O reactor optimization code in Israel and have tested the nuclear portion of the code against your measured values of buckling. The agreement between our calculations and your measurements was good.

I.A. MOSSOP: The paper refers to measurements of the conversion ratio "in a representative cross-section of the central fuel assembly". I assume this means that you have made a number of measurements within

the fuel clusters and have then taken an average. If this is the case, are you able to indicate the observed variations in conversion ratio between the various rings of the fuel cluster and also axially, particularly near the extremities of the fuel elements?

R.E. GREEN: We have determined the conversion ratio separately in the three fuel pencils which are at different radii in the cluster. I do not recall the values for the individual pencils offhand. As far as the variation of the conversion ratio along the length of the fuel bundle is concerned, there is certainly an effect due to the extra fuel surface exposed at gaps between the fuel bundles. We have measured this effect in one lattice and found it to be small. However, allowance must be made for this effect when determining the conversion ratio for the complete lattice.

G. CASINI: Could you give a few values for a comparison of the errors in the buckling measured directly from flux charts with those applicable when the buckling is deduced from detailed measurements (fine structure, neutron temperature, initial conversion factor, etc.)?

R.E. GREEN: A correlation such as that implied by your question has been done for the 7-rod UO_2 NPD-type fuel assemblies, and an internal Chalk River Report is available on this subject. The same type of correlation is being carried out for the 19-rod UO_2 assemblies and some preliminary results of this work are also available. In general, the bucklings deduced from the individual measured parameters agree with the measured bucklings, within the errors in the derived bucklings. However, in the case of the air-cooled assemblies the derived bucklings are consistently higher by ~ 0.1 to $0.3\ m^{-2}$.

COMPARISON OF THE WORTH OF CRITICAL AND EXPONENTIAL MEASUREMENTS FOR HEAVY-WATER-MODERATED REACTORS*

W.E. GRAVES AND E.J. HENNELLY
SAVANNAH RIVER LABORATORY, E.I. DU PONT DE NEMOURS AND CO.,
AIKEN, S.C., UNITED STATES OF AMERICA

Abstract — Résumé — Аннотация — Resumen

COMPARISON OF THE WORTH OF CRITICAL AND EXPONENTIAL MEASUREMENTS FOR HEAVY-WATER-MODERATED REACTORS. Critical and exponential experiments in general produce overlapping information on reactor lattices. Over the past ten years the Savannah River Laboratory has been operating a heavy-water critical, the PDP, and an exponential, the SE, in parallel. This paper summarizes SRL experience to give results and recommendations as to the applicability of the two kinds of facilities in different experiments.

Six types of experiments are considered below:

(1) Buckling measurements in uniform isotropic lattices

Here Savannah River has made extensive comparisons between single-region criticals, exponentials, substitution criticals, and PCTR type measurements. The only difficulties in the exponentials seem to lie in the radial-buckling determinations. If these can be made successfully, the exponentials can offer good competition to the criticals. Material requirements are greatest for the single-region criticals, roughly comparable for the substitution criticals and exponentials, and least for the PCTR measurements.

(2) Anisotropic and void effects

SRL experiments with the criticals and with critical-exponential comparisons are reviewed briefly here and at greater length in a companion paper.

(3) Evaluation of control systems

Adequately analysed exponential experiments appear to give good results for total-worth measurements. However, for adequate study of overall flux shaping, flux tilts, etc. a full-sized critical such as the PDP is required.

(4) Temperature coefficients

Exponential experiments provide an excellent method for determining the temperature coefficient of buckling for uniform lattice heating. A special facility, the PSE, at Savannah River permits such measurements up to temperatures of 215°C. For non-uniform lattice heating criticals are generally preferred.

(5) Mixed lattices

Actual reactors rarely use the simple uniform lattices to which the exponentials basically apply. Critical experiments with mixed loadings are used at SRL both in measuring direct effects in mock-ups and as a test for heterogeneous and two-dimensional diffusion calculations.

(6) Criticality studies of heavy-water lattice fuel in light water

The SRL exponentials have proved particularly valuable for criticality studies to determine safe methods of handling enriched fuel in light water.

* The information contained in this paper was developed during the course of work under contract AT(07-2)-1 with the US Atomic Energy Commission.

High accuracy is not required in this case, and the generalized exponential buckling studies are definitely preferable to the more particularized critical studies.

VALEUR RELATIVE DES MESURES CRITIQUES ET EXPONENTIELLES POUR L'ÉTUDE DES RÉACTEURS RALENTIS A L'EAU LOURDE. En règle générale, les expériences critiques et exponentielles sur des réseaux de réacteurs fournissent des renseignements qui font double emploi. Durant les dix dernières années, le Savannah River Laboratory (SRL) a fait fonctionner simultanément un ensemble critique à eau lourde (PDP) et un ensemble exponentiel (SE). Les auteurs exposent brièvement l'expérience acquise au SRL, indiquent les résultats obtenus et font des recommandations au sujet de la possibilité d'appliquer ces deux genres d'installations dans différentes expériences.

Les auteurs examinent les six types d'expériences ci-après:

1. Mesures du laplacien dans les réseaux isotropiques uniformes

Le SRL a procédé à de nombreuses comparaisons entre les mesures faites à l'aide d'ensembles critiques à une seule région, d'ensembles exponentiels, d'ensembles critiques à substitution et du réacteur d'essai des constantes physiques (PCTR). Il semble que les seules difficultés que présentent les expériences exponentielles résident dans les déterminations du laplacien dans le sens radial. Si l'on réussit à faire ces déterminations, les expériences exponentielles peuvent être comparées favorablement aux expériences critiques. Les ensembles critiques à une seule région nécessitent le plus de matières; viennent ensuite les ensembles critiques à substitution et les ensembles exponentiels dont les besoins sont en gros comparables; enfin le PCTR où les mesures en exigent le moins.

2. Effets anisotropiques et effets cavitaires

Des expériences à l'aide d'ensembles critiques et les comparaisons faites entre expériences exponentielles et expériences critiques font l'objet d'un aperçu dans le présent mémoire et d'un exposé détaillé dans un autre mémoire.

3. Evaluation des barres de contrôle

Une analyse appropriée des expériences exponentielles semble donner de bons résultats lorsqu'il s'agit de mesures de l'antiréactivité totale. Cependant, si l'on veut étudier convenablement certaines caractéristiques du flux, il faut un ensemble critique de dimensions normales tel que le PDP.

4. *Coefficients de température*

Les expériences exponentielles offrent une méthode excellente si l'on veut déterminer le coefficient thermique du laplacien pour un chauffage de réseau uniforme. Une installation spéciale (PSE) du SRL permet de procéder à ces mesures à des températures allant jusqu'à 215°C. Pour un chauffage non uniforme, on préfère généralement utiliser des ensembles critiques.

5. Reseaux mixtes

Dans les réacteurs, on utilise rarement les réseaux uniformes simples auxquels les expériences exponentielles s'appliquent essentiellement. Au SRL, on fait des expériences critiques à chargements mixtes tant pour mesurer les effets directs dans des maquettes de réacteurs que pour vérifier les calculs de diffusion hétérogènes et à deux dimensions.

6. Etudes, au point de vue de l'état critique, du comportement dans l'eau ordinaire d'un combustible destiné à un réseau à eau lourde

Les ensembles exponentiels du SRL se sont révélés particulièrement utiles pour les études visant à déterminer comment manipuler le combustible enrichi dans l'eau ordinaire.

Ces travaux ne nécessitent pas une très grande exactitude; les expériences exponentielles d'un caractère plus général sont nettement préférables aux expériences critiques d'un caractère plus particulier.

СРАВНЕНИЕ ЦЕННОСТИ КРИТИЧЕСКИХ И ЭКСПОНЕНЦИАЛЬНЫХ ИЗМЕРЕНИЙ ДЛЯ РЕАКТОРОВ С ТЯЖЕЛОВОДНЫМ ЗАМЕДЛИТЕЛЕМ. Критические и экспоненциальные эксперименты дают, как правило, частично перекрывающиеся данные по реакторным решеткам. В течение последних десяти лет в Лаборатории Саванна-Ривер работали параллельно тяжеловодная критическая установка PDP и экспоненциальная установка SE. Обобщается опыт с целью дать рекомендации в отношении применения этих двух установок для различных экспериментов. Рассматриваются шесть видов экспериментов:

1) . Измерения лапласиана в однородных изотопных решетках

Осуществлено широкое сравнение результатов, полученных при однородных критических, экспоненциальных и подстановочно-критических измерениях, а также измерениях типа PCTR. В экспоненциальных измерениях трудности, по-видимому, заключаются единственно в определении радиального лапласиана. При удачном выполнении экспоненциальные измерения могут успешно конкурировать с критическими. Наибольшее количество материала требуется для однозонных критических измерений, примерно одинаковое количество—для подстановочно-критических и экспоненциальных измерений и менее всего—для измерений типа PCTR.

2) Анизотропный и пустотный эффекты

Сравнения экспериментов лаборатории с критическими и критически-экспоненциальными приводятся в данной работе, а более подробно они излагаются в работе, которая сопровождает данную.

3) Оценка систем управления

Оказалос, что хорошо проанализированные экспоненциальные эксперименты дают хорошие результаты для измерений общей значимости. Однако для надлежащего изучения формирования общего потока, углов наклона потока и т.д. необходима полномасштабная критическая установка наподобие PDP.

4) Температурные коэффициенты

Экспоненциальные эксперименты являются превосходным методом определения температурного коэффициента лапласиана для нагревания однородной решетки. Имеющаяся в лаборатории специальная установка PSE позволяет производить такие измерения вплоть до температуры 215°C. Для нагревания неоднородных решеток предпочтение, как правило, отдавалось критическим экспериментам.

5) Смешанные решетки

Для настоящих реакторов редко применяются простые однородные решетки, для которых используются в основном экспоненциальные измерения. Критические эксперименты со смешанными загрузками используются как для измерения прямых эффектов в макетах, так и для испытания расчетов гетерогенной и двухразмерной диффузии.

6) Исследования критичности топлива, используемого в тяжеловодных решетках, в обычной воде воде

Экспоненциальные измерения оказались особенно ценными для исследования критичности с целью определить безопасные методы обращения с обогащенным топливом в обычной воде.

В этом случае не требуется большой точности, и обобщенные экспоненциальные исследования лапласиана являются определенно более предпочтительными, чем более конкретизированные критические исследования.

VALOR RELATIVO DE LAS MEDICIONES CRÍTICAS Y EXPONENCIALES PARA LOS REACTORES MODERADOS POR AGUA PESADA. Con los conjuntos críticos y los exponenciales se obtienen generalmente informaciones en parte repetidas sobre los reticulados de reactor. En los últimos diez años, en el Laboratorio de Savannah River (SRL) se ha venido trabajando con un conjunto crítico de agua pesada el PDP, y con un conjunto exponencial, el SE, en forma paralela. Los autores presentan una reseña de la experiencia así ad-

quirida en dicho laboratorio, exponiendo los resultados y formulando recomendaciones sobre cuál de los dos tipos de conjuntos resulta más adecuado para determinados experimentos.

A continuación se exponen seis tipos de experimentos:

1. Determinación del laplaciano en reticulados isotrópicos uniformes

En el SRL se han llevado a cabo extensas comparaciones entre mediciones efectuadas con ayuda de conjuntos críticos de región única, conjuntos exponenciales, conjuntos críticos de sustitución y del reactor PCTR (prompt critical test reactor). En el caso de los conjuntos exponenciales, aparentemente sólo se tropieza con dificultades en las determinaciones del laplaciano radial. Si se llegase a salvarlas, los experimentos exponenciales podrían rivalizar sin desmedro con los críticos. Los conjuntos críticos de región única son los que exigen más material; les siguen los conjuntos críticos de sustitución y los exponenciales, cuyas necesidades son, en términos generales, comparables; en último término figura el PCTR, cuyas exigencias son mínimas.

2. Efectos anisotrópicos y de cavitación

Se examinan brevemente los experimentos realizados en el SRL con conjuntos críticos y se establecen comparaciones entre éstos y los conjuntos exponenciales; en otra memoria se trata el mismo tema con más detalle.

3. Evaluación de los sistemas de control

Los experimentos exponenciales se prestan para efectuar mediciones de la eficacia global, siempre que sus resultados se analicen adecuadamente. No obstante, para un estudio cabal de la distribución general del flujo, de los gradientes de flujo, etc., se requiere un conjunto crítico de gran tamaño, como el PDP.

4. Coeficientes de temperatura

Los experimentos exponenciales constituyen un excelente método para determinar el coeficiente térmico del laplaciano para un calentamiento uniforme del reticulado. En el SRL hay una instalación especial, el PSE, que permite establecer dicho coeficiente hasta temperaturas de 215°C. En cambio, para un calentamiento no uniforme, se prefiere generalmente los conjuntos críticos.

5. Reticulados mixtos

En los reactores en funcionamiento raramente se usan los reticulados uniformes simples a los cuales se aplican básicamente los experimentos exponenciales. En el SRL se recurre a los experimentos críticos con cargas mezcladas, tanto para medir los efectos directos en maquetas, como para verificar la corrección de los cálculos de difusión en medios heterogéneos y bidimensionales.

6. Estudios de la criticidad en agua ligera de un combustible destinado a reticulados de agua pesada

Se ha comprobado que los experimentos exponenciales del laboratorio del SRL son particularmente valiosos para los estudios de criticidad encaminados a encontrar métodos seguros de manipulación en agua ligera del combustible enriquecido.

Estos trabajos no exigen una exactitud muy grande, y cabe señalar que los estudios de tipo general del laplaciano efectuados en conjuntos exponenciales son decididamente preferibles a los estudios especializados con conjuntos críticos.

1. INTRODUCTION

Over the past ten years the Savannah River Laboratory (SRL) has operated a large heavy-water critical facility, the PDP [1, 2], and an exponential

one, the SE [3]. Since 1958 the Laboratory has also operated a pressurized exponential facility, the PSE [4]. The purpose of this paper is to summarize the results of this SRL experience and to give recommendations as to the applicability of the two kinds of facilities in six fields of reactor experimentation:

(1) Buckling measurements in uniform lattices;
(2) Anisotropic and void effects;
(3) Evaluation of control systems;
(4) Temperature coefficients;
(5) Mixed lattices; and
(6) Subcriticality studies of fuel for heavy-water-moderated reactors.

A great deal of data bearing on these subjects from the point of view of experimentation at SRL was contained in two recent review papers by CRANDALL [5, 6]. Where such data are relevant in the present context they will be discussed, but only referenced rather than reproduced. Data given in detail in the present paper has been, for the most part, previously unpublished.

All six of the above listed topics involve macroscopic lattice parameters. Before dealing with them, a few words would be appropriate on the measurement of unit cell parameters such as thermal utilization, fast fission ratio, etc. by activation techniques. Although such measurements are more usually carried out in a critical than in an exponential facility there seems no a priori reason why this should be so, provided that the neutron flux is sufficiently high in the exponential. At SRL the neutron source for the SE is a small reactor, the SP [7], and fluxes of $\sim 10^9$ n cm^{-2} s^{-1} can be obtained at the bottom of the exponential tank. It has thus proved possible to make activation measurements of all types in the SE. While there is some reason to expect the measured microscopic parameters to change with leakage, in general the effects are small and/or correctable. Some discussion of such effects is given in the section on control systems. Extensive use of the SE for activation measurements has proved extremely convenient and has permitted the PDP to be used primarily for macroscopic measurements where its large size is a more positive advantage.

2. BUCKLING MEASUREMENTS IN UNIFORM LATTICES

At SRL our most accurate values for the bucklings of uniform lattices have been obtained by mapping the flux distributions in critical one-region loadings in the PDP and fitting the data to the appropriate functions. Such a procedure minimizes the possibility of systematic error. However the measurements are expensive, both in terms of critical facility usage and of fuel requirements. They therefore seem justified in only a few circumstances. Two types of lattices, in particular, suggest themselves:

(1) Lattices containing fuel assemblies destined for use in a prototype or full-size power reactor. Here the fuel is already available and there is strong incentive to obtain quite accurate results in order to optimize the operation of the reactor.

(2) Lattices which cover an extreme range of lattice parameters. Here the measurements have as their primary purpose the provision of accurate experimental data for comparison with lattice calculations.

Since SRL, almost alone among laboratories dealing with heavy-water lattice physics, has not been concerned in the immediate design of a prototype power reactor, we have felt free to pursue the second of the above alternatives in the PDP. Fuel assemblies used have included natural-uranium metal rod clusters [8, 9], natural-UO_2 rod clusters [10], and, more recently, natural-uranium metal tubular fuel assemblies. Since both sets of cluster measurements have already been fully reported, the tubular fuel assembly measurements are used as examples here. These latter measurements utilized two types of fuel assemblies: a single tube, and a rod surrounded by two concentric tubes. These assemblies are shown in Fig. 1. Bucklings were measured over a range of triangular lattice pitches in the PDP, using standard techniques [8, 10]. Both air and D_2O were used as "coolants" within the assembly housings. Buckling results are given in Table I.

A secondary purpose which measurements such as the above serve is to provide a set of reference lattices of known bucklings to test alternate and simpler methods of measuring bucklings. Such measurements include exponential measurements, critical substitution measurements, and null reactivity or PCTR-type measurements.

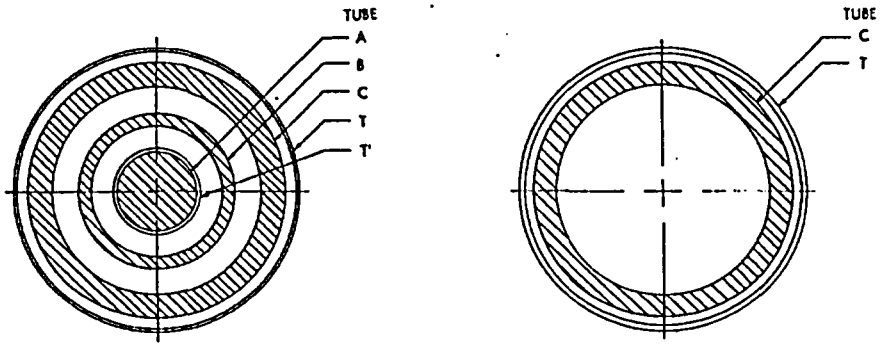

Fig. 1

Tubular metal fuel assemblies

Tube	O.D. (in)	I.D. (in)	Material
A	0.998		Natural U
B	2.120	1.760	Natural U
C	3.500	2.860	Natural U
T	3.890	3.840	Al (6063)
T'	1.090	1.026	Al (1100)

TABLE I

BUCKLINGS OF LATTICES CONTAINING TUBULAR NATURAL URANIUM FUEL ASSEMBLIES

Fuel assembly[b]	Triangular lattice pitch (in)	Coolant	Corrected experimental buckling		
			B_z^2 (m^{-2})	B_r^2 (m^{-2})	B_m^2 (m^{-2})
Two tubes and one rod	9.33	Air	2.12 ± 0.06	3.78 ± 0.05	(5.90 ± 0.08)[c]
		D_2O	1.17 ± 0.08	3.74 ± 0.03	5.52 ± 0.09
	12.12	Air	3.86 ± 0.06	2.12 ± 0.03	(5.98 ± 0.07)
		D_2O	3.31 ± 0.07	2.13 ± 0.02	5.44 ± 0.07
	14.00	Air	3.41 ± 0.06	1.64 ± 0.01	(5.05 ± 0.06)
		D_2O	2.82 ± 0.05	1.66 ± 0.02	4.48 ± 0.05
Single tube	9.33	Air	1.98 ± 0.05	3.74 ± 0.02	(5.72 ± 0.06)
		D_2O	2.90 ± 0.08	3.83 ± 0.03	6.73 ± 0.09)
	12.12	Air	3.12 ± 0.05	2.11 ± 0.03	(5.23 ± 0.06)
		D_2O	3.43 ± 0.05	2.16 ± 0.04	5.59 ± 0.06
	14.00	Air	2.71 ± 0.04	1.67 ± 0.02	(4.38 ± 0.04)
		D_2O	2.70 ± 0.04	1.69 ± 0.02	4.39 ± 0.04

[a] At 99.59 mol.% D_2O and 22°C
[b] See Fig. 1
[c] Bucklings enclosed in parentheses refer to anisotropic lattices

Exponential measurements of buckling have great potential advantages over one-region critical measurements in terms of reducing time and material requirements as well as the criticality hazards potential. The greatly reduced time requirements can only be realised in practice, however, if the experimental measurements on a given lattice consist solely of measuring the inverse relaxation area κ^2. Such measurements are particularly fast if the κ^2 measurement is made with a flux monitor which is remotely controlled and moves vertically in the lattice. The requirement for this simple type of experiment to be feasible is that changes in the radial buckling of the exponential tank with lattice loading must be small and calculable.

Strong anomalous changes in measured radial bucklings with changing lattice loadings were first observed at the Argonne National Laboratory [11]. The Argonne experiments showed that the changes were independent of the presence or absence of a small reflector and also indicated that the effects

did not arise from external reflectors or foreign materials outside the cadmium-covered exponential tank.

Similar observations were made independently at SRL in a programme to compare bucklings measured in one-region criticals and in exponentials. With an assumed constant radial buckling for the exponential, systematic differences appeared between the material bucklings measured in the two types of facilities [12]. Later measurements of radial bucklings in the exponential showed that essentially all of the differences could be ascribed to anomalously large changes in these bucklings [13]. The results of the Savannah River intercomparisons are shown in Fig. 2 [6]. This plot is, of course, only one method of presenting the results. An alternative presentation of the same data is shown in Fig. 3. In this plot the exponential-critical difference is essentially a single valued and rather linear function of the material bucklings of the lattices. A physical explanation of these results has not been forthcoming. Similar results have been observed in Switzerland [14]. On the other hand, unpublished measurements referenced by PERSSON [15] for the ZEBRA exponential gave radial bucklings which fell within the range which would be predicted by standard reactor theory [16].

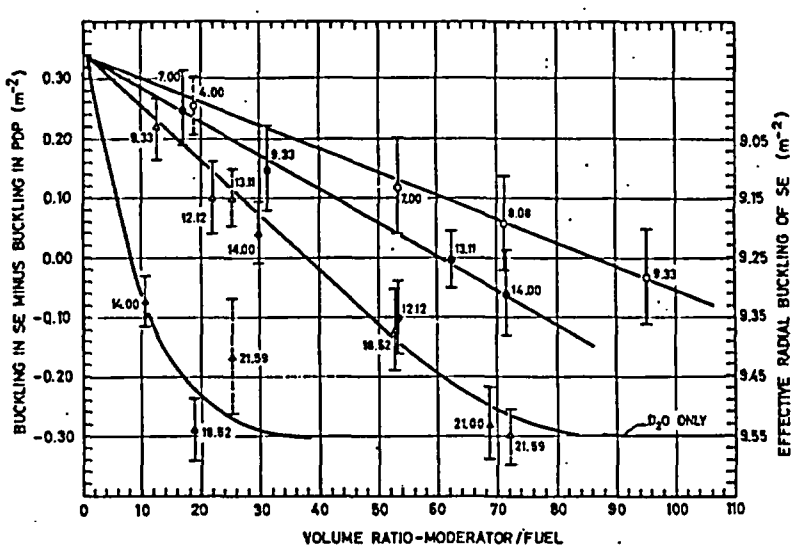

Fig. 2

Effect of moderator to fuel ratio on differences between exponential and critical bucklings for natural uranium rods in D_2O

Rod diameter; 0.998 in; buckling at 99.75% D_2O

○ Single rods ● 3-rod cluster

△ 7-rod cluster ▲ 19-rod cluster

Numbers adjacent to data points refer to lattice pitches in inches;

Dashed flags indicate measured radial buckling

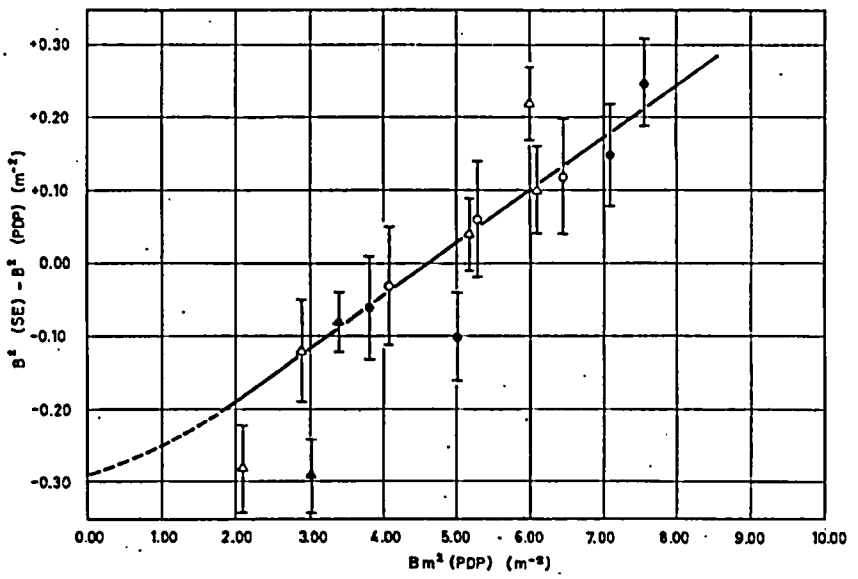

Fig.3

Effect of buckling on differences between exponential and critical buckling for natural uranium rods in D_2O

O Single rods ● 3-rod cluster

Δ 7-rod cluster ▲ 19-rod cluster

Another set of measurements bearing on radial buckling changes in exponentials was performed at Babcock and Wilcox [17]. These experiments indicated a strong dependence of radial buckling on the diameter of a cadmium aperture limiting the diameter of the source feeding the exponential.

The authors' conclusion from the above is that, at the present time, accurate exponential measurements in general require a measurement of the radial buckling as well as the inverse relaxation area κ^2, for each lattice studied. Under these conditions, exponentials sacrifice their speed advantages, although the advantage of requiring less material than the criticals is retained. The accuracy of the bucklings obtained will be limited by the accuracy of the radial buckling measurements.

In practice, however, it is probably preferable to use values of the radial buckling that were obtained from previous exponential experiments or from intercalibrations with critical experiments and accept the possibility of some small systematic error in the final result. Studies such as the SRL correlation [11] show that, within a fairly limited range of lattice parameters, the error may even be less than the error on a single measurement of radial buckling.

A related problem in exponential experiments arises from the fact that it is rarely convenient to use a lattice pitch such that the lattice fits exactly into the exponential tank, i.e. the number of fuel assemblies times the area of a unit cell is usually not equal to the area of the tank. It is usually as-

sumed that these effects do not change the radial buckling appreciably. This assumption is not a good one when the diffusion coefficient of the lattice is appreciably different from that of D_2O [18]. Furthermore, conventional two-group theory does not adequately predict the change in radial buckling [18]. It would thus appear advisable to measure directly the radial buckling in lattices which combine reflectors with air-filled housing tubes.

The critical substitution technique has been widely used at SRL as an alternative to the exponetials using comparable quantities of test fuel. In this technique the experiment begins with the measurement of the critical moderator height in a one-region loading of some standard lattice. Following this measurement, one or more of the central fuel assemblies are replaced by test fuel assemblies and the critical moderator height again measured. If this process is repeated one or more times with different numbers of test assemblies, it is usually referred to as a successive substitution technique. The buckling of the test lattice must be inferred from the measured critical moderator heights.

Of the random sources of error in this type of measurement, the most important are (a) uncertainty in the measurement of the moderator height itself, (b) uncertainty in the temperature changes in the lattice between critical runs, (c) uncertainty in the moderateur degradation between critical runs, and (d) quality control uncertainties in the test fuel assemblies. At SRL the relative moderator heights in the PDP are measured to ± 0.02 cm and the relative lattice temperatures to ± 0.03°C. These uncertainties contribute negligible error to the results. Frequent remeasurements of the one-region critical moderator height eliminate (c) as an important source of error. Our largest source of random error in this type of experiment has been in quality control of a small number of test fuel assemblies [19].

A more serious problem than random error is the avoidance of systematic errors in the conversion of measured moderator heights into lattice bucklings. A perturbation analysis described by PERSSON [15, 20] has enabled the Swedish group to obtain quite remarkable accuracy in interpreting successive substitution measurements. The use of this method of analysis at SRL has proved quite satisfactory over a large range of fuel assemblies, although quality control difficulties obscure systematic errors less than $0.05\,m^{-2}$ [19]. As an alternative the two-group, two-region critical equations for a single substitution measurement give satisfactory results if the mismatch in resonance escape probability between reference and test region is not large [19].

When fuel sufficient for an exponential loading is available, the same fuel used in critical successive substitution measurements in an appropriate host lattice will probably produce somewhat more accurate results with a somewhat greater expenditure of time. Such differences are not very important, however. The greatest usefulness of critical substitution measurements occurs when there is insufficient test fuel for an exponential loading. With the substitution technique, bucklings can be measured to within 0.10 to $0.15\,m^{-2}$ with as few as seven test assemblies (assuming a hexagonal lattice pattern).

There is no reason in principle why the substitution method could not be applied in a subcritical exponential and indeed such measurements have been performed at other sites [21, 22]. Random errors in the κ^2 measure-

ments become important in such measurements, however, and the accuracy of the results is lowered correspondingly.

The null reactivity method pioneered at the Physics Constants Testing Reactor (PCTR) and applied to exclusively heavy-water-moderated lattices at the Pawling Lattice Test Rig (PLATR) [23] requires smaller amounts of material than any of the buckling measurements described thus far. Somewhat offsetting this advantage is the more indirect nature of the measurement compared to the others just described. That is, after experimentally verifying that a given poisoned lattice has an infinite multiplication constant of unity, a two-step calculational process must follow to obtain the buckling of the unpoisoned lattice, which is the quantity of direct interest to the lattice designer. These steps are, of course, the calculation of the k_∞ of the lattice without poison and then the calculation of the buckling through a critical equation.

The agreement between measurements of bucklings at SRL and measurements of k_∞ by the null reactivity method at PCTR and PLATR [23] has been discussed by CRANDALL [6]. The essential conclusion was that no important systematic difference between the two types of measurements has been observed.

3. ANISOTROPIC AND VOID EFFECTS

Light-water lattices have an inherent anisotropy resulting from the large differences in diffusion coefficients between the fuel and H_2O. In general, this is not the case in heavy-water lattices where strong anisotropic effects are ordinarily encountered only when the lattices contain appreciable amounts of gas voids. As with the isotropic lattices, bucklings for the anisotropic heavy-water lattices are best measured in full-scale criticals. Examples of such measurements from the PDP programme are given in Table I and GRAVES et al. [10]. However, except for gas-cooled power-reactor lattices, the voided lattices are usually studied only for accident analysis and the accuracy of a full critical is usually not justified. Here buckling changes between the voided and unvoided lattice are usually obtained by critical substitution techniques [19]. Exponential measurements are ruled out if the lattices contain large void fractions, because of the anisotropy of the lattices.

However, simply determining changes in buckling between the voided and unvoided lattices is not sufficient. The primary usefulness of such data is in safety analyses of the consequences of the coolant boiling completely out of the fuel assemblies. In such analyses, the change in the effective multiplication constant, not the buckling, is the crucial factor. Hence changes in the migration area must also be known. Several methods which have been used at SRL to obtain this information experimentally are described below.

The first method of measuring migration areas involves positive period measurements in a critical facility. This technique, as applied to UO_2 rod cluster lattices, has been described previously [10, 6]. Briefly the procedure is as follows. The pile is held critical at a constant power for twenty

minutes or more to establish delayed neutron equilibrium and the critical moderator height is measured. The moderator is then pumped to a larger height, pile power being maintained constant by insertion of control rods. After the new moderator height has been measured the control rods are withdrawn rapidly, sending the pile on a positive period. The asymptotic period is obtained by monitoring the flux after a suitable [24] waiting time.

The change in vertical buckling can be computed from the moderator heights and known vertical extrapolation distances, while Δk_{eff} can be obtained from the measured value of the period plus an inhour relation. Values of vertical migration area are then deduced from $(-\Delta k_{eff}/\Delta B_z^2)$ and a (usually two-group) critical equation.

Errors in absolute values of migration areas obtained in this way depend not only on errors in the moderator height and period measurements, but also on uncertainties in the inhour relation and the critical equation. Such uncertainties are considerably larger in heavy-water lattices than in other lattices because of the importance of photoneutron production and the uncertainty in the escape probability from the fuel of gamma rays giving rise to photoneutrons. However, inhour equation uncertainties practically cancel out if one takes ratios of migration areas in lattices with D_2O in and D_2O out of the void channels. Such ratios are then subject only to the experimental uncertainties in moderator height and period measurements.

Previously reported results [10, 6] for this type of measurement in the PDP agreed rather well with predictions based on the Benoist theory [25,26]. The most recent PDP measurements of this type were made using the single natural-uranium metal tube shown in Fig. 1. Results are given in Table II. In this case the Benoist three-region model cannot be used directly to obtain calculated values. Instead, the Benoist theory was used to calculate the change in vertical diffusion coefficient on voiding the housing tube-fuel tube annulus alone, and the Behrens' theory [27] to calculate the change on voiding the space within the fuel tube alone. The two changes were simply added. Changes in effective thermal cross-section of the cell were computed using the P-3 approximation. The resulting calculated values of $L_z^2 + \tau_z$ are given in Table II for comparison with experiment. The agreement between experimental and calculated values is not bad, although outside of the assigned experimental error.

A less time consuming and in some ways more satisfactory approach to the problem of measuring lattice anisotropy effects lies in determining changes in diffusion coefficients rather than migration areas. Changes in both the radial and vertical one-group diffusion coefficients following D_2O coolant loss have been measured by this technique in the PDP. In the vertical measurement a single test assembly is placed in the central lattice position of the PDP with the rest of the pile containing reference fuel assemblies of well-known properties. The critical moderator height is then measured with various levels of D_2O coolant in the test assembly housing. In the corresponding radial measurement critical moderator heights are measured with coolant in and out of the test housing and with the test assembly placed in lattice positions at various radii in the pile. Remote expulsion of coolant must be used to take full advantage of the potential sensitivity of the method. Both sets of measurements are analysed by perturbation theory [20] to obtain $\delta D_z/D$ and $\delta D_r/D$. Lattice anisotropy can

TABLE II

PERIOD MEASUREMENTS

Single tube assembly, 9.33-in lattice pitch

Change in pile height (cm)	$-\Delta B_z^2$ (m^{-2})	Doubling time (s)	Experimental* $-\Delta k_{eff}/\Delta B_z^2$ (cm^2)	Experimental* $L_z^2 + \tau_z$ (cm^2)	Calculated $L_z^2 + \tau_z$ (cm^2)
Air filled assemblies					
1.87	0.0294	52	316 ± 5		
1.63	0.0256	61	325 ± 5		
1.46	0.0230	70	324 ± 5		
1.32	0.0208	80	328 ± 6		
1.08	0.0170	101	334 ± 7		
1.03	0.0162	109	330 ± 7		
			Average 326 ± 2.5	357 ± 2.5	360
D_2O filled assemblies					
1.46	0.0403	52	230 ± 4		
1.44	0.0398	52	232 ± 4		
1.23	0.0340	64	235 ± 4		
1.13	0.0313	74	230 ± 4		
1.12	0.0308	74	233 ± 4		
0.97	0.0269	87	238 ± 5		
0.97	0.0268	87	238 ± 5		
0.78	0.0215	113	241 ± 6		
			Average 235 ± 2.3	256 ± 2.3	245
$\frac{(L_z^2 + \tau)\text{ air filled}}{(L_z^2 + \tau)\ D_2O\text{ filled}}$				1.39 ± 0.04	1.47

* Assigned errors based upon known random errors only and do not include possible systematic errors in the experimental method or the period-reactivity relationship.

be obtained from these values. This method, as applied to UO_2 rod clusters, has been discussed in detail previously [19, 6].

Results are now available for changes in vertical one-group diffusion coefficients over a rather wide range of UO_2 tubular assemblies at two triangular lattice pitches, 9.33 in and 11.10 in. Cross-sections of the fuel assemblies are shown in Fig. 4. The natural UO_2 within the aluminium tubes

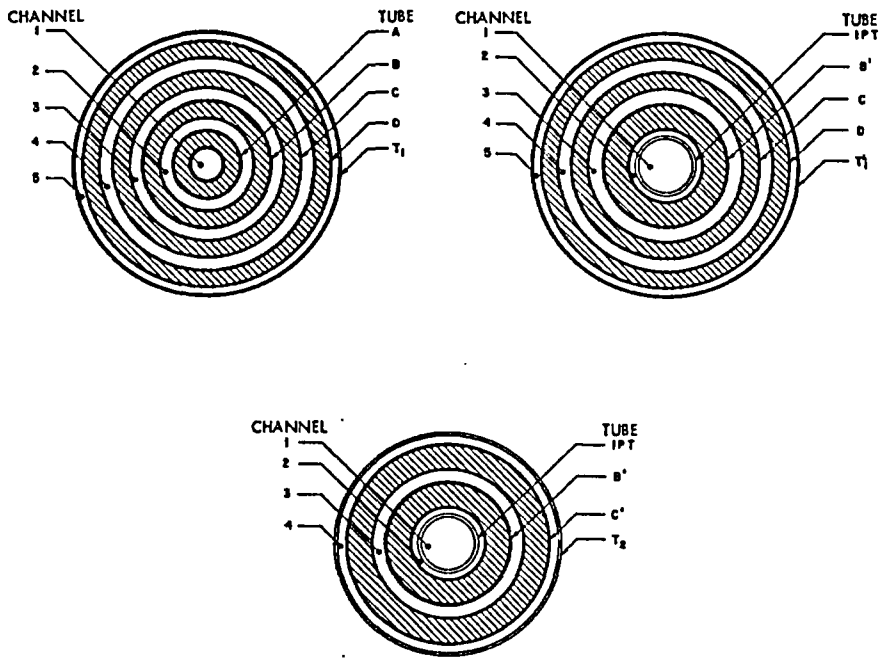

Fig. 4

Cross-sections of UO_2 tube assemblies

Tube	O.D. Clad. (in)	I.D. Clad. (in)	Material	Density (g/cm^3)
A	1.12	0.50	UO_2	8.896
B	2.10	1.48	UO_2	8.849
C	3.08	2.46	UO_2	8.872
D	4.06	3.44	UO_2	8.904
T_1	4.38 (O.D.)	4.30 (I.D.)	6061 Al	
IPT	0.97 (O.D.)	0.89 (I.D.)	1100 Al	
B'	2.10	1.18	UO_2	8.928
C'	3.38	2.46	UO_2	8.868
T_2	3.70 (O.D.)	3.62 (I.D.)	6061 Al	

NOTE: All cladding - 0.030 in thick, 1100 Al
ABCD oxide - 0.250 in thick
B'C' oxide - 0.400 in thick

was vibratorily compacted to a density of 8.9 g/cm^3. The assemblies were constructed to permit the partial or total expulsion of coolant from any coolant channel or combination of channels by compressed helium. The results obtained are plotted in Fig. 5 against void fraction in the cell. In principle, of course, the values of $\delta D_z/D$ are not a single valued function of the cell void fraction, but for the small void fractions involved in these assemblies the assumption is justified in practice.

Two calculated curves are also given in Fig. 5. The lower one was computed by homogenizing transport cross-sections. The resultant expression is $\delta D/D = X/(1-X)$ where X is the void fraction (ratio of void volume to cell volume). Since this method ignores streaming, $\delta D/D$ is underestimated. The higher curve is based on the Benoist model [25, 26] and assumes that $\delta D/D$ can be computed for each channel individually and the results added. The agreement between this latter curve and the experimental points is quite adequate.

Another type of anisotropy measurement, this time again yielding the change in migration area, involves only measurements of buckling changes. First, the buckling change on voiding the test assembly housings is measured by the critical substitution technique. Then the fuel assemblies are poisoned

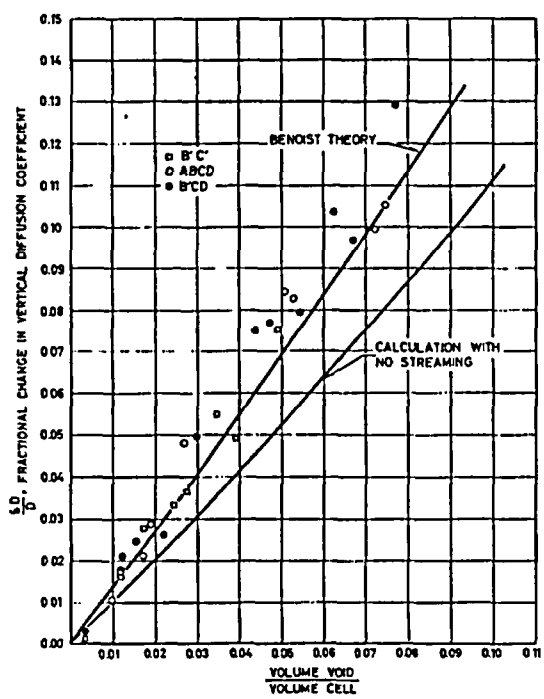

Fig. 5

Change in vertical diffusion coefficient on voiding coolant channels in UO_2 tube clusters

down and the buckling change remeasured. It is important that the poison be introduced quite close to the fuel, so that changes in flux ratios between poison and fuel on expelling the coolant can be reliably calculated by P-3 or other means. For tubular assemblies, copper sheet is convenient. Using one-group theory it is then possible to set up two simultaneous equations in two unknowns, Δk_∞ and ΔM^2 on voiding, and solve for these. The technique has been described in detail [28]. It has been used both with tubular and cluster type fuel assemblies at SRL. Our general conclusions on this method are that it is feasible but rather laborious and appears to offer no particular advantages over the perturbation method of obtaining diffusion coefficient changes already discussed.

Although the perturbation method yields values of lattice anisotropy, it would be desirable to have at least a few examples of lattice anisotropy measurements made in a more direct manner. The most direct method of measuring anisotropy, and therefore the one least subject to systematic error, would involve measuring the geometrical buckling of a lattice at critical in at least two different geometric configurations. A co-operative programme with CEA-Saclay is presently underway at SRL to make precisely this measurement in a highly anisotropic lattice. The fuel assembly is a cluster of 19 half-inch diameter UO_2 rods on a 0.650-in centre-to-centre spacing, contained in a 5-in outer diam. air-filled aluminium housing. The lattice pattern is square with a 9.09-in pitch. The identical fuel assemblies on a 9.33-in triangular pitch were previously used in anisotropy measurements by the perturbation techniques and yielded a ratio of vertical to radial diffusion coefficient of 1.20 [6]. Radial and vertical buckling measurements at critical are being made on the square lattice, first using the full radial size of the PDP and then a greatly reduced radius. The results should permit the ratios of vertical to radial diffusion coefficients to be specified to within ± 0.03. Perturbation measurements are also being made for comparison.

This same direct measurement of anisotropy can be accomplished by comparing results obtained in two different exponentials of greatly different radial bucklings. Such a comparison was made as part of an exchange programme between A.B. Atomenergi, Sweden, and SRL. The fuel assemblies consisted of four coaxial uranium metal tubes in aluminium pressure tubes. Buckling measurements were made with D_2O and with air within the housings in the 1-m diam. exponential ZEBRA [16] and later in the 1.52-m diam. SE. Data on the ZEBRA measurements have been reported by A.B. Atomenergi [29]. The comparison has been summarized by ROGERS [30]. The resulting anisotropies are plotted in Fig. 6.

4. EVALUATION OF CONTROL SYSTEMS

Two major questions arise in connection with reactor physics studies of control systems: the control system worth and the flux perturbations that it can introduce. If the control pattern is regular within the lattice, then the question of worth can be answered most conveniently by exponential measurements. Care must be exercised in analysing the results, however, as shown by the following illustration.

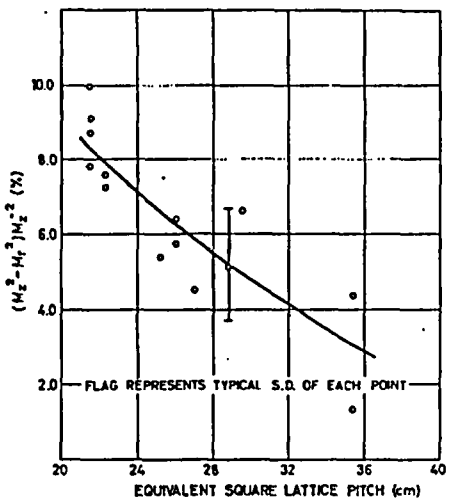

Fig.6

Anisotropy in migration area
Air-filled assemblies

An example of a lattice used for control rod measurements in the SE [31] is shown in Fig. 7. The triangular lattice pitch was 7 in. At this pitch, 61 lattice positions fall within the SE tank wall. Seven lattice positions were occupied with clusters of control rods as shown. This lattice pattern has been discussed previously in another connection [32]. Values of κ^2 were measured with no control rods in place, and then with various combinations of control rods in the clusters. To a first approximation, the buckling worth of any control rod combination is simply the difference between the κ^2 measured in that case and the κ^2 with no rods in place. To obtain a more

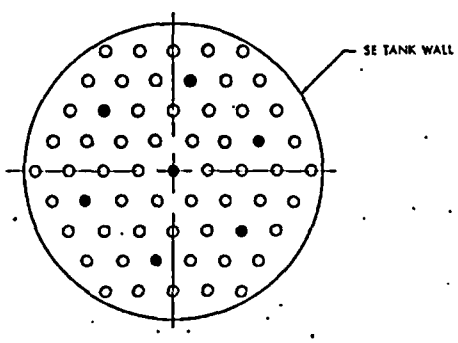

Fig.7

Lattice used in control rod worth measurements in the SE
O Fuel assemblies
● Control clusters

accurate result, one must look more critically at the difference between the exponential loading and the loading which is really of interest: i.e. a large section of lattice with exactly a six-to-one ratio of fuel to control clusters, in an approximately flat radial flux ($B_r^2 \sim 0$). It is evident that there are two effects in the exponential loading which would not be present in a larger uniform loading in a flat flux: (a) There are twelve extra fuel assemblies in the outer part of the exponential loading over and above the part of the lattice that has a six-to-one fuel-to-control ratio; and (b) The control pattern is centred in a highly buckled flux. The first effect will make the "first approximation" result underestimate the rod worths, while the second effect will make it overestimate the worths.

In analysing the SE experiment, the first step in taking account of these differences was to perform a two-group two-region calculation to obtain the buckling of the portion of the lattice with an exact six-to-one fuel-to-control ratio. The region comprising the inner 49 lattice positions was cylindricized. The region from this boundary to the extrapolated tank boundary was assumed to be filled with a lattice in which every lattice position was occupied by fuel. The buckling of such a lattice was known from previous experiments [31]. From calculated two-group parameters and measured values of κ^2, the effective material buckling of the inner region was computed. This buckling then had to be corrected to that which the lattice would have in a radially flat flux. The latter correction is most conveniently made by assuming that only the thermal utilization is affected and calculating the change in thermal utilization. It can easily be shown, if one ignores moderator absorption, that for this lattice, centred on a control cluster,

$$\frac{f-f'}{f} = (1-f)\,\frac{6\Sigma' J_0(B_r r) - \Sigma J_0(B_r r)}{f\Sigma J_0(B_r r) + 6(1-f)\Sigma' J_0(B_r r)}, \tag{1}$$

where f is ratio of fuel absorption to fuel-plus-control absorption in a radially flat flux, f' is the same quantity in a flux having a radial buckling of B_r^2, r is the distance from the central control cluster, Σ is the summation over the lattice positions at which fuel assemblies are located, and Σ' is the summation over the lattice positions at which control clusters are located. Calculated lattice parameters were used to convert the results of Eq. (1) to a buckling correction to be made to the "first approximation" values of rod worths. The final correction curve is shown in Fig. 8. From the direction of the correction it is evident that the favourable position of the control system, with respect to the centre of symmetry of the flux, was more important than the extra 12 fuel assemblies. The corrected rod worths were in closer agreement with critical facility results than the uncorrected ones [33].

The purpose of presenting the above example was to indicate that exponential measurements to determine the worth of control systems must be interpreted with some care even if the control pattern is quite regular. If the pattern is only slightly irregular, statistical weight arguments may permit proper analysis of exponential results. For really irregular lattices, however, one must resort to a mock-up in a critical facility. An example of such experiments in which the control system played an important part

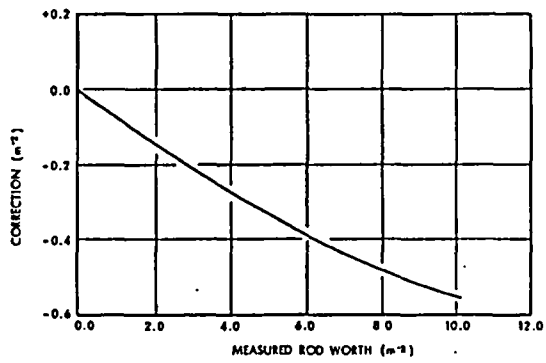

Fig. 8

Calculated correction to raw control rod worths measured in SE

is the set of measurements made in the PDP on a mock-up of the lattice of the Heavy Water Components Test Reactor (HWCTR) [34].

As one moves from the area of control system worths to the flux perturbations that the control systems can produce, the only alternative to critical experiments becomes calculation. The need for direct measurements in such an inhomogeneous lattice as that of the HWCTR [34] is obvious. However, these measurements can also be important for much more regular lattices. This need is particularly acute if one looks on the control system of a power reactor not as a producer of undesirable flux perturbations, but rather as a powerful means of flattening the flux distribution both radially and vertically and thus achieving a considerably higher total pile power under the same heat flux limitations. Such control systems have to be rather complex, and could lead to rather unexpected flux shapes if not used carefully. An example of such an effect was observed in the PDP some time ago. A lattice similar to that shown in Fig. 7 was loaded into the PDP, completely filling the tank. The control rods were placed so as to be slightly (~2 cm) off the theoretical lattice positions, and all in the same direction. The over-all pile flux was rather badly tilted as a result. Fluxes in many lattice positions were 20% higher than the fluxes at the corresponding positions on the opposite side of the pile [35].

5. TEMPERATURE COEFFICIENTS

It is rarely possible, in exponential or zero-power critical facilities, to measure directly the reactivity changes that would occur as the result of the non-uniform temperature changes that would obtain in the operation of a high-powered reactor. What is usually obtained by a temperature coefficient measurement in a zero-power facility is the change in lattice buckling as the lattice is heated uniformly. With natural-uranium systems in which there are no poisonous (target) materials, however, such measurements are usually sufficient to predict the actual temperature coefficient of an operating high-power reactor. The work is

most conveniently performed in an exponential facility because of the smaller quantities of heavy water involved. At SRL measurements up to about 90°C are carried out in the SE [3] while measurements up to 215°C are carried out in a pressurized facility, the PSE [4]. Buckling measurements at various temperatures are straightforward and no special techniques are required. An example of such measurements at SRL involved fuel assemblies for the Swedish R3/Adam reactor [36].

The agreement of experiment with calculation for natural-uranium lattices seems adequate for practical purposes [6] although the dependence of η on temperature remains uncertain.

Another type of experiment in which the small amount of heavy water involved gives the exponential an even more obvious advantage over a critical involves measuring the reactivity effects of contamination of heavy water with light water. Measurements in the SE have involved moderator purities ranging from 99.8 mol.% D_2O down to 92% D_2O [32].

6. MIXED LATTICES

Actual reactors rarely use the simple uniform lattices to which the exponentials basically apply. The most obvious lattice irregularity is the control system. The interpretation of exponential experiments in this case has already been discussed. Additional lattice irregularities appear in lattices which incorporate nuclear superheat, "spikes", or isotope production. In heavy-water exponentials of conventional size, it would usually not be possible to fit an integral number of the "supercells" which repeat the lattice pattern into the tank. In addition the measured value of κ^2 is sensitive to how the lattice is centred in the tank. For such lattices, critical experiments provide more easily interpretable measurements of reactivity.

There are two quite different sets of circumstances which have given rise to critical experiments with mixed loadings at SRL: (a) A specific lattice of a heterogeneous nature has been designed on the basis of calculation, but it is clear that the state of the art of calculation is not high enough to depend exclusively on calculation, a close mock-up is therefore assembled in a critical facility; and (b) it is desired to test fundamental methods of calculating the flux ratios and criticality of mixed loadings in general.

An example of measurements of type (a) is the set of experiments made in the PDP on a nuclear mock-up of the HWCTR [34]. A lattice diagram of the HWCTR is shown in Fig. 9. A glance at this diagram makes it clear that the uniform lattice calculation methods generally used in connection with heavy-water lattice physics are inapplicable here. The mock-up experiments served not only to prove the feasibility of the design and provide much information necessary to satisfactory operation, but also provided a wealth of experimental data on which to test calculational methods. The chief calculational method used thus far by the HWCTR group is based on the Westinghouse PDQ-3 code [37] and the auxiliary codes necessary to provide input information for it. Generally satisfactory agreement with experiment has resulted [38].

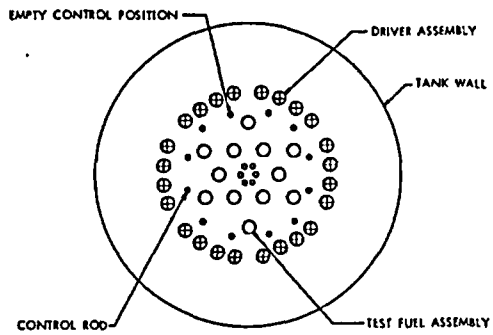

Fig.9

HWCTR lattice

Such a lattice as that of the HWCTR is not ideal, however, for providing a test of theory. It is too complex, with too much room for accidental compensating errors in the calculation. To provide a good test of calculational methods, more precise critical experiments with simpler heterogeneous lattices would seem preferable. Such a set of experiments has recently been completed in the PDP.

The philosophy behind this short set of experiments was to provide critical moderator heights and flux ratio measurements in a number of mixed lattices chosen on the basis of availability of fuel components and on the convenience of the predicted critical moderator heights. Cross-sections and dimensions of fuel and poison assemblies used in those experiments are shown in Fig.10. All lattices were assembled at a 7-in triangular pitch in the central 85 positions in the PDP. These 85 positions were contained within a boundary of 36 poison rods. The five lattices studied are shown in Figs.11-15. The inner radius of the PDP tank wall is 247 cm, so that the reflector beyond the poison rod boundary was effectively infinite.

Vertical flux traverses to determine the vertical extrapolation distances were made by irradiating gold pins. These extrapolation distances were applied to the critical moderator heights measured when the gold pins with their holders were removed from the lattice. A small correction to the critical vertical bucklings thus obtained accounted for the presence in the lattice of a few aluminium guide tubes for control rods (the rods themselves always being completely removed from the lattice at the time of the measurement of the critical moderator height). To make this correction the worth of a few representative guide tubes was measured by inserting extra tubes, and the worth of the tubes already present was inferred from statistical weights. These standard techniques have been described in more detail previously [10]. The corrected critical vertical bucklings then correspond to the idealized lattice diagrams of Figs.11-15, a moderator purity of 99.59 mol.% and a temperature of 22°C.

During the irradiation to determine vertical extrapolation distances, flux ratios were also measured between lattice components of different types.

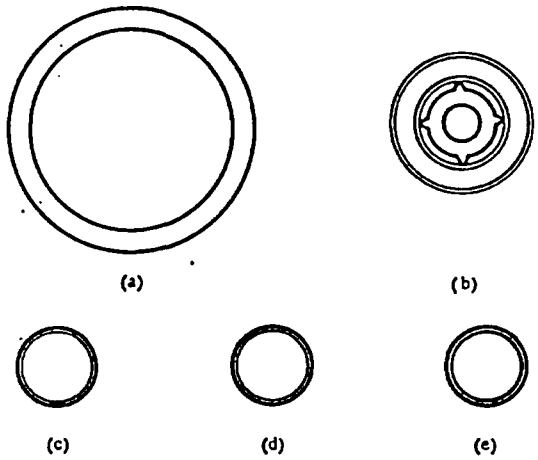

Fig. 10

Components used in mixed lattice experiments

(a) Natural uranium metal tube
Density 18.9 g/cm^3
Outer diameter 3.500 in
Inner diameter 2.860 in

(b) Clad uranium metal tube
Enrichment 0.947 wt.% U^{235}
Density 18.9 g/cm^3
Cladding and inner support tube material; 1100 aluminium
Clad outer diameter 1.974 in, inner diameter 1.166 in
Bare fuel outer diameter 1.914 in, inner diameter 1.226 in
Support tube outer diameter 0.832 in, inner diameter 0.532 in
Support tube rib diameter 1.146 in

(c) Natural uranium metal rod
Density 18.9 g/cm^3
Rod diameter 0.998 in
Sheath material; 1100 aluminium
Sheath outer diameter 1.090 in, inner diameter 1.026 in
Air between sheath and fuel

(d) Enriched uranium-aluminium alloy rod
Enrichment > 90% U^{235}
5.0 wt.% U^{235} in aluminium
Density 2.82 g/cm^3
Rod diameter 1.000 in
Sheath material; 1100 aluminium
Sheath outer diameter 1.090 in, inner diameter 1.026 in
Air between sheath and fuel

(e) Natural lithium-aluminium alloy rod
Lithium in aluminium wt.% 4.9
Density of alloy 2.35 g/cm^3
Rod diameter 0.930 in
Cladding and sheath material; 1100 aluminium
Cladding outer diameter 1.005 in, inner diameter 0.930 in
Sheath outer diameter 1.090 in, inner diameter 1.026 in
Air between sheath and clad rod

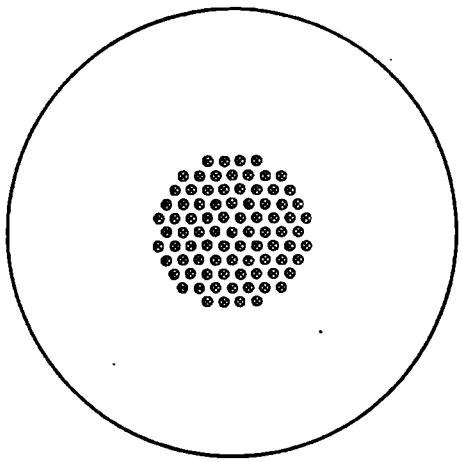

Fig. 11

Pile loading number 1
⊗ = (c), see Fig. 10

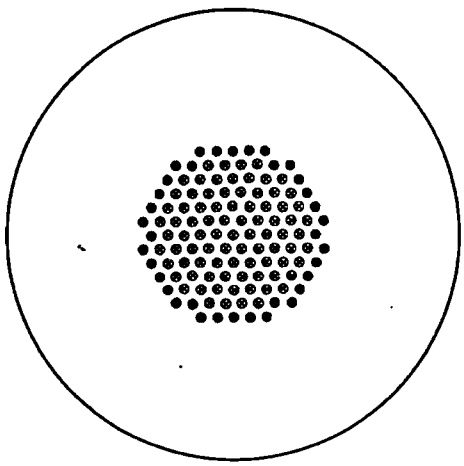

Fig. 12

Pile loading number 2
● = (e), ⊗ = (c), see Fig. 10

Copper foils machined to the same dimensions as the various fuel assemblies were enclosed in aluminium catcher foils and installed in their respective fuel assemblies. They were then irradiated and subsequently cut up and counted. Cadmium-covered copper foils placed at a different level in the

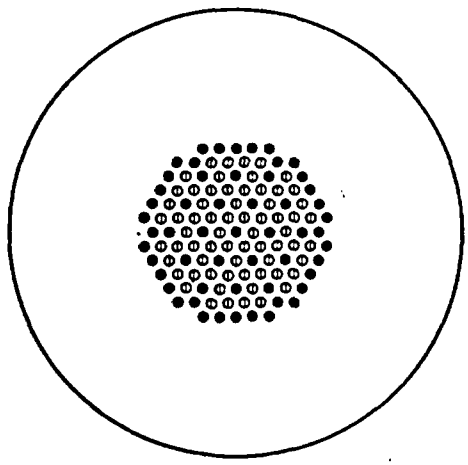

Fig. 13

Pile loading number 3
● = (e), ⦶ = (d), see Fig. 10

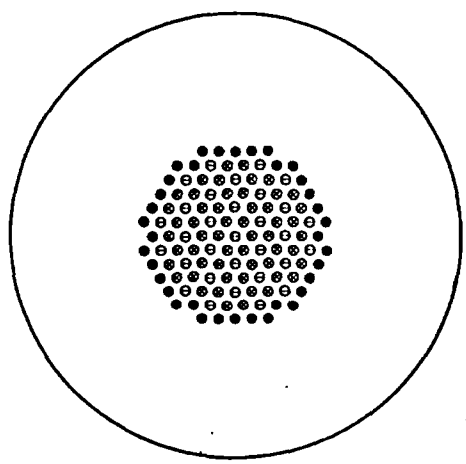

Fig. 14

Pile loading number 4
● = (e), ⊗ = (c), ⊖ = (a), see Fig. 10

lattice permitted epicadmium activations to be subtracted off the bare foil activities. A correction for the over-all radial flux shape in the pile then yielded the ratios of thermal fluxes averaged over the different lattice components in a flat radial flux. Results of these experiments are given in Table III.

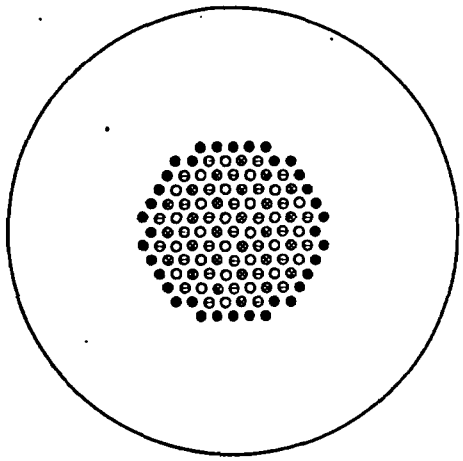

Fig.15

Pile loading number 5
● = (e), ⊗ = (c), O = (b), ⊖ = (a), see Fig.10

TABLE III

RESULTS OF MIXED LATTICE EXPERIMENTS

Lattice number [a]	Critical vertical buckling (m^{-2})		Average subcadmium neutron density ratios [b]	Average subcadmium neutron density ratios [b]
1	2.69		-	-
2	0.98		-	-
3	0.97	(d)/(e) [c]	1.63	0.676
4	2.23	(a)/(c)	0.828	3.37
5	3.41	(a)/(b)	1.04	1.61
		(a)/(c)	0.796	3.24

[a] See Figs.11-15

[b] In assembly (b), the flux and absorption refers to the fuel alone, not cladding or support tube. In assemblies (c) and (d), the flux and absorption refers to the one-inch diameter components, not including the aluminium containing tube. In assembly (e), they refer to the Li-Al alloy alone. Ratios are corrected to an over-all flat radial flux.

[c] See Fig.10

There are two general methods of calculation which should permit computation of the above results. One is the heterogeneous reactor theory methods associated with the names of FEINBERG [39] and GALANIN [40], while the other involves two-dimensional diffusion theory codes, such as PDQ-3 [37]. Both of these methods will be tested against the data in Table III, but calculational results are not yet available.

7. LIGHT-WATER SUBCRITICALITY STUDIES OF FUEL FOR HEAVY-WATER-MODERATED REACTOR

Most reactor physics studies with heavy water have involved the use of natural-uranium fuel. However, economic studies [41] have shown that improved operation can be achieved by slight enrichment of the natural-uranium fuel with U^{235}. The recycling of plutonium in heavy-water reactors containing predominately natural-uranium fuel is also attractive economically. Criticality problems will exist in the manufacturing, shipping and storage of U^{235}-enriched or plutonium-bearing fuel. A heavy-water exponential is an ideal facility for measuring the light-water reactivity of various arrangements because the usual size of an exponential (1 to 1.5 m diameter) provides a facility with an effectively infinite reflector of H_2O.

The data are all obtained using exponential techniques. The method used at SRL is outlined below.

(1) The test fuel array is added into the SE tank without any moderator present.

(2) The neutron multiplication is monitored as H_2O is added to the lattice to determine that it is in fact subcritical. Safety rods and safety circuits are provided which are actuated by signals from the neutron monitors.

(3) Exponential measurements of κ^2 are obtained for the lattice being studied. Regular rectangular or triangular lattice arrays are used.

(4) The transverse buckling is determined by measuring the vertical buckling for two or more different sizes of the same lattice arrangement. The material buckling is assumed constant for the different sized lattices. In this way it is possible to determine the value of the reflector savings and hence the transverse buckling that is consistent with all of the measurements.

(5) Addition of the vertical or exponential buckling and the transverse buckling gives the material buckling,

$$B_m^2 = B_{x,y}^2 - \kappa_z^2.$$

Maximum values of buckling as high as 90 m^{-2} have been studied in the SE for 3-in diam., 3 wt.% U^{235} uranium metal rods. Maximum bucklings as low as 2 to 3 m^{-2} have been measured for fuel of lower enrichment. Bucklings in the lower range cannot conveniently be measured in light-water criticals because the amount of material would be extremely large. The exponential has the same inherent advantages as mentioned previously for D_2O reactor-physics studies. Bucklings in the higher ranges can be

measured in critical facilities especially designed for that purpose, but in many cases the data are not as easy to interpret theoretically because regularly shaped lattices are not always achieved at criticality.

Experience at Savannah River has shown that the exponential technique outlined above is very useful, does not require additional facilities and the exponential facility can readily be converted for D_2O or H_2O measurements, as the need arises.

REFERENCES

[1] DUNKLEE, A.E., The Heavy Water System of the Process Development Pile, USAEC Rpt. DP-567 (1961).

[2] BAUMANN, N.P., Process Development Pile Measurements of Parameters of Natural Uranium in Heavy Water, USAEC Rpt. DP-407 (1959).

[3] TOWLER, O.A., Jr. and WADE, J.W., Exponential Measurements in Heavy Water Systems, Chem. Eng. Progr. Symp. Ser. 52 (1956) 177-81.

[4] HENNELLY, E.J., Pressurized Subcritical Facility, Nucleonics 19 3 (1961) 104-5.

[5] CRANDALL, J.L., Status of the United States Effort in D_2O Reactor Physics, USAEC Rpt. DP-787 (1962).

[6] CRANDALL, J.L., Efficacy of Experimental Physics Studies on Heavy Water Lattices, USAEC Rpt. DP-833 (1963).

[7] AXTMANN, R.C. et al., Initial Operation of the Standard Pile, USAEC Rpt. DP-32 (1953).

[8] HURLEY, T.J., Jr., FIKE, H.R. and O'NEILL, G.F., Experimental Bucklings of Heavy Water Moderated Lattices of Natural Uranium Metal Rod Clusters, Nucl. Sci. Engng 12 (1962) 341-7.

[9] HURLEY, T.J., Jr., Measured Lattice Parameters for Natural Uranium Metal Rod Lattices in D_2O, USAEC Rpt. DP-777 (1963).

[10] GRAVES, W.E., O'NEILL, G.F. and FIKE, H.R., Experimental Bucklings and Void Effects in Heavy Water Lattices of Natural Uranium Oxide Rod Clusters, Nucl. Sci. Engng 16 (1963) 186-95.

[11] REDMAN, W.C., Recent Experience with D_2O Subcritical Assemblies, Proc. University Subcritical Assemblies Conf., USAEC Rpt. TID-7619 (1961).

[12] WINGFIELD, E.C. and HENNELLY, E.J., Exponential Measurements of Natural Uranium Rods in Heavy Water and Comparisons with Critical Experiments, Nucl. Sci. Engng 12 (1962) 348-58.

[13] WINGFIELD, E.C., unpublished (see [6]).

[14] LUTZ, H.R. and MEIER, R., private communication.

[15] PERSSON, R., HELLSTRAND, E. and JOHANSSON, E., Experimental reactor physics work on heavy water lattices in Sweden, Heavy Water Lattices; Second Panel Report, Technical Reports Series No.20, IAEA, Vienna (1963) 305.

[16] PERSSON, R. and BLOMSJÖ, E., Exponential Pile Measurements with Natural Uranium and Heavy Water, J. nucl. Energy 3 (1956) 188-206.

[17] BARRETT, L.G. and MORTENSON, J.H., Exponential Experiments on Lattices Moderated by D_2O-H_2O Mixtures, USAEC Rpt. BAW-1232 (1962).

[18] ROGERS, W.B., Jr., Effects of Reflectors and Voids on Exponential Measurements in D_2O Natural Uranium Lattices, Trans. Amer. nucl. Soc. 5 1 (1962) 74.

[19] GRAVES, W.E., Analysis of the Substitution Technique for the Determination of D_2O Lattice Bucklings, USAEC Rpt. DP-832 (1963).

[20] PERSSON, R., One-Group Perturbation Theory Applied to Substitution Measurements with Void, A.B. Atomenergi Rpt. RFX-74 (1961).

[21] PERSSON, R. et al., Exponential Experiments on Heavy Water Natural Uranium Metal and Oxide Lattices, Proc. 2nd. UN Int. Conf. PUAE 12 (1958) 364-73.

[22] LUTZ, H., MEIER, R. and WINKLER, W., Unterkritische Zweizonenanordnungen, Neue Technik 3 6 (1961) 343-51.

[23] BROOKS, W.L. et al., Pawling Lattice Test Rig - Test Report No.1, PLATR-PCTR Comparison, USAEC Rpt. NDA-2131-40 (1961).

[24] TOPPEL, B.J., Sources of Error in Reactivity Determinations by Means of Asymptotic Period Measurements, Nucl. Sci. Engng 5 (1959) 88-98.

[25] BENOIST, P., General Formulation of the Diffusion Coefficient in a Heterogeneous Medium Which May Contain Cavities, CEA Rpt. SPM-522 (1958).
[26] BENOIST, P., A Simplified New Expression for the Radial Diffusion Coefficient for Fuelled Channels, CEA Rpt. SPM-710 (1962).
[27] BEHRENS, D.J., The Migration Length of Neutrons in a Reactor, U.K.A.E.A. Rpt. AERE T/R 877 (1956).
[28] DUNKLEE, A.E., PDP Measurements of Coolant Void Reactivity Coefficients, USAEC Rpt. DP-641 (1962).
[29] ERLANDSSON, I. and PERSSON, R., Exponential Measurements on the SRL Four-Tube Fuel Assemblies with Void, A.B. Atomenergi Rpt. RFX-89 (1962).
[30] ROGERS, W.B., Jr., Experimental Determination of Anisotropy in D_2O-Uranium Lattices Containing Voids, Trans. Amer. nucl. Soc. 6 1 (1963) 51-2.
[31] FIKE, H.R., unpublished.
[32] FINN, B.S. and WADE, J.W., Effects of the Contamination by Light Water on Lattices of Natural Uranium Rods in Heavy Water, Nucl. Sci. Engng 7 (1960) 93-6.
[33] TOPP, S.V., unpublished.
[34] GRAVES, W.E., Physics Data from a Mockup of the HWCTR Lattice in the PDP, USAEC Rpt, DP-457 (1960).
[35] CRANDALL, J.L. et al., unpublished.
[36] BAUMANN, N.P., GRAVES, W.E., HENNELLY, E.J. and O'NEILL, G.F., High Temperature Exponential Measurements and Room Temperature Critical Substitution Measurements on Swedish R3/Adam Fuel Assemblies in Heavy Water, Nukleonik 4 5 (1962) 200-8.
[37] CADWELL, W.R., PDQ-3, A Program for the Solution of the Neutron-Diffusion Equations in Two Dimensions on the IBM-704, USAEC Rpt. WAPD-T17-179 (1960).
[38] RUSCHE, B.C., private communication.
[39] FEINBERG, S.M., Heterogeneous Methods for Calculating Reactors; Survey of Results and Comparison with Experiment, Proc. UN Int. Conf. PUAE 5 (1956) 484-500.
[40] GALANIN, A.D., The Thermal Coefficient in a Heterogeneous Reactor, Proc. UN Int. Conf. PUAE 5 (1956) 477-83.
[41] BABCOCK, D.F. et al., An Evaluation of Heavy Water Moderated Power Reactors, USAEC Rpt. DP-830 (1963).

DISCUSSION

R. HEINEMAN: It is interesting to note that many laboratories have recently had to re-examine their assumptions concerning the radial (or lateral) bucklings in their experimental facilities. Three years ago, Dr. D.E. Wood at Hanford found discrepancies in the lateral bucklings in graphite exponential piles. These troubles can be interpreted as changes in the extrapolation distance with changes in reflector thickness, lattice heterogeneity, and position of the flux detector in the lattice cell. All the work on this subject is described in the Nuclear Physics Research Quarterly Report* of Hanford Laboratories. The difficulties encountered at the Savannah River Laboratory in comparing critical and exponential results can evidently be explained in terms of variations in radial buckling. The paper presented by Dr. Hellens** describes the corrections to previously reported results which are needed to account for non-asymptotic radial bucklings. The one presented by Dr. Green gives results recently obtained at Chalk River on variations in radial buckling. The troubles met with in

* HANFORD ATOMIC PRODUCTS OPERATION, Rep.HW-64866 (1960) 151 pp.

** ANDERSON, E. and HELLENS, R.L., "Some problems in the interpretation of exponential experiments", these Proceedings II.

these cases may be due to different causes but, in any event, the situation seems to be that the errors in bucklings derived in earlier years are all larger than had been thought. It is interesting that these findings are coming out at the same time.

I should also like to comment on your spoken remarks concerning buckling and k_∞ measurements. I think it is fair to say that the reactor designer wants to know both these quantities. Primarily he wants to know how much larger than just critical the reactor must be, in order to ensure that the excess reactivity is sufficient to overcome long-term, isotopic changes in the fuel, to cope with temperature coefficients upon going to power, to overcome xenon transients, and to allow sufficient control rod insertion to ensure a shutdown margin in reactivity. If only one of the two quantities B^2 and k_∞ can be obtained, the error in the final reactivity balance will be smaller if B^2 is known for small systems with high leakage and if k_∞ is known for large systems with low neutron leakage.

G. BLAESSER: As regards the applicability of heterogeneous methods of reactor theory to the calculation of mixed lattices, I should like to mention that we did Feinberg-Galanin and PDQ-calculations in a study of the physics of the test reactor ESSOR, which has a configuration similar to that of the HWCTR. Both types of calculations agreed very well (even when we used a two-group kernel in the Feinberg-Galanin approach). We also used three-dimensional kernel-type calculations for control rod studies. Although no experimental checks are yet available, we feel quite confident about the reliability of these methods.

A.G. WARD: I was interested in Dr. Graves' comments, in his oral presentation, about flux shaping in large power reactors. In D_2O-moderated natural uranium reactors for power generation, fuel costs become high if absorbers are used to shape the flux. In our studies we have chosen, instead, to use the distribution of irradiated fuel as a means of controlling the flux shape. Precise computation of the flux shape for very large power reactors will subject our current methods of calculations to a severe test. Since instrumentation for detailed measurement of the power distribution is also costly, there is a strong incentive for relying as far as possible on calculation.

A. HITCHCOCK: In connection with Dr. Ward's remarks on the matter of shaping the flux by means of absorbers and other techniques, I should like to report that we recently made some comparisons between the methods of calculation used for this purpose in the AGR project in the United Kingdom and those used at the Oak Ridge EGCR project. In the calculations of the same system by the two different techniques, there were differences of up to approximately 20% in the power distribution of selected channels and differences of some 6-7% in the radial averaging factor. It is clear that there is still a good deal of work to be done in defining these methods of calculation. I am therefore extremely interested in the case where the Feinberg-Galanin and PDQ-calculations showed close agreement.

G. BLAESSER: We found that the maximum difference in k_∞ was about 1%.

DETERMINATION OF D_2O-2% ENRICHED URANIUM LATTICE PARAMETERS BY MEANS OF A CRITICAL SYSTEM

N. RAIŠIĆ, S. TAKAČ, H. MARKOVIĆ AND T. BOŠEVSKI
BORIS KIDRIČ INSTITUTE OF NUCLEAR SCIENCES, BELGRADE, YUGOSLAVIA

Abstract — Résumé — Аннотация — Resumen

DETERMINATION OF D_2O – 2% ENRICHED URANIUM LATTICE PARAMETERS BY MEANS OF A CRITICAL SYSTEM. The paper describes a series of experiments performed to determine the basic parameters of a D_2O-2% enriched-uranium lattice. The fuel elements were hollow cylinders, canned in aluminium and wetted by heavy water both on the inside and outside. The experiments were performed on the RB critical assembly of the Boris Kidrič Institute of Nuclear Sciences in Belgrade. The clean geometry of this system enables a rather simple theoretical interpretation of experimental results, and straightforward comparison with two-group diffusion-theory calculations.

Measurements performed for ten different lattice configurations included determination of buckling, water-level reactivity coefficient and disadvantage factors for thermal-and epithermal-neutron flux inside a reactor cell. Techniques for these measurements are described. The experimental data are then used to derive the lattice parameters defined by the four-factor formula and two-group diffusion-theory treatment of the reactor core. The results are compared with the standard calculations of the same parameters for measured lattice configurations. Deviations are found in the value of n and resonance integral for U^{238}. In conclusion, an analysis is made of the usefulness and accuracy of information obtained from critical experiments for design and exploitation of a research reactor, composed of D_2O and enriched uranium.

DÉTERMINATION DES PARAMÈTRES D'UN RÉSEAU URANIUM ENRICHI A 2%-EAU LOURDE AU MOYEN D'UN ENSEMBLE CRITIQUE. Les auteurs décrivent une série d'expériences qu'ils ont faites pour déterminer les paramètres fondamentaux d'un réseau uranium enrichi à 2%-eau lourde. Les éléments combustibles étaient des cylindres creux, gainés d'aluminium et baignant dans l'eau lourde, à l'intérieur comme à l'extérieur. Ils se sont servis de l'assemblage critique RB de l'Institut Boris Kidrič des sciences nucléaires à Belgrade. La géométrie de cet assemblage non empoisonné a permis d'interpréter le résultat expérimental à l'aide d'une théorie assez simple et de le comparer directement aux calculs faits par la théorie de la diffusion à deux groupes.

Les mesures, pour dix configurations de réseau différentes, comportaient la détermination du laplacien, du coefficient du niveau d'eau et des facteurs de désavantage pour le flux de neutrons thermiques et épithermiques à l'intérieur d'une cellule. Le mémoire décrit les méthodes de mesure. Les auteurs utilisent ensuite les données expérimentales pour en déduire les paramètres de réseau déterminés par le calcul du cœur du réacteur au moyen de la formule des quatre facteurs et dans une théorie de diffusion à deux groupes. Ils comparent ces résultats avec les calculs classiques des mêmes paramètres pour des configurations de réseau ayant fait l'objet de mesures. Ils ont constaté des écarts dans la valeur de n et de l'intégrale de résonance pour ^{238}U. En conclusion, les auteurs analysent l'utilité et l'exactitude des informations recueillies à l'aide des montages critiques en vue de l'étude et de l'exploitation d'un réacteur de recherche à uranium enrichi et eau lourde.

ОПРЕДЕЛЕНИЕ С ПОМОЩЬЮ КРИТИЧЕСКОЙ СИСТЕМЫ ПАРАМЕТРОВ РЕШЕТКИ С 2%-НЫМ ОБОГАЩЕНИЕМ УРАНА И С ЗАМЕДЛИТЕЛЕМ D_2O. Дается описание серии опытов, выполненных с целью определения основных параметров решетки с 2%-ным обогащением урана и с замедлителем в виде D_2O. Топливные элементы представляли собой полые цилиндры, покрытые алюминием и смоченные как снаружи, так и изнутри водой. Опыты проводились на критической сборке RB Института ядерных наук им. Бориса Кидрича в Белграде. Удобооптекаемая геометрическая форма этой системы дает возможность сравнительно просто теоретически объяснить результаты опытов и провести непосредственное готовое сравнение с расчетами двухгрупповой теории диффузии.

Измерения, выполненные для десяти различных конфигураций решетки, включали определение лапласиана, коэффициента реактивности уровня воды и блок-эффекта для потока тепловых и надтепловых нейтронов внутри камеры реактора. Описывается методика этих измерений. Данные опытов используются для выведения параметров решетки, определяемых по формуле четырех сомножителей и при применении к активной зоне реактора двухгрупповой теории диффузии. Результаты сравниваются со стандартными расчетами тех же параметров для измеряемых конфигураций решетки. Отмечаются отклонения в величине η и резонансного интеграла U-238. В заключение проводится анализ полезности и точности полученной в результате проведения критических экспериментов информации для проектирования и эксплуатации исследовательского реактора на обогащенном уране с тяжеловодным замедлителем.

DETERMINACIÓN, MEDIANTE UN CONJUNTO CRÍTICO, DE LOS PARÁMETROS DE UN RETICULADO DE D_2O Y URANIO ENRIQUECIDO AL 2%. En la memoria se describe una serie de experimentos efectuados con objeto de determinar los parámetros básicos de un reticulado de D_2O y uranio enriquecido al 2%. Los elementos combustibles consistían en cilindros huecos, revestidos de aluminio, con agua pesada en el interior y en el exterior. Los experimentos se realizaron en el conjunto crítico RB del Instituto de Ciencias Nucleares «Boris Kidrič» (Belgrado). La geometría sencilla de este conjunto facilita la interpretación teórica de los resultados experimentales, así como la comparación directa con cálculos efectuados según la teoría de difusión de dos grupos.

Entre las mediciones efectuadas para diez configuraciones diferentes de reticulado, figuraban la determinación del laplaciano, del coeficiente de reactividad del nivel de agua y de los factores de desventaja para un flujo de neutrones térmico y epitérmico dentro de una celda del reactor. En la memoria se describen las técnicas utilizadas en las mediciones. Los datos experimentales sirvieron a continuación para deducir los parámetros del reticulado, definidos por la fórmula de cuatro factores y el estudio matemático del cuerpo del reactor con arreglo a la teoría de difusión de dos grupos. Los resultados obtenidos se comparan con los valores corrientemente asignados a los mismos parámetros para configuraciones de reticulados medidos. Se presentan las desviaciones halladas en el valor de η y en la integral de resonancia para el ^{238}U. En conclusión, se analiza la utilidad y precisión de los datos obtenidos con los experimentos críticos para la construcción y explotación de un reactor de investigación de D_2O y uranio enriquecido.

1. INTRODUCTION

In order to specify the experimental techniques for the few standard measurements sufficient to give a consistent set of lattice parameters, a series of experiments were performed on the RB heavy-water zero-power reactor [1] using 2% enriched fuel elements of tubular shape. The results obtained were compared with the standard two-group diffusion theory calculation and the correlative data for basic nuclear constants, such as η, effective resonance integral etc., were determined.

One can expect that by using the input data chosen in such a way that the conventional calculation methods can be applied for a fairly exact determination of the lattice parameters necessary at the design stage of a research reactor.

It is known that this approach to the determination of basic lattice parameters is rather sophisticated. It is assumed that the standard calculation recipes are exact, if proper input data are given. According to the results published so far for different types of lattices, it is true for a rather narrow range of reactor core compositions and usually fails when complicated fuel element geometries, unusual core compositions or a high fuel-to-moderator ratio are used.

In this paper the experimental results as compared with the theory indicate that the above method can be used with a high degree of accuracy even for a complicated type of fuel element over a broad variety of lattice con-

figurations. The reactor parameters thus obtained are reliable for the optimization study concerning the criticality and the reactivity of the reactor core.

2. CHARACTERISTICS OF THE RB REACTOR

The RB reactor is an unshielded critical assembly intended mainly for lattice-parameter investigations in heavy-water systems. The reasons for constructing an unshielded critical system were the following:

(a) To allow clean critical experiments in a simple geometry;

(b) To provide flexibility in performing experiments even in cases where major changes in the core composition are to be made; and

(c) To reduce the time and cost of construction.

The present construction of the RB reactor satisfies most of these requirements. On the other hand, all efforts are made to protect the personnel and ensure the highest possible safety in reactor operation. When the reactor is operating, there is no admission to the reactor hall and all operations are performed from a shielded control room. In order to avoid high radiation levels in the reactor building and the radioactivity of the reactor core, the power for continuous operation is limited to 2 W. Short irradiations only are done at higher powers and these never exceed 10 W. This makes it possible to keep the radiation dose rate at the reactor tank as low as 10 mr/h when changes in the core are to be made.

When operating at the standard power of 2 W the thermal neutron flux at the reactor centre is about 2.5×10^7 n $cm^{-2}s^{-1}$, which allows neutron measurements in most experiments.

2.1. Reactor

The reactor tank is a cylindrical vessel with a flat bottom. The internal diameter is 199.86 cm and the height 230 cm. The bottom of the tank is made of 15-mm thick aluminium, while the thickness of the side wall is 10 mm. An aluminium lid strengthened by radial ridges tightly covers the reactor tank. The lid has a 50 mm × 1900 mm slot along the diameter which serves for neutron irradiations inside the reactor core. This slot can be hermetically shut with an easily movable cover.

The reactor tank is mounted on a platform and placed in the centre of a basin with dimensions 8000 cm × 8000 cm × 1500 cm. The aluminium structure supporting the reactor tank is designed for a working load of 15 t.

Two platforms supported by a separate structure are built around the reactor. These platforms are used by the personnel for all operations with the reactor core.

No additional reflectors or shields are built around the reactor core.

To allow a broad variety of investigation lattices, a changeable lattice pitch is procured by a system of fuel supporting plates. One plate is fixed at the bottom of the reactor tank and other about 20 cm below the lid, on top of the tank. The fuel elements are inserted in holes drilled in the plates. The system of holes gives a possibility of arranging about five different lattice configurations. At present square lattices are being investigated

and the existing holes in the plates allow an arrangement of the following configurations:

(a) Main pitch and integer multiples of the main pitch (na);
(b) Multiples of the main pitch with $\sqrt{2}$ and $n\sqrt{2}$; and
(c) A function of the main pitch of the form $\sqrt{(na)^2 + a^2}$, where a is the main pitch.

With three pairs of supporting plates it was possible to arrange the following lattices:

Main pitch (cm)	7		8		9	
na $\sqrt{2}$	9.9	19.8	11.3	22.7	12.7	25.4
na	14	21	16	24	18	
$\sqrt{(2a)^2 + a^2}$	15.6		17.9		20.1	

With a sufficient number of fuel elements it is possible to arrange a radially bare reactor system. In the axial direction the reactor is bare in most cases. This makes it possible to treat the reactor as a bare system in a large number of experiments. By approaching criticality, the bare systems with a buckling as low as $7.6 \times 10^{-4}\ m^{-1}$ can be investigated.

There are several facilities for reaching the interior of the reactor core. For neutron flux distribution measurements, dismountable horizontal and vertical channels passing through the reactor core are provided. The vertical channel is in the central position and can be used either for neutron flux distribution measurements or for sample oscillations in connection with oscillator work. The horizontal channel is at a height of 60 cm from the bottom of the tank and it can reach either the central axis or pass through the reactor. For neutron flux distribution measurements these channels are used in connection with various techniques applied. Normally for all measurements with micro-BF_3 or semi-conductor counters the measuring devices are moved along the experimental channels. When activation techniques are applied the foil holders are directly inserted in the channels.

For all experiments where the fuel should be reached, there is a 7-cm wide slot on the reactor lid. An additional opening on the tank lid serves to insert and remove specially prepared fuel elements for intracell measurements.

2.2. Heavy-water circulation system

When the reactor is not operating, the heavy water is stored in a storage tank with a capacity of 7 t: The tank is located in an underground room. The circulation of the moderator from the storage tank to the reactor tank and back is realized through a stainless-steel pipe system. A canned rotor pump is used to pump the moderator into the reactor tank through a tube 28 mm in diameter. By reversing the direction of rotation two pumping speeds are possible, i.e. 2.5 cm/min and 0.8 cm/min of the level raise in the tank.

The moderator can be dumped by gravity either through a stainless-steel tube of 45-mm inner diameter or through the pumping circulation sys-

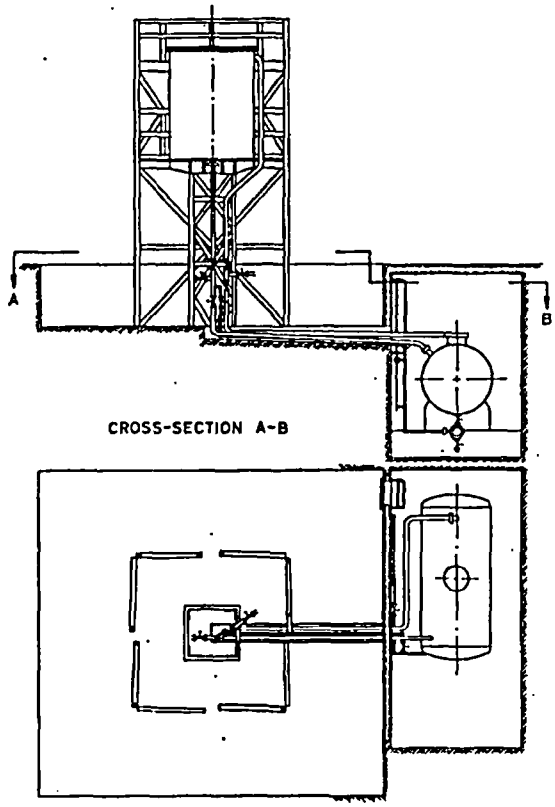

Fig. 1

Schematic view of the reactor

tem. Pumping or draining of the moderator is controlled by pneumatic valves which are actuated by DC magnetic valves.

The air pressure difference, between the reactor tank and the storage tank is equalized through an aluminium tube. A scheme of the water circulation system is given in Fig. 1.

The heavy-water temperature is measured by a platinum resistance thermometer which permits an accuracy of ±0.2°C.

For continuous moderator level measurements one of the safety rods is used. This rod differs mechanically from the normal safety rod because a separate cog-wheel system with a synchro generator is added. The accuracy of measuring the relative heavy-water level is better than ±0.02 cm.

In addition to the continuous water level monitoring equipment, there are two stable level meters in the reactor tank which serve to control the pumping speeds (fast pumping limiter) and the maximum height of the heavy water in the reactor tank (maximum level limiter).

The fast pumping limiter is placed far below the critical level. Its height is adjusted so that k_{eff} for a given system does not exceed 0.9. After reaching this level a contact probe activates a relay which stops the pump.

The maximum water level limiter is placed above the critical level. Its height is determined so that the maximum excess reactivity does not exceed 600 pcm. After reaching this level the contact probe scrams all safety and control rods and stops the pump.

2.3. Control and safety

Reactivity of the reactor is normally controlled by varying the heavy-water level. These operations are performed manually. In addition, there is one rod which can be used for automatic power control. The rod position is controlled by an error signal which is a function of the difference between the actual and required power.

The reactor is equipped with three safety rods. Safety rod No. 3 serves simultaneously as a follow-up point contact probe by which the heavy-water level in the reactor tank is measured both manually and automatically.

Position of the follow-up level meter and of the control rod are indicated on the control console by synchro position indicators while the two safety rods are provided only with signal lights for indicating the limit positions.

The control console of the reactor is equipped with six measuring channels:

(a) Two pulse channels with BF_3 counters for operation in the sub-critical range;

(b) Two logarithmic DC channels for the measurement of the power level and period. The power indication from one of these channels is included in the automatic power control loop. Both channels use compensated boron chambers, type CCP1N10, with a sensitivity of the order of 1.5×10^{14} ampères per n $cm^{-2}s^{-1}$.

(c) Two linear DC channels with compensated boron chambers, type CCP1N10, for the power level measurement. One of these two channels is used for the automatic power control.

Safety rods can be withdrawn only if all circuits are closed and if one of the start-up channels indicates at least 5 pulses per second. To ensure the presence of this minimum signal a Ra-Be source of 0.5 c is injected pneumatically in a position immediately below the reactor tank where it is locked by an electric magnet.

The control rod can be withdrawn only if the two safety rods are in the upper limit position. To withdraw the third safety rod (the follow-up level meter) it is necessary that all the safety circuits are closed. When operated the safety system will result in (a) dropping of all three safety rods, (b) dropping of the control rod, and (c) stopping any further increase in the heavy-water level.

The safety system is designed on the principle of one of two. There are 12 circuits which will cause the safety system to operate giving also an optical indication of the fault that has caused the scram. A manual scram button is also included in the safety circuits. Safety circuits of the instrument channels are automatically blocked if the instruments are disconnected from the main supplies.

3. LATTICES STUDIED

In the present series of experiments 2%-enriched metallic uranium fuel elements in different lattice configurations were studied. These elements are normally used in the RA high flux reactor of the Boris Kidrič Institute in Belgrade.

The fuel is manufactured in tube-shaped slugs canned from both sides with aluminium.

Overall dimensions of the fuel slug are outside diameter of aluminium canning 37 mm, outside diameter of the uranium tube 35 mm, inside diameter of the uranium tube 31 mm, inside diameter of aluminium canning 29 mm and length of the slug 110 mm.

Inside the slug there is an additional aluminium tube, serving as a spacer for D_2O coolant flow. The tube has an outer diameter 23 mm and 1-mm wall thickness. The cross-section of a fuel slug is shown in Fig. 2.

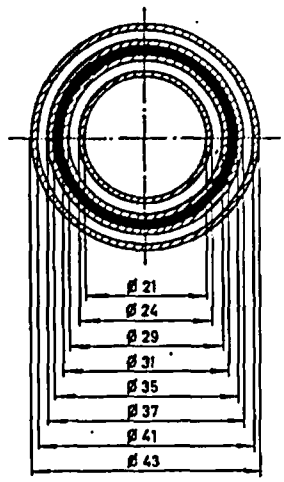

Fig. 2

Cross-section of the fuel element

D_2O; Al; U(2% U^{235})

Ten to fifteen such fuel slugs are placed in an aluminium tube whose overall dimensions are 43/41×2250 mm. Thus the total length of a fuel element could be changed, in accordance with the requirements of experiment. The shrouds could be either open at the bottom or closed if lattices with void are investigated. The total number of fuel elements is limited. In most experiments 52 fuel elements were used.

The lattices recently investigated are made of square shaped cells. The lattice pitches as expressed by the distance between the axis of two fuel elements are 7, 8, 9.9, 11.3, 14, 16, 17.9 and 19.8 cm.

4. TECHNIQUES IN BUCKLING DETERMINATION

For all the investigated lattices buckling was measured by flux mapping. Several neutron detection techniques such as; foil activation, semi-conductor counter or BF_3 miniature counter techniques were tested. Although the measurements by means of a counter proceed much faster and the results are suitable for theoretical interpretation, the foil-activation technique has proved to be more reliable. The main reason is the difficulty in keeping the reactor power steady when the counter moves through the reactor core. Oscillation in reactor power usually introduce much higher errors in the overall flux distribution obtained by counters than the foil activities plot.

The foils used are made of copper for thermal or gold for epithermal neutron flux mapping. They are disc shaped with a diameter of 10 to 17 mm and a thickness of 0.2 mm.

To irradiate the foils, they are arranged on an aluminium foilholder and inserted in one of the channels passing through the reactor. The relative foil position was better than 1 mm and the mutual distance 5 to 7 cm.

The axial and radial flux distributions are measured separately. In one distribution more than 20 foils are used. For each lattice thermal and epithermal neutron flux distributions as well as the cadmium ratios were measured.

The foils activities are measured by four intercalibrated G-M counters. The measuring and waiting times are automatically regulated by means of an electronic timer. The data obtained are corrected for radioactive decay, the counter dead time and the foil weight by means of an electronic computer.

In all lattices studied the core configurations were arranged in such a way that no axial reflectors were present. Owing to the fact that the number of the available fuel elements was limited, it was not possible to avoid a radial reflector in most lattice configurations. For close packed lattices the reflector was as large as 70 cm compared to the 60-cm diameter of the reactor core.

4.1. Determination of α^2 and β^2

Owing to the fact that the reactor is axially bare, the thermal neutron flux distribution can be represented in the elementary one-group diffusion theory by the function $n(x) = A \sin \alpha x$. To find the axial buckling from the neutron flux distribution it is sufficient to fit the experimental value to a sine function and to obtain the α value by the least squares method. This process is somewhat lengthy unless an electronic computer is used and in our case an easier method was adopted which gave the same accuracy.

From the flux distribution measured three successive points are selected.

The three selected points on the $\sin \alpha H$ distribution can be represented as:

$$n_1 = A \sin \alpha (H + \Delta H)$$

$$n_2 = A \sin \alpha (H)$$

$$n_3 = A \sin \alpha (H - \Delta H),$$

where α is the axial buckling and ΔH the distance between the points.

By developing the expressions for n_1 and n_3 as $\sin(\alpha \pm \beta)$, adding the two expressions and dividing the result by n_3 one obtains:

$$\beta_1 = \frac{1}{\Delta H} \arccos \frac{n_1 + n_3}{2n} .$$

Any set of three equidistant points can be presented in this form and the β_1 value obtained. The advantage of this method is that the distance ΔH can be fixed with high precision and it is not necessary to make the normalization. The mean value for β can be found from a series of β_1 obtained. The standard error can be easily determined by using the standard deviation and the expression for β_1.

In most of the lattices investigated the reflector influence on radial flux distribution was very much pronounced, so the thermal neutron flux distribution could not be simply represented by the $AJ_0(\alpha r)$ function. Cadmium ratio measurements have shown that there was no pronounced region in the reactor where the ratio between thermal and epithermal flux could be taken as constant and where the simple one-group diffusion theory could not be applied.

What follows is based on the two-group diffusion theory. It assumes that the thermal and epithermal flux distributions could be presented by the following formulae:

$$\phi_f = AJ_0(\mu r) - BI_0(\nu r)$$

$$\phi_s = S_1AJ_0(\mu r) + S_2BI_0(\nu r),$$

where μ is the radial buckling to be determined. If the epithermal flux distribution is multiplied by the reflector coupling coefficient S_2 and the two distributions added, the obtained distribution must have a $J_0(\mu r)$ form, where the μ value can be easily found using the least squares method. Both distributions have to be properly normalized beforehand which is easily done by measuring the absolute ratio between fast and thermal fluxes at the reactor centre. For this purpose the cadmium ratio at the reactor centre was measured by means of thin gold foils. After self-absorbtion corrections the Westcott r value was found and the absolute ratio between 2200 m/s thermal and epithermal fluxes was determined.

$$R = \frac{2}{\sqrt{\pi}} r \left(\frac{T}{T_0}\right)^{1/2} \int \frac{dE}{E},$$

where T is the neutron temperature in the core and T_0 2200 m/s neutron temperature. The integration is made over the epithermal region. This method includes the use of the theoretical value of S_2, but the buckling obtained is not very sensitive to the possible inaccuracy in this value.

The factors affecting the accuracy of the total bucklings include the statistical errors in the foil counting and positioning and uncertainty in the

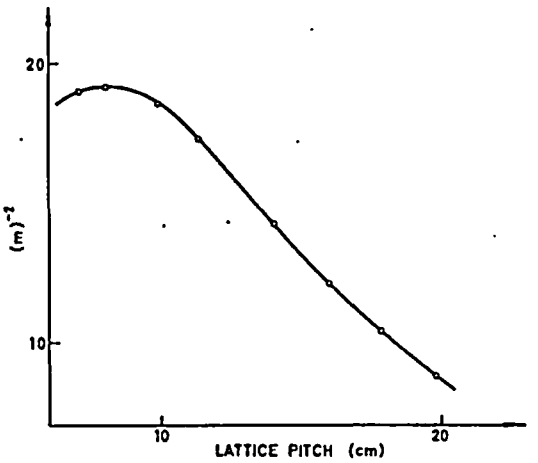

Fig.3

Total buckling plotted against lattice pitch

corrections applied, especially in S_2 and ϕ_{th}/ϕ_{epi} values. If all these errors are estimated independently and statistically combined, the standard error in buckling is ± 1%.

The results obtained reduced to D_2O concentration 99.80 and temperature 20°C are represented in Fig.3.

5. FLUX DISTRIBUTION INSIDE A CELL

Thermal neutron distribution measurements within an elementary cell were carried out on a specially prepared fuel element which was mounted in the central position of the core. The fuel element was drilled with a 3-mm diam. diamond drill close to the middle of the active height and the hole was painted with colourless lacquer to avoid a release of fission products. A special small tube with detector foils was placed in the hole. The uranium in the fuel element is only 2-mm thick. To enable the detection of particular thermal flux variations in different diffusion media, one should obtain the highest possible resolutions between the points measured. According to the experimental results it was evident that a high statistical accuracy of the activities measured and strict positioning of the detector foils were required to make these micro-effects visible.

Small intercalibrated foils of dysprosium-aluminium alloy were used as detectors. Owing to its highly effective activation cross-section, moderate decay and slight departure from the 1/v law, dysprosium proved to be a convenient detector for intracell measurements.

To define more accurately the positions of the detector foils, a special small tube was made of Plexiglass of 2.1-mm internal and 2.8-mm external diameter. Within this tube the foils 2 mm in diameter and 0.15 mm thick were arranged on a sandwich principle by using Plexiglass cylindrical

spacers 2-mm in diameter. The distance between the foils was kept constant (1mm or 2.5 mm) in order that the shadowing factor might remained unchanged. All the elements included in the sandwich were machined to an accuracy of ± 0.01 mm.so that the relative position of the detector was known to within ± 0.1 mm.

Intracell irradiation was carried out along the side and the diagonal of the square lattice. At least two irradiations were performed in each direction for each lattice. The beta activities were measured in cycles with four independent G-M channels of approximately identical efficiencies. The measurement intervals were chosen in such a way as to obtain a standard error of about ± 0.3% in all channels.

The results obtained were corrected for the foil weight, decay and the counter dead time to present the thermal neutron flux distribution inside a cell. Fig.5 shows the measured distributions for several lattice pitches. Both side and diagonal direction distributions are given.

From the curves obtained experimentally the measured average thermal neutron fluxes were calculated for particular material regions. The obtained values are used to calculate the thermal utilization factor as well as the diffusion length for the core composition.

According to the definition of the thermal utilization factor f, i.e. the number of thermal neutrons absorbed in the fuel per neutron absorbed in the reactor, the f value is calculated from the formula:

$$f = \frac{N_u \Sigma_{au} V_u F_u}{N_i \Sigma_{ai} V_i F_i},$$

where N is atomic density.

Σ_{ai} - BNL-325 absorption cross-section (for fuel absorption cross-section allowance is made for the difference of 40°C in neutron temperature)

V - volume of the zone

F_i - thermal flux averaged over the material zone.

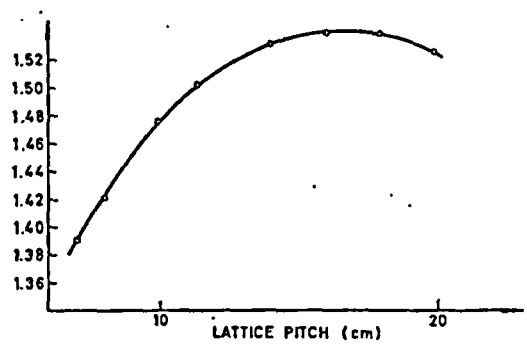

Fig.4

Infinite multiplication factor

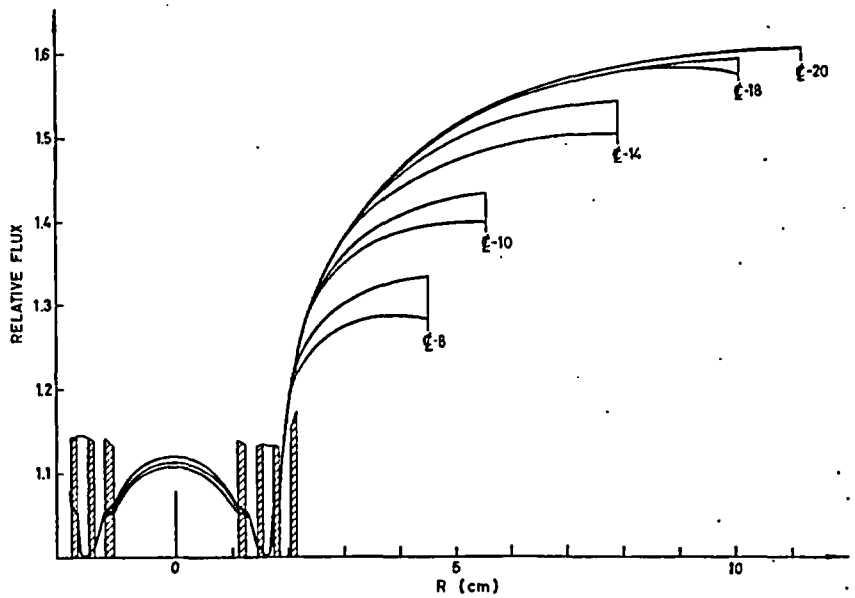

Fig. 5

Neutron flux distributions elementary cells

The diffusion length is determined from the formula:

$$L^2 = \bar{D}/\bar{\Sigma}_a,$$

where $\bar{D}$ and $\bar{\Sigma}_a$ are the mean values of the diffusion constant and the absorption cross-section for the core composition.

All the calculations were performed by means of an electronic computer. The computer programme prepared for this purpose employs the foil counting rate as an input, making all the necessary corrections, calculates the average fluxes in various zones, the thermal utilization factor and the diffusion length. Table I gives the result for f and L^2 as obtained for different lattices.

5.1. Determination of the infinite multiplication constant

The experimental data for bucklings and L^2 offer the possibility of determining the infinite multiplication constant k_∞ using the two-group diffusion theory expression

$$k_\infty = (1+L^2B^2)(1+\tau B^2).$$

There is no direct method for measuring the slowing-down length and the usual way to determine k_∞ is to use the calculated τ. This way of approach was applied in the case under consideration.

TABLE I

RESULT FOR f AND L^2 AS OBTAINED FOR DIFFERENT LATTICES

Lattice pitch	f	L^2
7		46.0
8	0.9488	61.0
9.9	0.9461	99.0
11.3	0.9432	137.0
14.0	0.9378	212.0
16.0	0.9331	282.0
17.9	0.9275	352.0
19.8	0.9205	430.0

The slowing-down length was determined from the expression

$$\tau = \tau_0\left(1+\frac{V_u}{V_m}\right)\left(1+2\cdot\frac{V_{al}}{V_{tot}}\right).$$

The value $\tau_0 = 118\ cm^2$ is adopted for 99.80% D_2O. The above expression is recommended by DESSAUER [2] and out of several formulae existing in the literature is chosen because of its simplicity. The infinite multiplication constant as a function of the lattice pitch is given in Fig. 4.

An effective way of checking the calculated values for τ is to measure the water level reactivity coefficient $d\rho/dH$ which can be expressed by:

$$\frac{d\rho}{dH} = \frac{2\pi^2}{H_{ex}^3}\left(1+\frac{\partial\alpha^2}{\partial\beta^2}\right)\left(\frac{L^2}{1+L^2B^2}+\frac{\tau}{1+\tau B^2}\right)$$

where H_{ex} is the extrapolated water height at criticality, and $\partial\alpha^2/\partial\beta^2$ the radial reflector coefficient.

By direct measurements of $d\rho/dH$ it is possible to determine experimentally $[L^2/(1+B^2L^2)+\tau/(1+B^2\tau)] = M$, and compare it with the same expression obtained with the theoretical calculation.

The water level reactivity coefficient was obtained by measuring the stable reactor period for a fixed value of ΔH. The reactivity was calculated from the inhour relation. For this purpose a programme was written for the electronic computer Z-23 where 14 delayed neutron groups were taken into account. Photoneutrons were weighted by the non-escape probability for fission product gamma rays of energies higher than 2.23 MeV.

From a series of measurements of the reactivity as a function of ΔH, $d\rho/dH$ is obtained by the least-squares method, assuming a linear variation of ρ as a function of H in the vicinity of the critical height.

The $\partial\alpha^2/\partial\beta^2$ is the radial reflector coefficient. It is primarily a function of the geometrical characteristics of the reactor core and can be obtained theoretically during criticality calculations. When the criticality determinant was calculated by varying the radial and axial buckling values, the reflector coefficient is obtained as a ratio between

$$\frac{\partial\alpha^2}{\partial\beta^2} = \frac{\partial\Delta}{\partial\beta^2}\Big/\frac{\partial\Delta}{\partial\alpha^2} .$$

The experimentally obtained results for M are compared with those calculated on the bases of the theoretical τ and the experimental B^2 and L^2. This comparison is shown in Fig. 6. As one can see, the theoretical curve represented by the full line shows a rather good agreement with the experimental points, although a number of points are scattered around the theoretical curve. This is due to low accuracy in $d\rho/dH$ determination.

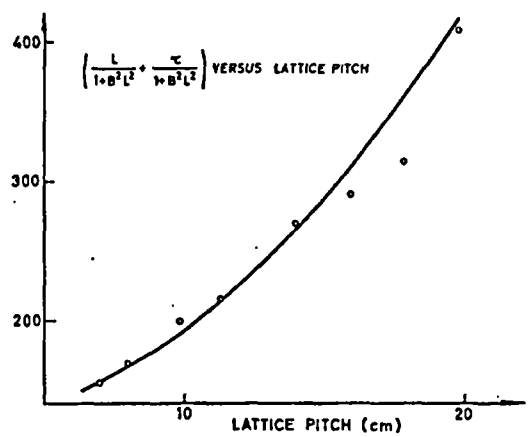

Fig. 6

Comparison of experimental results for M with those calculated on the bases of the theoretical τ and the experimental B^2 and L^2.

This comparison shows that the values for τ are rather well computed, but at the same time indicates that the method of direct determination of τ by means of $d\rho/dH$ is not suitable.

5.2. *Correlative data for η and the effective resonance integral*

The k_∞ and f factors experimentally determined offer a possibility of estimating the value of η and the effective resonance integral. The method is described by MUMMERY [3] and consists in expressing the logarithm of

k_∞/f as a function of the fuel to moderator ratio $N_u V_u/N_m V_m$. The straight line theoretically given by

$$\log \frac{k_\infty}{f} = \log \epsilon\eta - \frac{N_u V_u}{N_m V_m} \frac{1}{\xi \sigma_s} \int \sigma_a \frac{dE}{E}$$

gives the logarithm of $\epsilon\eta$ at its intersection with the vertical axis. The slope of the straight line represents the effective resonance integral divided by $\xi\sigma_s$.

Such an analysis is made for eight measured values of k_∞ and f, and the log $\epsilon\eta$ as a function of $N_u V_u/N_m V_m$. is expressed in Fig. 7. The extrapolated value for log $\epsilon\eta$ is 0.528 which, with ϵ = 1.008, gives η_{corr} =1.676. The slope obtained by least squares is 2.99. When the usual value of $\xi\sigma_s$ for D_2O is used ($\xi\Sigma_s$ = 0.177) one obtains for the effective resonance integral $\int \sigma_a dE/E$ = 15.92 b.

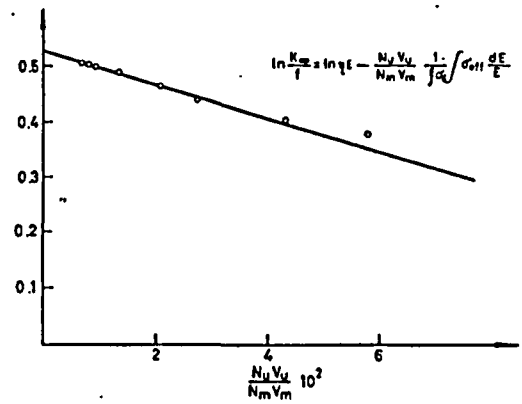

Fig. 7
Log $\epsilon\eta$ as a function of $N_u V_u/N_m V_m$

6. COMPARISON WITH THEORY

Critical bucklings were calculated for all the lattices studied, using the four-factor model and two-group diffusion theory. The BNL-325 cross-sections with Westcott notation were used. Because some arbitrariness in the choice of the formulae for lattice parameter calculation cannot be avoided, in all cases where it was possible, the expressions which allow a direct experimental check were used. For those parameters where direct measurement was not possible, no special effort was made to improve the calculation methods, but simple empirical formulae were applied.

In this way the lattice parameters were divided in two categories: (a) where the definition allows a direct experimental check, and (b) where a number of miscellaneous processes are lumped together and no strict definition is possible.

The theoretical model gives a relation between these two categories and offers the possibility of determining the correlative data for the parameters in the second category. As the measurable parameters f, ϵ, L^2, and B^2 are taken, the correlative parameters are p, k_∞, η and τ. This is an arbitrary choice based on the existing experimental methods.

The results obtained as compared with experiments are as follows.

6.1. *Thermal utilization*

Computations of the thermal utilization factor were done using the expression previously mentioned. The disadvantage factors were calculated according to the diffusion theory, using corrections based on the P_3 approximation to the neutron transport theory.

The results obtained for f are higher by 0.3% in comparison with the experiments. For close packed lattices this discrepancy is somewhat lower. The difference appears primarily from the error in moderator disadvantage factors. As some preliminary calculations show, it can be completely reduced if more exact treatment of neutron flux distribution is made. The fuel disadvantage factor is small because the uranium tube thickness is too small and as a result the error cannot influence the result appreciably.

6.2. *Fast fission factor*

Although it was possible to measure the fast to thermal fission ratio and obtain this factor the experimental way, the computed value was used through the whole analysis. The expression identical to that submitted by SPINRAD [4] was adopted for the calculation. The moderator influence inside the fuel element was not taken into account. The obtained value is $\epsilon = 1.008$.

6.3. *Thermal reproduction factor in fuel*

Using $\nu = 2.46$ and BNL-325 cross-sections, one obtains $\eta = 1.73$. As shown before, the $\ln k_\infty/f$ plot gives a much lower η value, $\eta = 1.676$. At the same time this is the largest disagreement between the theory and the experiments.

6.4. *Resonance absorption*

The exponential expression was chosen for computation of the factor p. From several rather different formulae for the effective resonance integral reported in the literature, the semi-theoretical expression given by GALANIN [5], for the same type of fuel element was taken:

$$p = \exp(-\Psi) \quad \text{and} \quad \Psi = \frac{5.6}{S_m}\left[\sqrt{\rho_1}\sqrt{\rho_1^2-\rho_2^2}\,1.2 + 0.55(\rho_1^2-\rho_2^2)\right].$$

This assumes a $\sqrt{S/M}$ dependence of the effective resonance integral.

To allow for the influence of the moderator inside the fuel tube the surface depending part of the resonance integral was increased by 20%. The resonance integral computed in such a way appears higher by 12% in comparison with that obtained from the ln k_∞/f plot. This influences the discrepancy in the p value ranging from 0.2% up to 2% for close packed lattices.

6.5. Infinite multiplication factor

The discrepancy in η was completely reflected in k_∞. The calculated values are higher by 2 to 3%.

6.6. Bucklings B^2

The most pronounced discrepancy between theory and experiments was observed in the material bucklings. The percentage error in total buckling values is of the order of 10 to 15%. The computed radial bucklings are in a good agreement with experiments, owing to the fact that it is practically the function of the geometry only. The axial buckling as the final aim of calculation was influenced by all discrepancies previously mentioned and the difference between calculated and measured values is rather high.

7. CONCLUSIONS

The experiments and comparison with theory show that if the directly measurable lattice parameters are determined with a reasonable degree of accuracy, then according to the adopted theoretical model it is possible to obtain the correlative data for other parameters necessary for criticality and reactivity calculations. In any case the lattice parameters where the correlative data should be taken are η and the effective resonance integral.

In our case $\eta_{corr} = 0.969$. η is recommended, which is in good agreement with the reported values from critical experiments for natural-uranium heavy-water lattices.

As the correlative value for the effective resonance integral the following formula is recommended:

$$I_{res.} = 3.68 + 21.1\sqrt{\frac{S}{M}},$$

which is the same expression as used by GALANIN [5], but the moderator inside the fuel tube increases the surface part of the resonance integral by 4% instead of 20% as originally taken.

Critical bucklings calculated in such a way are in very good agreement with experiments for the whole range of lattices studied except for very close packed configurations, where the calculations are giving somewhat lower values. This deviation could be explained by the fact that the fast fission factor is calculated without the ineraction between the separate fuel elements.

REFERENCES

[1] JOVANOVIĆ, S. et al., Zero Energy Reactor RB, NPY-Y-2 (1963).
[2] DESSAUER, G., Physics of Natural Uranium, D_2O Lattices, Proc. 2nd. UN Int. Conf. PUAE 12 (1958) 320.
[3] MUMMERY, P. W., The Experimental Basis of Lattice Calculation, Proc. UN Int. Conf. PUAE 5 (1956) 282, 323.
[4] SPINRAD, B. I., Fast Effects in Lattice Reactors, Nucl. Sci. Engng. 1 (1956) 455.
[5] GALANIN, A. D., et al., Experiments on D_2O Reactor, Proc. 2nd. UN Int. Conf. PUAE 12 (1958) 380.

DISCUSSION

C.E. COHN: Could you give us some further details on your automatic power-level control system? What sort of servo system do you use, what is the total reactivity worth of the automatically controlled rod, and finally in what sort of experiments do you make use of this facility?

N. RAIŠIĆ: Our automatic power system is operated by means of an error signal which is based on the difference between the required and the actual power of the reactor. Details are given in the paper. The total reactivity worth of the automatically controlled rod is between 300 and 400 pcm, depending on the core configuration. Automatic control is used for irradiation work whenever the reactor has to operate at high power for fairly long periods of time.

C.E. COHN: I should have thought that you could avoid the necessity of controlling the power level by using a monitor counter in a fixed position and normalizing your traverse count against the monitor counter.

A.E. PROFIO: Since this is a critical assembly and has very little room return of neutrons, it should be possible to use it for investigating the anomalous variation of radial buckling with lattice configuration. Have you made enough measurements in assemblies without a radial reflector to be able to say anything about this problem?

N. RAIŠIĆ: The room return of neutrons is extremely small. We did make some measurements changing the radial buckling but the idea was really to determine experimentally the radial reflector coefficient in connection with the interpretation of $d\rho/dH$. Unfortunately we did not carry out simultaneous measurements of the bucklings so the effect you mentioned was not observed. I hope however that we shall be able to undertake measurements of this sort soon.

VOID REACTIVITY EFFECTS IN THE SECOND CHARGE OF THE HALDEN BOILING WATER REACTOR

J.E. LUNDE
OECD HALDEN REACTOR PROJECT,
NORWAY

Abstract — Résumé — Аннотация — Resumen

VOID REACTIVITY EFFECTS IN THE SECOND CHARGE OF THE HALDEN BOILING WATER REACTOR. The reactivity effect of voids caused by boiling inside the coolant channels in the second fuel charge of the Halden Boiling Heavy Water Reactor has been measured both in void-simulated zero-power experiments and under actual power conditions.

The void-simulated experiments consisted of measuring the reactivity effect of introducing void columns inside thin-walled tubes to various depths. The tubes were placed at different positions between the stringers in a single 7-rod cluster element practically identical with the normal second-charge fuel elements. This experiment enables an investigation of the reactivity dependence upon void fraction, and also the reactivity dependence of steam-bubble position in the coolant channel. The experiment was carried out in the Norwegian zero-power facility NORA, with a core consisting of 36 second-charge elements and with a lattice geometry identical to the one in HBWR.

The temperature dependence of the void effect was investigated in a zero-power experiment with the 100 fuel-element core of HBWR. In a single fuel element the water level inside the coolant channel was depressed to various depths, and the reactivity effect of this perturbation was measured at different temperatures in the temperature interval 50°C-220°C.

The power void reactivity has been measured in HBWR as a function of nuclear power at different moderator temperatures between 150°C and 230°C at powers up to about 16 MW at the highest temperature. The power-void reactivity coefficient is an important quantity in determining the dynamic behaviour of a boiling-water reactor. The theoretical determination of this quantity is, however, complicated by the fact that knowledge about the void distribution in the core is required. The detailed power-void distribution is not easily amenable to experimental determination, and accordingly the void-simulated experiments represent a better case for testing the reactor physics calculation of void effects.

Preliminary theoretical comparisons are made for these experiments. Two-group diffusion theory is applied, and the conclusion can be drawn that fair agreement is obtained between theory and experiment for the perturbations in the lattice parameters for a void fraction equal to one, both at low and high temperatures. For intermediate void fractions, however, somewhat less satisfactory agreement is found.

EFFETS CAVITAIRES DANS LA DEUXIÈME CHARGE DU RÉACTEUR A EAU LOURDE BOUILLANTE DE HALDEN (HBWR). L'auteur a mesuré, aussi bien lors d'expériences avec vide simulé à puissance nulle que dans les conditions normales de puissance, l'effet cavitaire, provoqué par l'ébullition qui se produit à l'intérieur des canaux du refroidisseur, dans la deuxième charge de HBWR.

Les expériences avec vide simulé ont consisté à mesurer les effets que produit sur la réactivité le fait d'enfoncer à des profondeurs différentes des tubes plus ou moins vides à paroi mince. Les tubes ont été placés en plusieurs endroits entre les barres, dans une seule cartouche formée de sept barres en grappe et pratiquement identique aux cartouches de combustible de la deuxième charge. Cette expérience permet de déterminer comment la réactivité varie en fonction du volume cavitaire relatif et de l'emplacement des bulles dans le canal du refroidisseur. L'expérience a été effectuée dans le réacteur NORA de puissance zéro, avec un cœur composé de 36 cartouches de la deuxième charge de HBWR et dans une géométrie de réseau identique à celle de ce réacteur.

L'auteur a observé comment l'effet cavitaire variait avec la température dans un ensemble de puissance zéro avec le cœur à 100 cartouches de HBWR. Dans une seule cartouche, il a abaissé le niveau de l'eau à l'intérieur du canal de refroidissement à des niveaux différents et mesuré l'effet de cette perturbation sur la réactivité à différentes températures comprises entre 50 et 220°C.

L'auteur a mesuré l'effet cavitaire, à l'intérieur de HBWR et dans les conditions de puissance, en fonction de la puissance nucléaire à des températures différentes du ralentisseur comprises entre 150 et 230°C et, à la température la plus élevée, pour des puissances allant jusqu'à 16 MW. Le coefficient cavitaire est une quantité qu'il importe de connaître lorsqu'on veut déterminer le comportement dynamique d'un réacteur à eau bouillante. Or, la détermination théorique de cette quantité est difficile du fait qu'il faut connaître en détail la répartition des cavités dans le cœur. Cette répartition dans les conditions de puissance ne se prête pas facilement à une détermination expérimentale de sorte que les expériences avec vide simulé conviennent mieux pour vérifier les calculs de physique des réacteurs portant sur les effets cavitaires.

Les données de ces expériences ont été comparées aux résultats théoriques. On a appliqué la théorie de la diffusion à deux groupes et on peut conclure qu'il y a bon accord entre la théorie et l'expérience en ce qui concerne les perturbations dans les paramètres du réseau pour un coefficient cavitaire égal à 1, tant aux basses qu'aux hautes températures. Toutefois, pour les valeurs intermédiaires du coefficient cavitaire, l'accord est moins bon.

Pour le calcul macroscopique de l'effet sur la réactivité, on utilise une théorie de perturbation.

ЭФФЕКТЫ ПУСТОТНОЙ РЕАКТИВНОСТИ ВО ВТОРОЙ ЗАГРУЗКЕ HBWR. Эффект реактивности пустот, вызванных кипением в каналах для теплоносителя во второй загрузке Халденского кипящего тяжеловодного реактора (HBWR) был измерен как в экспериментах нулевой мощности с имитацией пустот, так и в условиях фактической мощности.

Эксперименты с имитированными пустотами состояли в измерении эффекта реактивности пустотных колонн, вводимых в тонкостенные трубки на различную глубину. Трубки были установлены в разных положениях между продольными ребрами в одиночной сборке, состоящей из семи стержней, практически идентичной нормальным топливным элементам второй загрузки. Этот эксперимент позволил изучить зависимость реактивности от пустого объема, а также зависимость реактивности от положения пузырьков пара в канале для теплоносителя. Эксперимент был выполнен на норвежской установке нулевой мощности NORA с активной зоной из 36 элементов второй загрузки и с геометрией решетки, аналогичной геометрии решетки реактора HBWR.

Температурная зависимость пустотного эффекта была изучена на экспериментальной установке нулевой мощности, имевшей активную зону из 100 топливных элементов реактора HBWR. В одиночном топливном элементе уровень воды в канале для теплоносителя снижался до различных глубин и влияние на реактивность этого отклонения от нормальных условий измерялось при различных температурах в интервале температур 50–220°C.

Влияние пустотной реактивности на мощность было измерено на реакторе HBWR как функция ядерной энергии при различных температурах замедлителя в диапазоне 150–230°C при мощностях до 16 мгвт (при самой высокой температуре). Коэффициент пустотной реактивности на мощности является важным показателем при определении динамического поведения кипящего реактора. Однако теоретическое определение этого показателя усложняется тем, что необходимо знать распределение пустот в активной зоне. Подробные данные о влиянии распределения пустот на мощность трудно поддаются экспериментальному определению, и поэтому эксперименты с имитированными пустотами были пригодны для проверки расчетов эффектов пустоты.

Для этих экспериментов делаются предварительные теоретические сравнения. Применяется двугрупповая теория диффузии, и можно сделать вывод о том, что достигнута справедливая согласованность между теорией и экспериментом для пертурбаций в параметрах решетки при пустотной части равной единице при низкой и высокой температурах. Однако для промежуточных пустотных частей установлена менее удовлетворительная согласованность.

Для макроскопического расчета эффекта реактивность применяется теория возмущений.

EFFECTOS DE CAVITACIÓN EN LA SEGUNDA CARGA DEL REACTOR DE AGUA PESADA HIRVIENTE DE HALDEN (HBWR). La ebullición que se produce en el interior de los canales refrigerantes de la segunda carga de combustible del reactor de agua pesada hirviente de Halden provoca efectos de cavitación que afectan a la reactividad. Este efecto se ha medido tanto en experimentos con vacío simulado de potencia nula como en condiciones de régimen normal.

Los experimentos con vacío simulado consistieron en medir las alteraciones de la reactividad al introducir hasta diversas profundidades tubos vacíos de paredes delgadas, que se colocaron en distintas posiciones entre las piezas de unión de un haz combustible de siete barras, prácticamente idéntico a los que constituyen la segunda carga de combustible. Este experimento permite investigar las variaciones de la reactividad en función del volumen relativo de los vacíos y de la posición de las burbujas de vapor en el canal refrigerante.

Se ejecutó en el conjunto noruego de energía nula, NORA, con un cuerpo consistente en 36 elementos de la segunda carga dispuestos en un reticulado de geometría idéntica a la del reactor HBWR.

El autor estudió la variación del efecto de cavitación en función de la temperatura en un conjunto de potencia nula provisto de 100 elementos combustibles. En un elemento redujo el nivel de agua en el interior del canal refrigerante a varios valores y midió el efecto que ejercía esta perturbación sobre la reactividad a temperaturas comprendidas entre 50°C y 220°C.

El efecto de los huecos sobre la reactividad a régimen normal se ha medido en el reactor HBWR en función de la potencia para temperaturas del moderador que oscilaron entre 150°C y 230°C, alcanzándose a esta última temperatura hasta unos 16 MW. El coeficiente de cavitación en régimen normal constituye un parámetro que conviene conocer cuando se trate de determinar el comportamiento dinámico de un reactor de agua hirviente. Sin embargo, su determinación teórica se complica por el hecho de que es preciso conocer la distribución de las cavidades en el cuerpo. Tampoco es fácil determinarla por vía experimental con exactitud cuando el reactor funciona a régimen normal y, por tanto, los cálculos de física de los reactores de los efectos de las cavidades se comprueban mejor simulando los huecos experimentalmente.

Se han efectuado comparaciones preliminares entre los resultados de esos experimentos y los datos teóricos. Los cálculos se realizan por una teoría de difusión de dos grupos y se aprecia que los resultados teóricos y experimentales sobre las perturbaciones de los parámetros del reticulado, para un volumen relativo de los vacíos igual a 1, concuerdan satisfactoriamente tanto a temperaturas bajas como a temperaturas elevadas. La concordancia es menos satisfactoria para valores intermedios del volumen relativo de los vacíos.

El efecto de reactividad se calcula macroscópicamente mediante una teoría de las perturbaciones.

1. INTRODUCTION AND SUMMARY

The Halden Boiling Water Reactor (HBWR) is a natural-circulation boiling heavy-water reactor. Heavy water circulates by natural convection of the moderator and steam is generated inside shrouds around the fuel elements. The heavy-water steam generated in the reactor pressure vessel circulates by natural convection through a primary steam circuit to a heat exchanger where the steam is condensed. The second fuel charge consists of 1.5 t of uranium oxide enriched to 1.5%. The 100 fuel elements are 7-rod clusters clad in Zircaloy-2.

A very important parameter related to the dynamic behaviour of a boiling-water reactor is the effective void reactivity coefficient, expressed for instance in pcm/MW, expressing the integrated effect of steam voids under actual boiling conditions. The reactivity effect of these steam voids in a given fuel geometry is a complicated function of space and temperature. For the prediction of integral reactivity effects a good knowledge of the boiling void distribution throughout the reactor is required. The void distribution varies greatly over the core, the void fraction being zero at the lower end of the fuel channel and having values up to around 80% at high-power levels in the upper end of the channel. Comparisons between experimental and theoretical values for the power void reactivity thus become a test of the ability to predict the combined effect of a thermodynamic quantity and reactor-physics quantities.

Low-power experiments with simulated voids (for instance by air) in single elements, however, permit the investigation of reactor-physics quantities alone, since the amount of voids is controllable and the distribution is uniform.

As a part of the reactor statics experiments with the second fuel charge of HBWR, a series of experiments have been made in order to enable tests

of the theoretical models to be made from various angles. The following experiments were performed:

(a) Differential experiments in the Norwegian zero-power facility NORA with a 36-element core of HBWR fuel elements. The reactivity effect of introducing void columns inside thin-walled tubes to various depths was measured. The tubes were placed at various positions between the stringers in the 7-rod cluster. The experiment enables an investigation of the reactivity dependence upon void fraction and upon the void position in the coolant channel to be made.

(b) Differential experiments in HBWR with the normal 100-element core. The reactivity effect of completely voiding one fuel element to various void depths at five different temperatures in the temperature interval 50 to 220°C.

(c) Integral experiments consisting of measuring the void reactivity as a function of nuclear power at different temperatures between 150 and 230°C at power levels up to 18 MW at the highest temperature. The measurements then give an experimental value for the power void coefficient.

Some of the experiments have been compared with theoretical values, a full theoretical comparison will be given in References [1-3]. The theoretical values are based upon two-group diffusion theory, using the Swedish lattice parameter recipe BURNUP 5 [4] when calculating the dependence upon void fraction of the lattice parameters. The conclusion can be drawn from NORA differential experiments that good agreement is obtained between experiment and theory for the cases with the largest void perturbations, void fraction = 1, which is homogeneous radially within the coolant channel. When the void distribution is strongly inhomogeneous, the theoretical approach of smearing out the void over the channel does not give good agreement with experiments. The disagreement seems particularly strong in the diffusion coefficients and seems to call for extension to a multi-zone model in the diffusion coefficient calculation, if inhomogeneous void geometries are considered to be of practical interest. Inhomogeneous void distributions might be found in large clusters.

The temperature dependence of the voided lattice parameters is further well represented by the theory. Since the radial void distribution in a coolant channel of HBWR is expected to be fairly homogeneous, the conclusion from the analysis of differential experiments is that the integral effect of power voids should be fairly well predicted provided that the void distribution calculation can be relied upon. A fair agreement is actually found between experimental and theoretical values for the integral void experiments, although the theoretical values presented here do not include the effect of control rods, which were actually present in the core during the experiments.

Rather similar experiments, both differential and integral, were performed for the first fuel charge of HBWR; they are reported in [5]. Since these experiments were performed in HBWR itself at a number of different lattice positions with a core geometry practically identical with the one used for the power core, it was found possible to extrapolate from the pure experimental results of the differential experiments in such a manner that a prediction of the power void coefficient could be made.

In a general boiling-water power-reactor design, however, it is very unlikely that differential void experiments can be made in the final power core geometry. Such low-power experiments are normally made in a core geometry considerably smaller than the power core. In this case, direct extrapolation from the differential experiments to the power void reactivity based upon experimental data only is not possible. The differential experiments will then be used by the theoretical reactor physicist to test the methods he wants to apply for calculating the integral void effect. The role of low-power critical experiments concerning void effects and theory thus seems to be of equal importance for prediction of power void reactivity in a boiling-water reactor in the immediate future as long as new fuel elements designs for boiling-water reactors are proposed and methods for the calculation of void effects are not well established.

2. GENERAL DESCRIPTION OF THE EXPERIMENTS

2.1. Fuel elements

The fuel elements of the second charge of HBWR consist of a cluster element with seven stringers containing 1.5% enriched UO_2 pellets, 1.26 cm in diameter and canned in Zircaloy-2. The stringers form a hexagonal pattern, with one of the stringers at the centre of the hexagon. The design of the fuel element is shown in Fig. 1.

Each stringer is made up of two segments, which are screwed together. At each end of the enriched fuel in a segment there is a pellet of natural UO_2. The stringers are connected to top and bottom end grids through Zircaloy-2 extension rods. The end grids are of stainless steel and fix the end position of the stringers. A shroud made of Zircaloy-2 surrounds the stringer assembly and serves the purpose of defining the coolant flow.

Spacing and stiffening of the stringers is provided by stainless-steel spacing plates at the end of the fuel part of the stringers. The stringers are mounted on the central spacer plate, which is supported by the shroud. Thus, the extension rods are free to expand through the holes in the end grids. The fuel element assembly is supported by the bottom plate through the extension piece screwed on to the lower end grid.

2.2. Reactor cores

2.2.1. NORA experiments

The differential experiments in NORA were performed in a core consisting of 36 Halden second-charge fuel elements in an open hexagonal lattice with a 13-cm pitch (Fig. 2). The fuel elements were suspended in the cylindrical tank of the NORA reactor which was filled with D_2O to the level where criticality was reached. The bottom cone of the fuel elements was kept 5 cm above the bottom of the tank. Due to the presence of extension pieces in the fuel elements, the fuel region starts at 49 cm above the bottom of the reactor tank. The equivalent core radius is 50.16 cm and the tank radius 112.5 cm, leaving a D_2O side reflector of 62.34 cm. Outside the reactor tank a graphite side reflector of 50 cm and a bottom reflector of

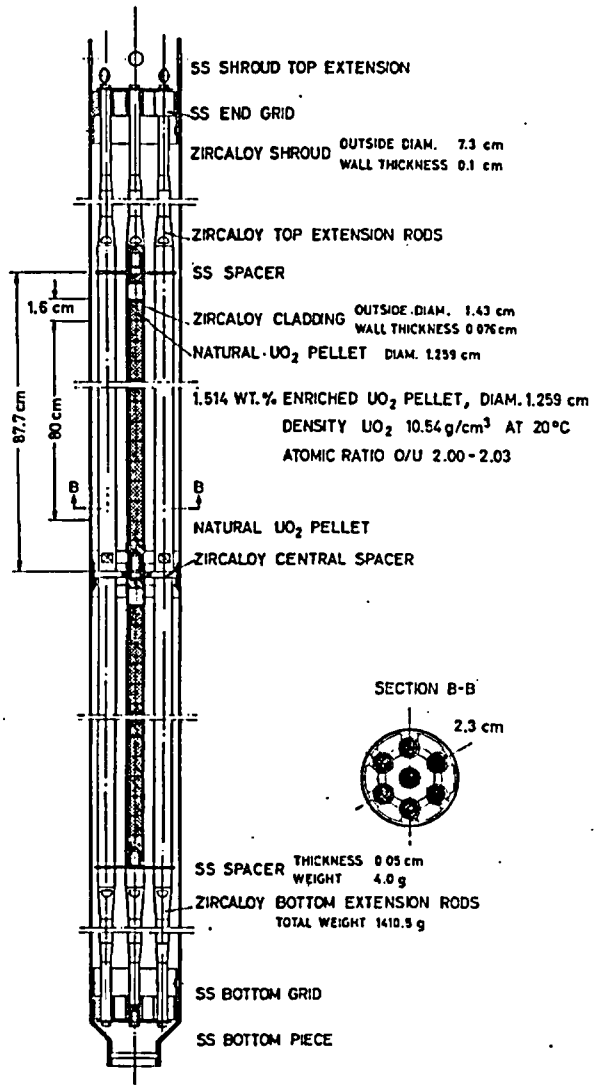

Fig.1

HBWR second-charge fuel element assembly

70 cm thickness were present. A full description of the NORA Critical Facility is given in [6].

2.2.2. HBWR experiments

The differential and integral void experiments in HBWR were performed in a core with 100 second-charge fuel elements in an open hexagonal lattice

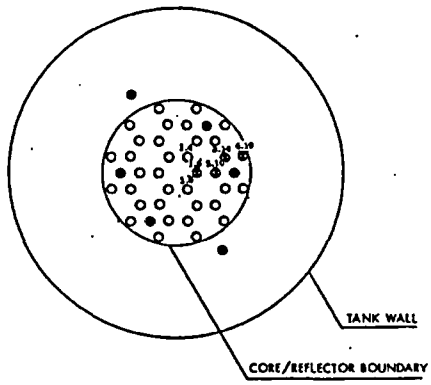

Fig.2

Horizontal cross-section through NORA core

- o Fuel element
- • Position of voided fuel element
- • Safety rod

with a lattice pitch of 13.0 cm. A diagram of the core loading is shown in Fig.3. The equivalent core radius is 83.6 cm and the D_2O side reflector has a thickness of 51.4 cm. The bottom reflector, consisting of a mixture of D_2O, steel and Zr, has a thickness of 38.3 cm.

For the differential experiment the reactor tank was filled with D_2O until criticality was reached at each temperature. The water level was thus considerably below the upper end of the fuel in all these experiments. No control rods were inserted in the core.

During the integral void experiments the water level was high enough to form a top reflector with a thickness of 13 to 21 cm, depending upon the temperature. The excess reactivity was shimmed off by three to four fully-inserted control rods and a regulating rod.

2.3. Experimental techniques

2.3.1. NORA differential experiments

The differential void measurements in NORA consisted essentially of measuring the reactivity worth of voids as a function of void depth in a single test element. Fig.2 shows the lattice positions in which the experiments were performed. A full description of the experiment is found in [1]. The coolant channel in the test element was subdivided into a number of subchannels by thin-walled aluminium tubes, and the reactivity effect of completely voiding various combinations of subchannels, using air, was investigated. Two methods were used for measuring the reactivity effect, the oscillating method and the static method.

2.3.1.1. Test fuel element. When operating HBWR at power, void fractions (defined as the ratio between the volume of steam and the volume of the

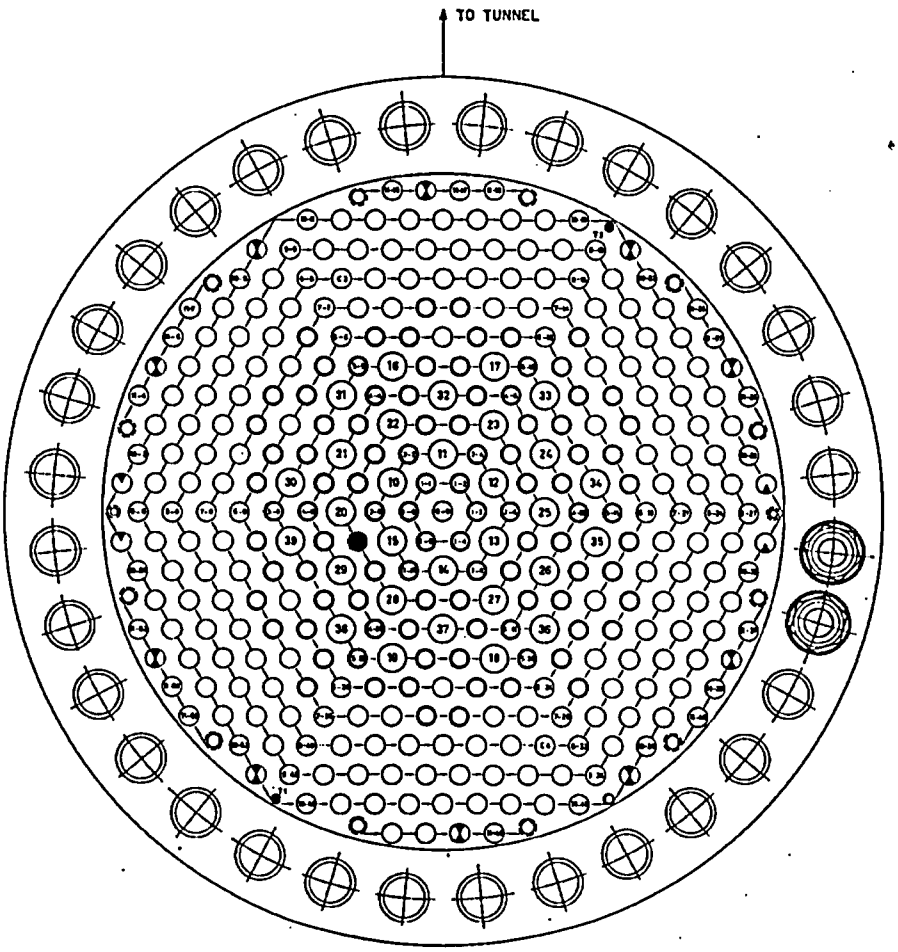

Fig.3

Core loading

Condens. in		2
Subcooled water-bottom		2
Subcooled water-top		12
Steam pipe drain		2
Thermocouples		
C3	Ionization chamber	
•	Void element	
Pressure meter P14 and P5		1
Nuclear instr.		2
Bolts		32
Plugged holes for exp. equipment		201
Control station		30
Fuel element		100
Steam out		10

Control rods 10-19 bank 1
control rods 20-29 bank 2
control rods 30-39 bank 3
control rods 20-22-23-25-27-28 are of smaller type
control rods 31-35-38 are regulating rods

coolant channel) between 0 and 0.8 will occur. It is expected that the void will have a fairly homogeneous distribution radially inside the coolant channel. In order to simulate these conditions by using air, it is necessary to subdivide the volume inside the shrouds into airtight sections. The coolant volume was subdivided by the insertion of 12 aluminium tubes between the fuel stringers, see Fig. 4. The void tubes were made of 0.012-cm thick aluminium foil by bending this around a rod and connecting the sides with Araldite. In this way tubes with uniformly thin walls were obtained. Above the active part of the core the tubes were glued to pipes with greater wall thickness. Hexagonal spacers were keeping the bundle of void tubes and spacers in the centre of the shroud. The tubes were grouped together in groups of three as indicated in Fig. 4 to form a void channel. The volume outside the tubes also forms a void channel.

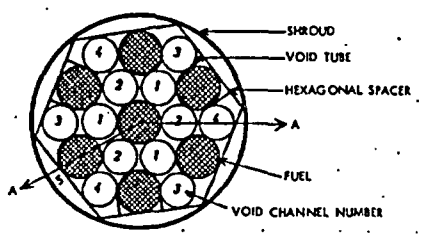

Fig. 4

Fuel assembly with 12 void tubes

2.3.1.2. Oscillating method. The technique for oscillating void measurements has been described in detail elsewhere [7] and will be only briefly outlined here. Each void channel was connected to pneumatic equipment [8] by which the water level inside the individual channel or combination of channels could be depressed to a certain depth. This water level could also be oscillated automatically with a period of 36.5 s between any two preset levels.

The response of the reactor to the coolant oscillations was detected by a fission chamber and analysed electronically by means of standard pile oscillator equipment, including a sine-cosine multiplier, synchronized with the pneumatic system to rotate with the fundamental period of pressure oscillations. By means of the calculated zero-power transfer function for HBWR, the fundamental mode amplitude of the flux response was converted into reactivity amplitude. Uncertainties in the calculated zero-power transfer function mainly caused by uncertainties in the delayed neutron data is within ± 4%, which is reflected in an equal systematic error in all reactivity data.

The periodic oscillations of void depth were very nearly rectangular in waveform. Small deviations in the waveform from the square wave were measured and corrected for in the amplitude of the fundamental mode. In most cases the correction was smaller than 1%.

A large correction had to be applied to the primary reactivity data because of oscillations in the bulk moderator level, caused by the local oscillations in one fuel element. The displaced volume of water could be calculated accurately and the water level coefficient of reactivity was determined experimentally with an accuracy of 0.3% by oscillating the bulk water level.

With the pneumatic equipment the water level in the coolant channels could also be adjusted manually to a preset depth. This could be done in any combination of channels, independent of any oscillations in the other channels. Interaction effects between voided regions could then be determined by measuring the void reactivity effect in a particular channel either with or without void in other channels. Interacting static voids were always introduced to full depth in a channel, because it was demonstrated [9] that interaction effects do not depend upon the depth of the static void as long as this depth is larger than the one to which the water level is oscillated in the other channel.

2.3.1.3. Static method. The manual adjustment was also used to perform static measurements of void reactivity. The procedure was then to keep the reactor balanced at a certain power level by adjusting the bulk water level in the reactor tank whenever the water level in the void channels was changed. The changes in bulk water level were measured with an electric water-level feeler gauge of high sensitivity. They were converted into reactivity by means of values of the water level reactivity coefficients, determined as described in 2.3.1.2. The level feeler gauge of the NORA reactor operates automatically with a preselected period. The reproducibility of consecutive measurements was usually within a few hundredths of a millimetre. In order to obtain an accurate determination of the water level each measurement was repeated ten times. Standard deviations corresponding to less than 0.2 pcm were obtained in many cases.

In the procedure of determining the critical water level enters also the uncertainty in criticality of the reactor. With the available recorder on the control panel of NORA a deviation of 0.2% in power over 2 min can be detected and corrected for. This corresponds to a deviation from criticality of 0.5 pcm.

2.3.2. HBWR differential experiments

The differential void experiments in HBWR were performed in order to investigate the void reactivity dependence upon temperature up to the maximum operating temperature of HBWR which is 230°C. The coolant level in a single fuel element was depressed by gas under pressure. The position of the test fuel element in the core is shown in Fig.3.

2.3.2.1. Test fuel element. The construction of one fuel element was altered in such a way that there were no upper flow holes in its shroud. Its upper extension tube and upper extension rods were removed and it was connected to a tube leading to a flow system outside the reactor tank. The connection between the tube and the reactor tank was made by welding the tube in a standard plug of the reactor top lid. This construction could withstand operating temperature and pressure of the reactor without giving rise

to leakage. The bottom of the fuel element was plugged in order to prevent pressure effects from subcooler flow.

2.3.2.2. Pneumatic system. The flow system outside the reactor tank was designed in such a way that pressurized argon from outside the reactor hall could be led into the fuel element when a valve was opened from the control room. The coolant level could be reduced gradually by using a pressure reduction valve. A differential pressure cell was connected to the top of the fuel element on one side and to the steam space in the reactor tank on the other side.

The void depth in the test fuel element was determined by the readings of this differential pressure cell. There were two calibration points: when the cell was bypassed and the moderator level in the reactor tank was equal to the coolant level in the shroud and when the argon reached the bottom flow holes of the fuel shroud. The void depth could be determined with an accuracy of ± 2 mm. The reading of the cell was continuously recorded.

2.3.2.3. Measurement of reactivity. The reactivity effect of voiding part of the test fuel element was determined in two independent ways. The first method was to measure the positive asymptotic reactor period when a certain amount of void was released. The temperature had to be quite stable during the measurements. It was therefore monitored with an accuracy of 0.02°C by reading the voltage of a thermocouple in the moderator with a compensator. The asymptotic period method is limited to the measurement of reactivities between 60 and 100 pcm. If the reactivity is smaller it is no longer possible to keep the reactor conditions stable over the long period during which the asymptotic doubling time has to be measured. Larger positive reactivities were not tolerated because of safety considerations. For the present experiments the limitation was quite serious, as the reactivity to only a few void depths could be measured in this way.

The second method consisted of calculating the reactivity directly from reactor power with an analogue computer [10]. In order to achieve this, the space independent reactor kinetic equations were programmed on an analogue computer in such a way that the output of an ionization chamber in the reactor core could be used as input to the computer, which would then give reactivity as output. In this way one does not have to wait for asymptotic periods to develop after a step in reactivity. The output from the reactivity meter was recorded continuously (synchronous with the void depth). This method is quite rapid and it allows measurements of small reactivity changes. However, because of the rapid response of the meter, it is quite sensitive to reactor noise. At low temperature there was very little noise, but at high temperature the noise was considerable. Many measurements were therefore performed and the averages were calculated for the reactivity effects of voiding the fuel element to various depths.

A systematic uncertainty both in the asymptotic period method and the reactivity meter method of ± 4% may exist because of uncertainties in delayed neutron data. The accuracy of the asymptotic period method is of the order of ± 1% in reactivity, while the standard deviation in the reactivity meter measurements is of the order of ± 2 pcm. The uncertainty in the measured bulk water level correction introduces an uncertainty of the order of ± 2% in the reactivity data.

2.3.3. HBWR integral experiments

The integral void experiments in HBWR were performed in order to investigate the boiling void reactivity as a function of nuclear power. The measurements were performed at different temperatures and also with different degrees of subcooling of the liquid coolant entering the lower end of the fuel channel. The subcooling affects the void distribution in the channels and thereby also the void reactivity.

A number of corrections, such as xenon reactivity and moderator temperature drift, have to be applied to the experimental results. Since the power void reactivity cannot be separated from fuel temperature reactivity experimentally, the two effects are lumped together even in the theoretical comparison.

2.3.3.1. Reactivity measurements. The experiment was started by balancing the reactor at a power level slightly in excess of subcooling power and heat losses, thus representing a condition of practically no void. The nuclear power level was raised in steps and the reactor was rebalanced at each step by means of the regulating rod. The regulating rod was calibrated reactivity-wise both in the condition of no void and at a high power level with appreciable amounts of void. In a boiling-water reactor the reactivity worth of a control rod obviously depends upon the power level, since the presence of voids normally changes the physics characteristics of the core considerably. Calibration of the regulating rod at high power levels was enabled by the use of the reactivity oscillator installed in the central core position. For a description of the oscillator see [11]. The regulating rod was inserted stepwise in the core, counteracting the added reactivity by removing reactivity at a constant amount by changing the rotor setting of the oscillator, while keeping nuclear power constant.

The constant amount of reactivity from the oscillator was afterwards found by measuring the reactivity-to-power-transfer function when rotating the oscillator at a frequency so high that the power transfer function is equal to the zero-power transfer function. The procedure outlined was repeated to cover the whole range of rod insertion.

2.3.3.2. Void fraction measurements. During this experiment an instrumented fuel assembly was present in the core. The instrumented fuel assembly will be used for extensive investigations of the dynamic behaviour of various parameters such as fuel temperature and void fractions, and in the integral void experiment measurements of the exit void fraction could be performed.

Instruments such as impedance void gauge and inlet and outlet turbines were used in the void fraction measurements. For a description of the instrumented fuel assembly see [12]. Measurements of the exit fraction thus indicate how well one can predict the void distribution in the core.

2.3.3.3. Correction for xenon reactivity. Corrections for the variations in the reactivity caused by xenon poisoning had to be applied to the experimental data. Some measurements of the xenon reactivity were made after a sequence of measurements at increasing power levels by going back to the starting condition of no void. The corrections were obtained by simulating the xenon equations on an analogue computer and running the power

history from the experiment in an accelerated time scale. The reactivity results obtained are in good agreement with the xenon reactivity measurements performed during the integral void experiment and also with a special xenon experiment performed earlier. The uncertainty in the xenon corrections are of the order ± 30 pcm.

2.3.3.4. Corrections for temperature drift. The moderator temperature as measured by thermocouples installed in the core could be measured with an accuracy of 0.025°C. By changing the moderator temperature while operating at power, the moderator temperature coefficient could be measured using the calibrated control rod. Temperature reactivity corrections for temperature drifts during the measurements could thus be made.

3. EXPERIMENTAL RESULTS AND ANALYSIS

The experimental results as presented below represent only a selection of all the various conditions investigated. For instance the NORA differential experiment involved more than forty different void geometries. Complete descriptions can be found in [1-3].

3.1. NORA differential experiments

Some of the experimental results in the NORA void experiment are given in Figs. 5 to 9. The curves show the reactivity effect of void as a function of the void depth. It should be mentioned that all reactivities are negative.

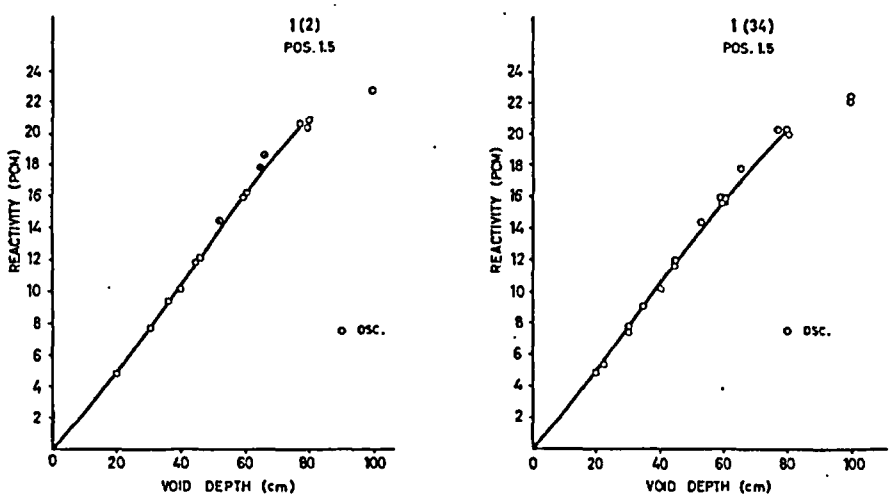

Fig. 5

Reactivity effect of void in three central tubes

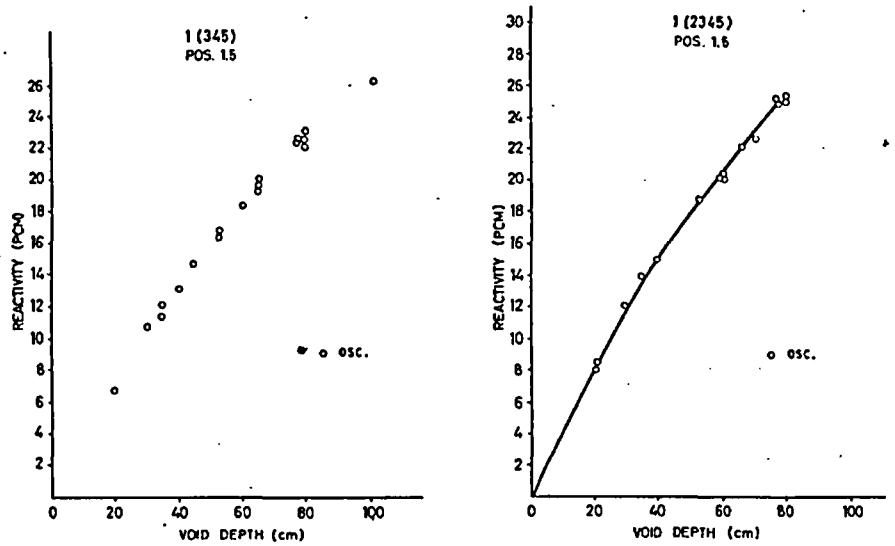

Fig. 6

Reactivity effect of void in three central tubes

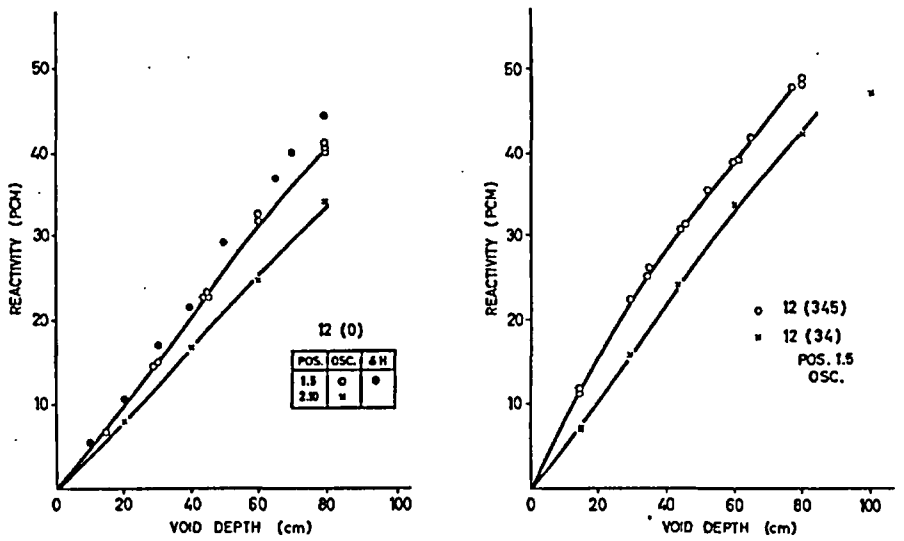

Fig. 7

Reactivity effect of void in six central tubes

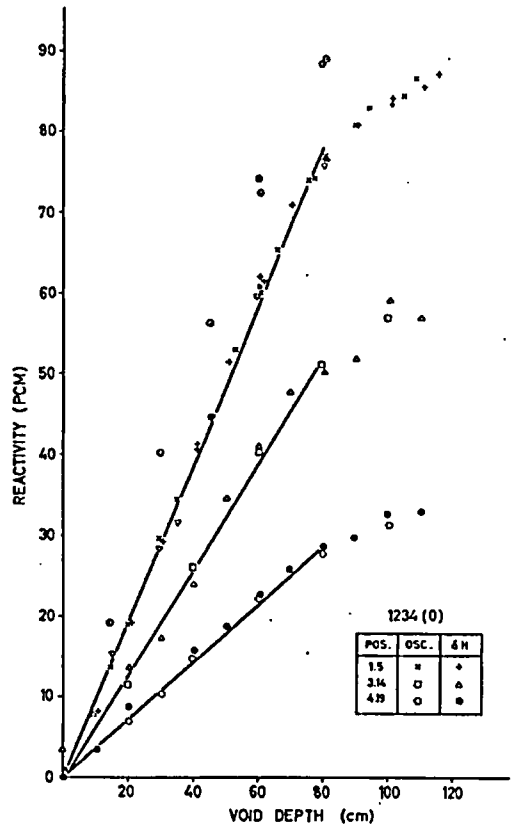

Fig. 8

Reactivity effect of void in 12 tubes

The symbolism used for indicating the void geometry is given by the following examples: 12(34) means the reactivity effect of voiding channels 1 and 2 (see Fig. 4) while channels 3 and 4 contain static void. 12(0) means that no static void is present when voiding channels 1 and 2. The type of experimental technique and the lattice position (see Fig. 2) in which the measurements were performed are also given in these figures.

For comparison between experiment and theory it is of course quite meaningful to compare reactivity values directly. It is well-known, however, that the introduction of void in a coolant channel changes practically every lattice parameter within the diffusion theory picture: diffusion coefficients and homogenized cross-sections as well as the multiplication factor. The results from the differential experiment can be analysed in a manner which permits experimental parameters to be found that represent in principle the void dependence of various lattice parameters separately by a least squares fitting procedure. A more severe test upon the theoretical lattice parameter can thus be made. This procedure assumes that

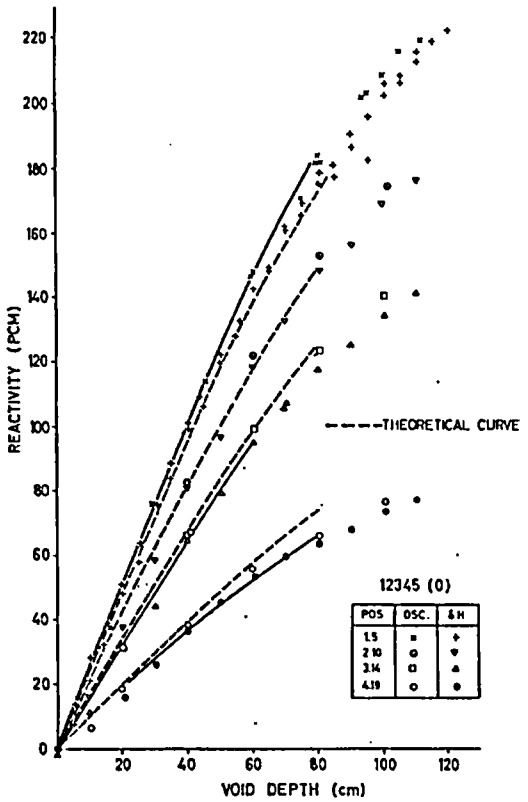

Fig. 9

Reactivity effect of void in all channels

perturbation theory is valid. The assumption has been tested and it was found that perturbation theory gives about 3% too low reactivity values for a void fraction equal to one. The measurements have been analysed by first-order perturbation calculations based upon two-group theory for an anisotropic reactor.

Assume the following diffusion equations to hold for the fluxes in the critical reactor:

$$\frac{1}{r}\frac{\partial}{\partial r}\left(r D_{fr}\frac{\partial \varphi_f}{\partial r}\right)+\frac{\partial}{\partial z}\left(D_{fz}\frac{\partial \varphi_f}{\partial z}\right)-\Sigma_f\varphi_f+\frac{k}{p}\Sigma_t\varphi_t=0$$

$$\frac{1}{r}\frac{\partial}{\partial r}\left(r D_{tr}\frac{\partial \varphi_t}{\partial r}\right)+\frac{\partial}{\partial z}\left(D_{tz}\frac{\partial \varphi_t}{\partial z}\right)-\Sigma_t\varphi_t+p\Sigma_f\varphi_f=0$$

with the adjoint equations: (1)

$$\frac{1}{r}\frac{\partial}{\partial r}\left(r D_{fr}\frac{\partial \varphi_f^+}{\partial r}\right)+\frac{\partial}{\partial z}\left(D_{fz}\frac{\partial \varphi_f^+}{\partial z}\right)-\Sigma_f\varphi_f^+ + p\Sigma_f\varphi_f^+ = 0$$

$$\frac{1}{r}\frac{\partial}{\partial r}\left(r D_{tr}\frac{\partial \varphi_t^+}{\partial r}\right)+\frac{\partial}{\partial z}\left(D_{tz}\frac{\partial \varphi_t^+}{\partial z}\right)-\Sigma_t\varphi_t^+ + \frac{k}{p}\Sigma_t\varphi_t^+ = 0.$$

These equations have been solved with the two-dimensional code made by HASSIT [13] for the unperturbed system. The fluxes and their adjoints obtained in this way have been used in the following first-order perturbation expression, which is derived from the two-group equations.

$$\rho = \frac{\delta k_{eff}}{k_{eff}} = A\left[\frac{k}{p}\Sigma_t I_0\right]^{-1}\left\{-\delta(\Sigma_f)I_1 + \delta(p\Sigma_f)I_2 + \delta\left(\frac{k}{p}\Sigma_t\right)I_3 - \delta(\Sigma_t)I_4 - \delta(D_{fr})I_5 - \delta(D_{tr})I_6 - \delta(D_{fz})I_7 - \delta(D_{tz})I_8\right\} \quad (2)$$

in which

$$I_0 = 2\pi\iint_{core}\varphi_f^+(r,z)\,\varphi_t(r,z)\,r\,dr\,dz$$

$$I_1 = \int_{z=0}^{z}\varphi_f^+(r_1,z)\,\varphi_f(r_1,z)\,dz$$

$$I_2 = \int_{z=0}^{z}\varphi_t^+(r_1,z)\,\varphi_f(r_1,z)\,dz$$

$$I_3 = \int_{z=0}^{z}\varphi_f^+(r_1,z)\,\varphi_t(r_1,z)\,dz$$

$$I_4 = \int_{z=0}^{z}\varphi_t^+(r_1,z)\,\varphi_t(r_1,z)\,dz$$

$$I_5 = \int_{z=0}^{z}\frac{\partial\varphi_f^+}{\partial r}(r_1,z)\,\frac{\partial\varphi_f}{\partial r}(r_1,z)\,dz$$

$$I_6 = \int_{z=0}^{z}\frac{\partial\varphi_t^+}{\partial r}(r_1,z)\,\frac{\partial\varphi_f}{\partial r}(r_1,z)\,dz$$

$$I_7 = \int_{z=0}^{z} \frac{\partial \varphi_f^+}{\partial z}(r_1, z) \frac{\partial \varphi_f}{\partial z}(r_1, z)\, dz$$

$$I_8 = \int_{z=0}^{z} \frac{\partial \varphi_f^+}{\partial z}(r_1, z) \frac{\partial \varphi_f}{\partial z}(r_1, z)\, dz.$$

In order to calculate the integrals $I_0 - I_8$ a code was developed for a Ferranti Mercury computer. The integrals $I_1 - I_8$ are calculated to an arbitrary depth at an arbitrary radius in the core. The flux matrices of the two-dimensional flux calculation are used as input to the programme.

In Eq.(2) the integrals are calculated by the computer code to the same depths at which ρ has been measured for a particular combination of void channels in the test rod. If one inserts an arbitrary set of differential lattice parameters in Eq.(2), one can then find a set of values for ρ_{fitted}, corresponding to the experimental void depths. In order to define in a unique way which set of differential lattice parameters shall be chosen, $\Sigma(\rho_{fitted} - \rho_{meas})^2$ is taken to be a minimum. In other words, using the calculated values for the perturbation integrals one makes a least squares fit to the observed reactivity data to obtain best apparent values for the individual differential lattice parameters. A unique set is obtained if a sufficient number of measured values to various depths is available for ρ.

There are two practical limitations to this procedure. In the first place there is an uncertainty up to ± 2% in the experimental values for ρ (not taking into account the systematic uncertainty of ± 4% in the transfer function). If a large number of measurements to various depths are available for a particular combination of void channels, a least squares fit will still give good results. However, another limitation is set by the computed perturbation integrals. If some of them are nearly proportional to each other, the parameters calculated from the least squares fit may not represent the differential lattice parameters, even though a good fit to the experimental points can still be obtained. In this case the calculated parameters may become very large without necessarily making the total value of the perturbation expression large, as could occur when the parameters have opposite signs. Even in this case the method can still be valuable in obtaining more detailed information about lattice parameters than the simple comparison of reactivities can give.

For example, in the present case it turned out that the first six integrals were proportional within a few per cent, though the fifth and sixth terms are small due to the small radial leakage. The differences between the first four integrals are of the same order as the uncertainties in the experimental points. It is, therefore, not justifiable to use them separately in a least squares fit so that a single integral (I_2) has been used for all terms. The same holds for the integrals I_7 and I_8, so that the terms containing these have also been grouped together and a single integral (I_7) has been used. Least squares fits to the experimental points were therefore made with two parameters, one (P) essentially representing the changes in multiplication properties of the lattice contained in the first four terms, the other (Q) representing the changes in axial leakage due to voidage of a coolant channel.

The factor $A[\frac{k}{p}\Sigma_t I_0]^{-1}$ has been combined with the integrals and is therefore not contained in P and Q. The parameters calculated in this way are listed in Table I for various void geometries. The accuracy of a combination

TABLE I

EXPERIMENTAL AND THEORETICAL VALUES OF VOID PARAMETERS FOR THE NORA EXPERIMENT

Position 1.5

Experimental					Theoretical Equivalent void fraction
Void configuration	1(0)	1(0)*	2(0)		α_{eff}=0 - 0.105
P	3.16	3.02	3.23		3.03
Q	3820	4510	3670		2314
Void configuration	12(0)	12(0)*	23(0)		α_{eff}=0.0 - 0.211
P	6.30	6.66	5.42		5.68
Q	8070	9160	7880		4933
Void configuration	34(0)	34(0)*	14(0)	14(0)*	α_{eff}=0.0 - 0.211
P	4.72	4.77	5.57	6.19	5.68
Q	7860	8480	7780	8510	4933
Void configuration	1234(0)	1234(0)			α_{eff} = 0 - 0.422
P	11.2	8.21			11.45
Q	16600	23750			11346
Void configuration	5(0)	5(0)*			α_{eff}=0 - 0.564
P	13.3	13.2			15.83
Q	20300	21750			16680
Void configuration	12345(0)	12345(0)*			α_{eff}=0 - 0.982
P	23.8	23.5			26.94
Q	45300	44700			45990
Void configuration	1(2)	2(1)			α_{eff}=0.105 - 0.211
P	3.15	4.33			2.66
Q	4280	3500			2619
Void configuration	1(34)				α_{eff}= 0.211 - 0.317
P	3.02				2.91
Q	4250				3008

* Static method

TABLE I (Cont'd)

Experimental					Theoretical Equivalent void fraction
Void configuration P Q	12(34) 6.38 8780	14(23) 5.43 9040	34(12) 4.73 11840		α_{eff}=0.211 - 0.422 5.77 6413
Void configuration P Q	14(5) 5.33 11150				α_{eff}=0.211 - 0.774 5.03 10283
Void configuration P Q	1(234) 3.00 4960	1(234)* 3.06 3660			α_{eff}=0.318 - 0.422 2.87 3405
Void configuration P Q	5(1234) 12.6 28400				α_{eff}=0.422 - 0.982 15.48 34643
Void configuration P Q	1(5) 2.89 5350				α_{eff}=0.564 - 66.9 2.23 4738
Void configuration P Q	1234(5) 10.5 25000				α_{eff}=0.564 - 0.982 11.1 29309
Void configuration P Q	1(345) 2.70 6390				α_{eff}=0.744 - 0.880 2.77 8064
Void configuration P Q	12(345) 5.70 13770	14(235) 4.93 14200	34(125) 4.28 14200		α_{eff}=0.771 - 0.982 6.03 19026
Void configuration P Q	1(2345) 2.76 7620				α_{eff}=0.877 - 0.982 3.31 10962

* Static method

of two parameters for a particular case is the same as the accuracy of the experimental points, though the individual uncertainty of the calculated parameters may in an unfavourable case be as large as 10%.

The fully drawn curve in Fig.5 to 9 represent then the least squares fitted curves, and it is seen that the procedure gives an excellent fit to the measurements. The fitting has only been made down to a depth of 80 cm, since larger depths are outside the core region.

The study of the dependence of void reactivity on void fraction in the coolant channel of the test rod with 12 aluminium tubes is complicated by the fact that the combinations of void channels do not represent a homogeneous distribution of voids in the fuel assembly.

The experimental results for a void depth of 60 cm are shown in Fig.10. No inhomogeneity effect is present for the fully voided channel (point 12345), and the straight line joining this point with the origin thus represents a linear dependence on void fraction. Inhomogeneous observed points lie on or below this line, indicating that the curve representing the effect of a truly homogeneous void fraction lies slightly below the straight line. Point 5, in which 80% of the void lies outside the fuel, represents a lower extreme which should lie below the true curve.

In Fig.10 it was evident that there was a dependence of void reactivity on the location of the void inside the fuel element. It is of interest to consider this variation in more detail. Ideally one should measure the effect of equal void volumes at different radii, but this was not possible with the

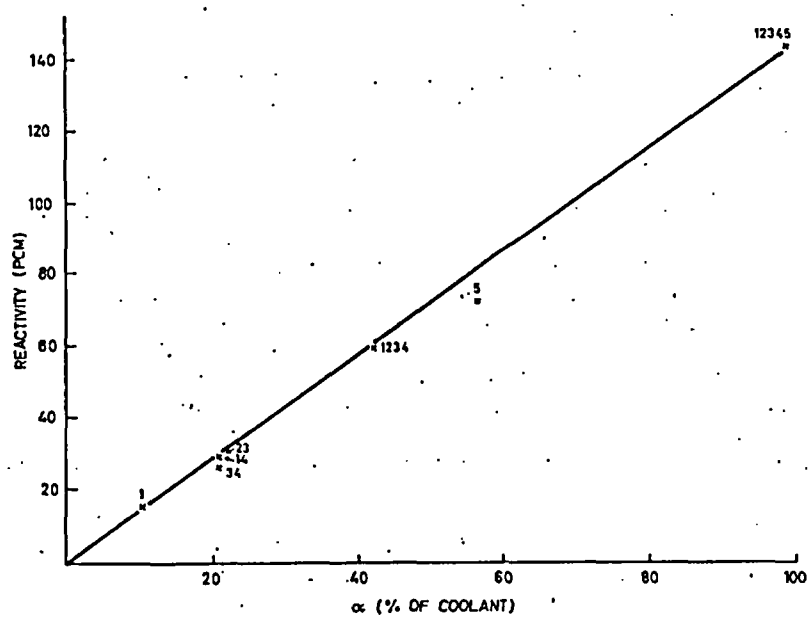

Fig.10

Dependence of void reactivity on void fraction

present apparatus. However, if one expresses the reactivity effect of a particular channel per cm^2 cross-section of this channel, it is possible to get an idea of the radial dependence of void reactivity, because the channels are at different locations in the fuel assembly. It can be seen from Fig.11

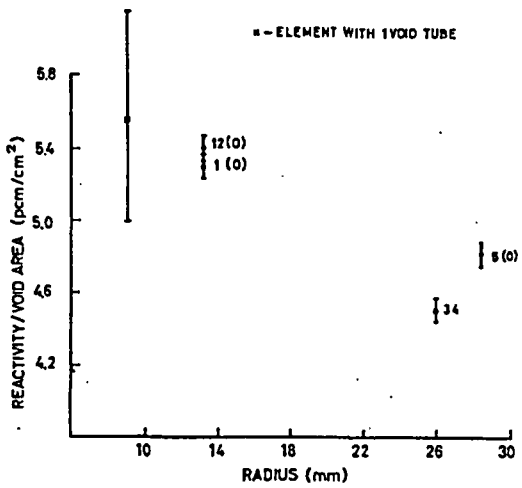

Fig.11

Variation of void reactivity with radial position within the fuel element

that the reactivity effect decreases in value with the distance from the centre of the assembly. In particular there is no tendency towards a positive reactivity effect in the centre of the fuel cluster. Because of void interaction effects, it is not feasible to derive quantitative conclusions from the measurements, qualitatively, however, the trend appears quite clear.

In order to investigate the mutual effect of voids in neighbouring channels, a systematic series of measurements was made of interaction effects on channel 1, which consisted of three tubes close to the centre of the fuel assembly. The void reactivity effect at a 60-cm depth in channel 1 is plotted in Fig.12 with void in various combinations of other channels. It can be seen in Fig.12 that an increasing void fraction in the fuel assembly increases the effect of void in channel 1. The effect is not linear. Note that the points including channel 2 all lie above the dotted curve, indicating that the interaction effect per cm^2 is largest for channel 2. (This channel is closer to the axis of the test rod than the other channels and closest to channel 1).

The fitted parameters show that more than 2/3 of the reactivity effect of voiding channel 1 is due to axial leakage of neutrons when there is still moderator in all other channels. The axial leakage doubles when all other channels are voided. On the other hand the multiplication parameter decreases slightly (~15%) when all moderator of the fuel assembly is removed. It can therefore be concluded that the main effect of voids in neighbouring channels is to increase the axial leakage of neutrons from channel 1.

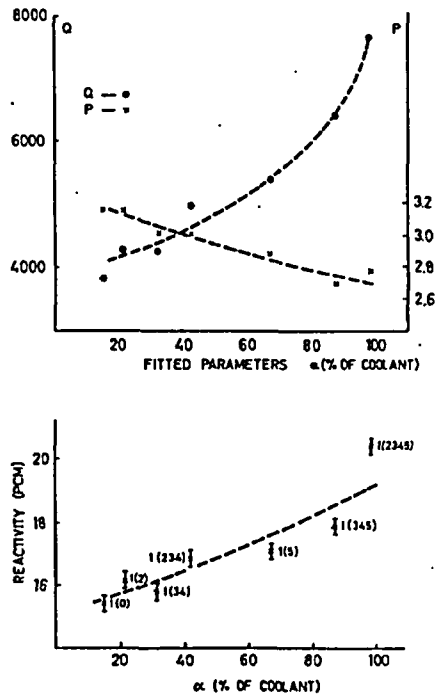

Fig.12

Void interaction effects on channel 1

3.2. HBWR differential experiments

The differential experiments performed in HBWR at various temperatures are analysed in exactly the same way as for the NORA experiment. The experimental values at different temperatures are given in Figs.13, 14 and 15. The experimental P and Q values are given in Table II.

3.3. HBWR integral experiments

The reactivity effect of power void and fuel temperature is presented as a function of nuclear power in Figs.16 and 17 at two different moderator temperatures. The uncertainties in the experimental points are about ± 40 pcm and ± 0.5 MW. The experimental points for exit void fraction in the instrumented fuel assembly as a function of assembly power is given in Fig.18.

4. THEORETICAL COMPARISONS

The theoretical comparisons with the various void experiments given below should be regarded as preliminary. They are made in order to obtain

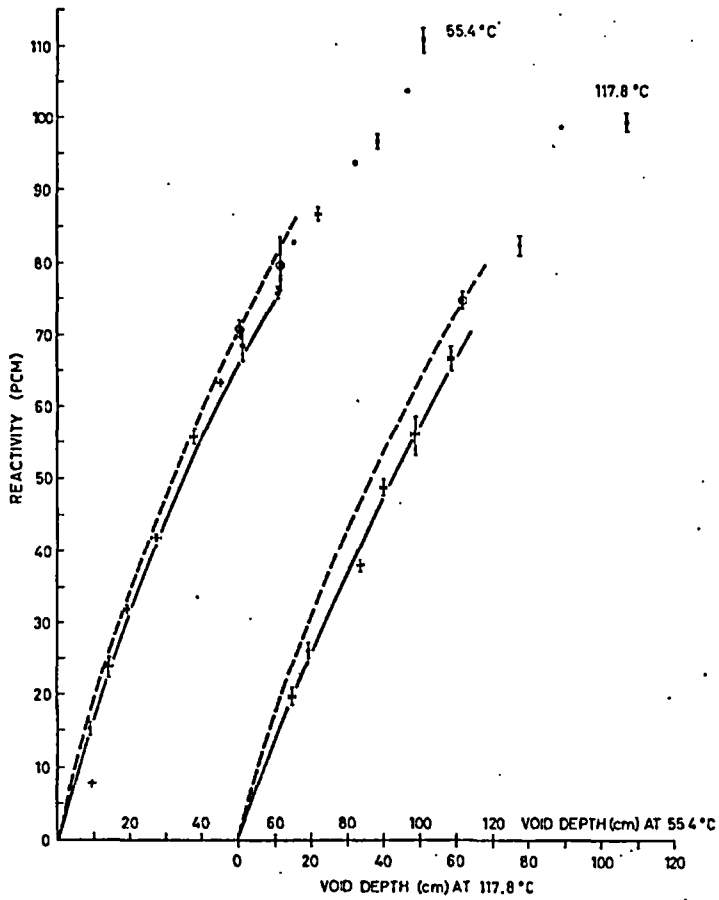

Fig. 13

Void reactivity as a function of void depth

- Reactor period measurement
- Output from 'reactivity meter'
- --- Calculated
- — Fitted to measured points

a feeling for the direction in which to concentrate further theoretical efforts in order to explain void effects. Improved methods are at present being developed and the final theoretical comparisons will be found in [1-3].

For D_2O-moderated and cooled reactors, two-group diffusion theory usually gives adequate descriptions of various reactivity effects and this frame has been adopted for the interpretation of the HBWR experiments.

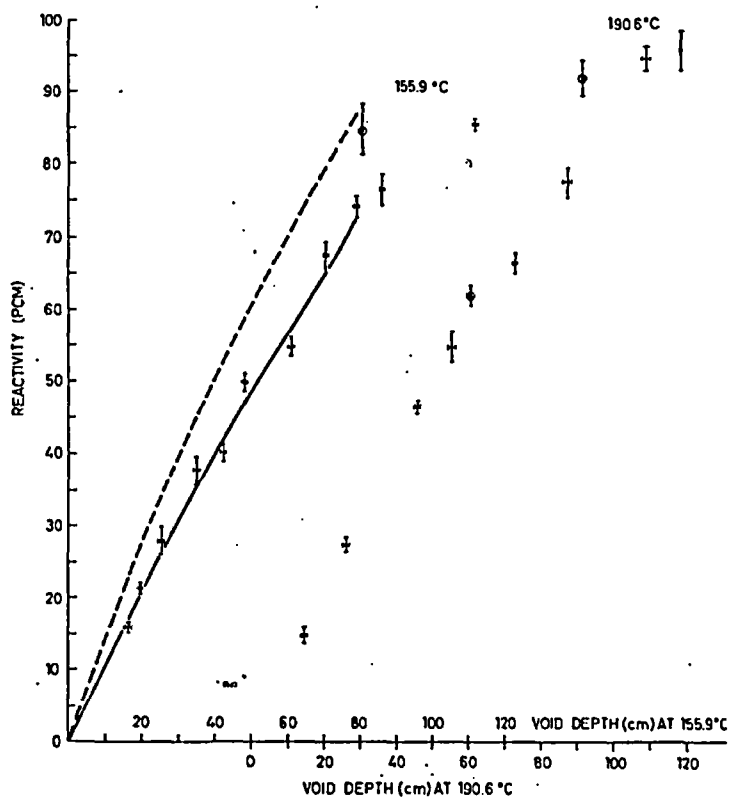

Fig. 14

Void reactivity as a function of void depth

- Reactor period measurement
- Output from 'reactivity meter'
- --- Calculated
- —— Fitted to measured points

For calculation of the two-group homogenized lattice parameters the Swedish recipe called BURNUP [4] has been used. The main characteristics of this code can be summarized in the following:

(i) Thermal neutron cross-sections. The thermal neutron absorption and fission cross-sections are calculated using Westcott formalism. In the present calculations the g- and s_4-factors from the 1960 Westcott compilation [14] were applied. The effective neutron temperature is an input to the programme. The neutron temperature was assumed to be equal to the true moderator temperature in the present calculations. The spectrum factor r is calculated as for a homogeneous reactor, but with corrections for non-uniform slowing-down density distribution and thermal flux depression in the fuel elements.

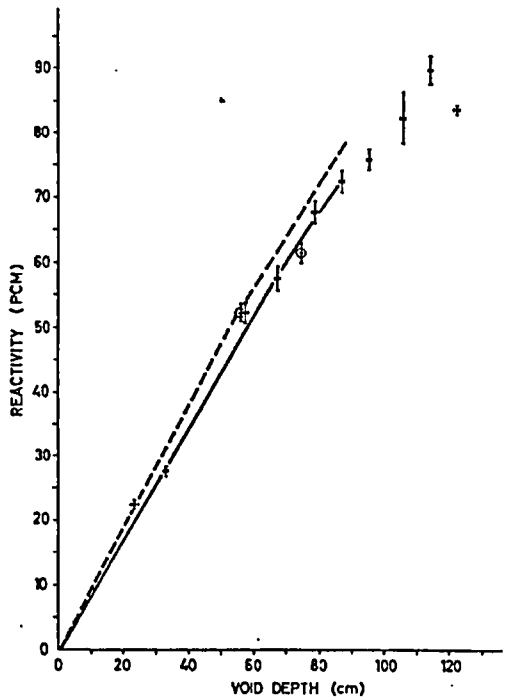

Fig. 15

Void reactivity at 220.3°C as a function of void depth

- Reactor period measurement
- Output from 'reactivity meter'
- --- Calculated
- — Fitted to measured points

(ii) Diffusion coefficients, etc. The diffusion coefficients are calculated according to BENOIST [15] as modified by WEISSGLASS [16]. It should be mentioned that the calculation is made in a three-region lattice cell model, the three regions consisting of the fuel and coolant within a rubber band around the fuel cluster, the remaining coolant between the rubber band and shroud, and the moderator outside the shrouds. The Fermi age, the thermal neutron diffusion area and the thermal utilization are calculated according to the methods presented by PERSHAGEN et al. [17].

(iii) Fast-fission. Only the fast fission in U^{238} is treated by the programme. The calculation is performed according to ALMGREN [18].

(iv) Resonance escape probability. The resonance absorption is treated separately for U^{238} and materials of construction by the inclusion of two resonance escape probabilities, p_{28} and p_s. In the present calculation the resonance integral of U^{238} is divided in two energy groups, corresponding to a two kernel fit of the measurements of

TABLE II

EXPERIMENTAL AND THEORETICAL VALUES OF VOID PARAMETERS HBWR DIFFERENTIAL EXPERIMENTS

(α = 0 - 1.0 in all experiments)

Temperature (°C)		Experimental	Theoretical
55.4	P	23.1	25.5
	Q	46100	49300
117.8	P	24.5	23.4
	Q	41400	49900
155.9	P	21.6	23.4
	Q	38500	51600
220.3	P	22.5	22.5
	Q	46200	52700

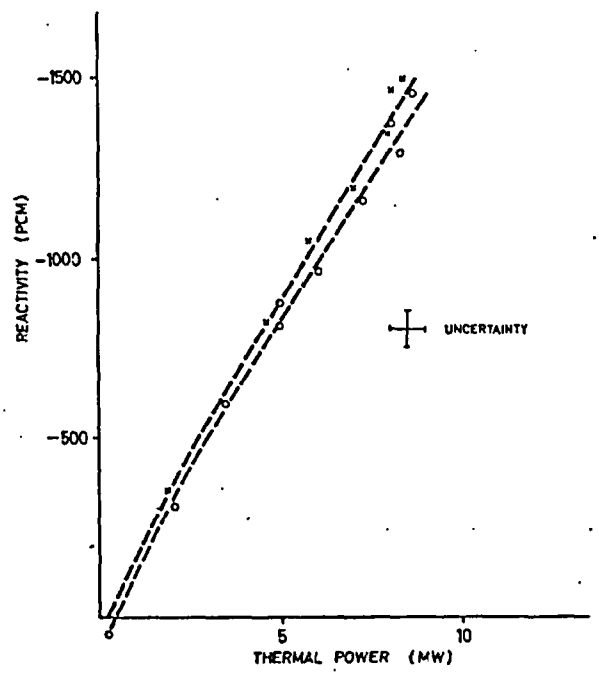

Fig. 16

Power void and fuel temperature reactivity plotted against thermal power (T = 190°C)

o Maximum subcooling
× Minimum subcooling

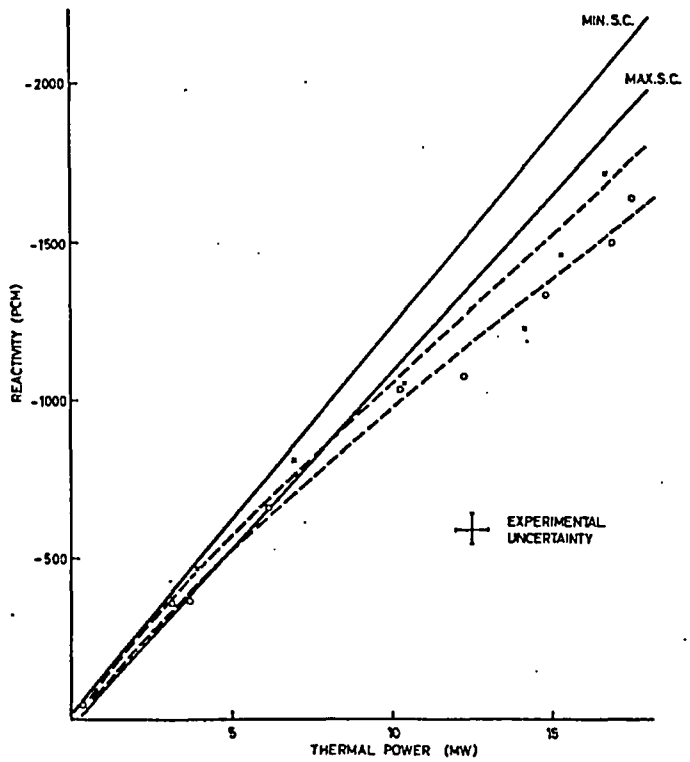

Fig.17

Power void and fuel temperature reactivity plotted against thermal power (T=230°C)

o Maximum subcooling
x Minimum subcooling
– Theoretical curves

the slowing-down distribution in heavy water. The value of the total resonance integral is taken from the measurements of HELLSTRAND [19]. The temperature dependence of the resonance integral is taken from the measurements made by HELLSTRAND et al. [20]. For cluster elements the Dancoff-Ginsburg correction for the surface within the cluster is treated by the approximate method of Carlvik-Pershagen [17]. In the calculation of the resonance escape probability, correction for the non-uniform slowing-down distribution is made.

This lattice parameter code has been used both for calculating the parameters for the non-voided core which then were used for calculation of the unperturbed flux distributions as mentioned in sections 3.1 and 3.2, and also for calculating the dependence of these parameters upon void fraction both for the differential and integral experiments.

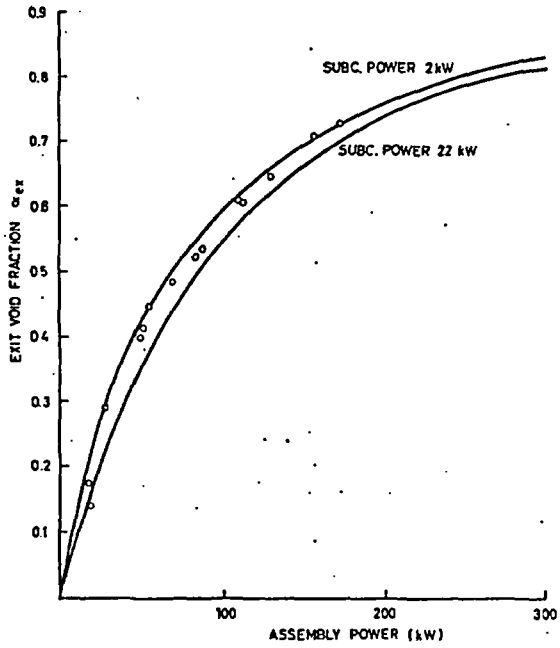

Fig.18

Exit void fraction plotted against assembly power

o Measured with instrumented fuel assembly at T = 230°C and Q_{sc} = 10 kW
— Calculated

4.1. *Differential experiments*

Having calculated the dependence of lattice parameters upon void fraction, the theoretical values for P and Q are obtained from the following formulae:

$$P_{theor} = -\delta(\Sigma_f)I_1 I_2^{-1} + \eta\,\delta(p\Sigma_f) + \delta(\frac{k}{p}\Sigma_t)I_3 I_2^{-1} - \delta(\Sigma_t)I_4 I_2^{-1} - \delta(D_{fr})I_5 I_2^{-1} - \delta(D_{tr})I_6 I_2^{-1} \tag{3}$$

and

$$Q_{theor} = -\delta(D_{fz}) - \delta(D_{tz})I_8 I_7^{-1}. \tag{4}$$

The main limitation to the theoretical comparisons with the NORA experiment is the fact that the lattice parameter code cannot treat void geometries which are inhomogeneous, so that direct comparison between experi-

ment and theory can only be made for geometry 12345(0) and also for all HBWR differential experiments. However, the various NORA measurements have been grouped together in Table I in groups having the same average void fraction when the voids are smeared out over the coolant channel and compared with the theoretical results for the same average void fractions. The theoretical results are also included in Table I. It is seen that in most cases the agreement between experiment and theory is not good, particulary in the diffusion coefficient parameter Q.

For the case 12345(0) where void-geometry used in experiment and calculation coincide, the agreement is good, the P values are somewhat too high. This could be expected, since comparison between experimental and theoretical buckling measurements for a number of voided lattices [21] also shows the same tendency. In these measurements the discrepancy was removed by using P_3-calculation for the intra-cell flux distribution rather than the approach used in the lattice parameter code.

In Table II corresponding comparisons are made for the HBWR differential experiment. Figs. 9, 13, 14 and 15 also show the calculated void reactivity versus void depth for completely voided coolant channels.

One might conclude from these comparisons that the agreement between theory and experiment is fair for the cases with void fraction equal to 1 and that the theoretical approach of smearing the void out over the coolant channel does not give a good agreement for the various void geometries.

Since a direct comparison cannot yet be made for void fractions less than 1, an indirect comparison can still be made by transforming the experimental reactivity data in such a manner that parameters for homogeneously distributed voids with void fractions less than 1 can be inferred.

Reactivities for a certain void depth can obviously be added together according to a principle demonstrated by the following examples:

$$\rho(1(0))+\rho(2(1)) = \rho(12(0))$$

or

$$\rho(1(0))+\rho(2(1))+\rho(3(12))+\rho(4(123))+\rho(5(1234)) = \rho(12345(0)).$$

Various cross-checks of this principle can be made from the measurements. We now want to find the reactivity value with an arbitrary void fraction α equal in each channel. The assumption is made that the interference term for a certain channel caused by void in the neighbouring channel is linear with the void fraction in this neighbouring channel, and further that the void reactivity for a certain channel is proportional to the void fraction in this channel. The assumptions are the same as used in [5] and [9], but there a different addition principle was used. We then obtain:

$$\begin{aligned}\rho(\alpha) = {} & \alpha\,\rho(1(0)) + \alpha[\rho(1(0)) + \alpha[\rho(1(2)) - \rho(1(0))]] \\ & + \alpha[\rho(34(0)) + \alpha[\rho(34(12)) - \rho(34)0))]] \\ & + \alpha[\rho(5(0)) + \alpha[\rho(5(1234)) - \rho(5(0))]].\end{aligned} \tag{5}$$

The formula is obviously correct in the limit of infinitely small channels. ρ can be substituted by P or Q, and $P(\alpha)$ and $Q(\alpha)$ inferred from the measurements can be evaluated from Eq.(5) and compared with theoretical values. Such a comparison is made in Table III for various α's.

TABLE III

COMPARISON BETWEEN EXPERIMENTALLY INFERRED AND THEORETICAL P- AND Q-VALUES

α=		0.25	0.50	0.75	1.0
From Eq.(5) and measurements	P	6.0	11.9	18.0	24.0
	Q	10000	21500	34000	48000
Calculated with BURNUP	P	6.8	13.6	20.5	27.3
	Q	6300	14000	26000	46000

It is seen that P is practically linear and is overestimated by the order of 10% by theory for all α's.

The Q-values, however, agree well at $\alpha = 1$ but discrepancies of up to the order of 30% too low theoretical values are found for intermediate void fractions. The discrepancy in P can probably be removed by performing improved intracell flux calculations. The discrepancy in Q can either be caused by the fact that the number of void channels used in the experiment are too few, or that the diffusion coefficient calculation is not adequate for intermediate void fractions.

The preliminary conclusion can then be drawn from the differential experiments that prediction of the integral void effect using the theoretical methods described can be expected to show a fair but not close agreement with experimental values.

4.2. Integral experiments

Fig.18 shows the measured and calculated exit void fraction as a function of fuel element power, indicating that the methods for calculating void distributions in HBWR can be relied upon.

Knowing the void distribution, the integral void reactivity effect can be calculated in various ways. One method is using perturbation theory as for the differential experiments, this was the method adopted for the first fuel charge [5]. Another method can be used by performing two-dimensional macroscopic calculations dividing the core into a number of zones with approximately equal void fractions.

The latter method has been used in some calculations for HBWR and the results of power void and fuel temperature reactivity versus nuclear power are given in Fig.17. It should be mentioned that the effect of control rods which were actually present in the core during the experiment were

not taken into account in these calculations and further that the theoretical void distribution calculation is not quite consistent with the present method from which the results in Fig.18 were obtained. Very detailed conclusions can thus not be made from Fig.17. The discrepancy between experimental and theoretical values is of the order of 25%.

A computer code which enables to take into account the effect of control rods is presently being made, and detailed comparisons will be made in Reference [3].

APPENDIX

LIST OF SYMBOLS

D_{fr}	radial fast diffusion coefficient
D_{fz}	axial fast diffusion coefficient
D_{tr}	radial thermal diffusion coefficient
D_{tz}	axial thermal diffusion coefficient
φ_f	fast flux
φ_t	thermal flux
k	infinite multiplication factor
p	resonance escape probability
Σ_f	macroscopic fast cross-section
Σ_t	macroscopic thermal cross-section
k_{eff}	effective multiplication factor
$\delta(Q)$	Q_2-Q_1, in which index 2 refers to the parameter Q after the perturbation (differential lattice parameter)
A	area of a lattice cell
ρ	reactivity
12(34)	void reactivity measured of channel 12 with static void present in channel 34 (see Fig.5) (example of symbolism in Tables and Figures)

REFERENCES

[1] HABERMANN, F.A., JAHREN, K., LUNDE, J.E. and ØYE, O., Coolant Void Reactivity Effect in the Second Fuel Charge of HBWR, Part I, Differential Experiments at Low Temperature, forthcoming Institutt for Atomenergi HPR Rpt.

[2] HABERMANN, F.A., Coolant Void Reactivity Effect in the Second Fuel Charge of HBWR, Part II, Differential Experiments at High Temperature, forthcoming Institutt for Atomenergi HPR Rpt.

[3] HABERMANN, F.A., JAHREN, K., LUNDE, J.E. and ØYE, O., Coolant Void Reactivity Effect in the Second Fuel Charge of HBWR, Part III, Integral Experiments, forthcoming Institutt for Atomenergi HPR Rpt.

[4] AHLSTRÖM, P.E., Calculation of Lattice Parameters as a Function of the Irradiation, EAES Symp. Mesurements and Calculations of the Influence of Burnup on Reactivity. Risø, Denmark (1961).

[5] BLOMBERG, P. and SOKOLOWSKI, E., Differential and Integral Investigation of Void Effects in HBWR, Institutt for Atomenergi Rpt. HPR-17 (1962).

[6] Hazards Summary Report for the NORA Critical Facility SS-NO, Institutt for Atomenergi, Norway (1961).

[7] ERIKSEN, V.O., Void Effects in Boiling Heavy Water Reactors, Proc. 2nd. UN Int. Conf. PUAE 11 (1958) 466.

[8] HANSSON, P.T., private communication.

[9] BERNANDER, G. et al., HBWR Void Experiments HPR-6.

[10] SASTRE, C.A., The Measurement of Reactivity, Nucl. Sci. Engng 8 (1960) 5.

[11] HBWR Quarterly Progress Report October - December 1962, Institutt for Atomenergi Rpt. HPR-29.
[12] AGER-HANSSEN, H. et al., Experience from the Operation of the Halden Heavy Water Boiling Reactor on its First Fuel Charge June 1959 to April 1961, HPR-26 (1961).
[13] HASSIT, A., A Programme for Solving the Multigroup Neutron Diffusion Equations in Two Space Dimensions on the Ferranti Mercury Computer, U.K.A.E.A. Rpt. AERE T/R 2487 (1958).
[14] WESTCOTT, C.H., Effective Cross Section Values for Well-Moderated Thermal Reactor Spectra, AEC Rpt. AECL-1101 (1960).
[15] BENOIST, P., Formulation générale et calcul pratique du coefficient de diffusion dans un réseau comportant des cavités, J. nucl. Energy, Part A: Reactor Science 13 (1961) 97-111.
[16] WEISSGLAS, P., Theoretical Calculation of the Effect on Lattice Parameters of Emptying the Coolant Channels in a D_2O-Moderated and Cooled Natural Uranium Reactor, Nukleonik 3 3 (1961) 53-7.
[17] PERSHAGEN, B. et al., Calculation of Lattice Parameters for Uranium Rod Clusters in Heavy Water and Correlation with Experiments, Proc. 2nd. UN Int. Conf. 12 (1958) 341.
[18] ALMGREN, B., On the Calculation of the Fast Fission Factor, A.B. Atomenergi Rpt. AE-27 (1960).
[19] HELLSTRAND, E., Measurements of the Effective Resonance Integral in Uranium Metal and Oxide in Different Geometries, J. appl. Phys. 28 12 (1957) 1493-502.
[20] HELLSTRAND, E. et al., The Temperature Coefficient of Resonance Integral for Uranium Metal and Oxide, Nucl. Sci. Engng 8 (1960) 497-506.
[21] AHLSTRÖM, P.E. and APELQVIST, G., personal communication.

DISCUSSION

C.F. HØJERUP: You mentioned that all the void reactivities measured in your experiments were negative. Could you tell me what the moderator-to-fuel ratio is in the second charge of the Halden reactor and how this is related to the optimum value?

J.E. LUNDE: The moderator-to-fuel ratio in HBWR is such that the lattice is slightly over-moderated.

G. LAUTENBACH: Do you make provision in the experimental set-up for measurements of increasing fractional void distribution in the core during operation of the HWBR? I would expect that there will be a greater specific void fraction in the upper part of the fuel-moderated region due to the accumulation of steam bubbles. Did you try to measure the void coefficient by introducing a linear increasing void fraction in the upper region of the core?

J.E. LUNDE: The test fuel element is voided to various void depths from the moderator water level downwards.

R. PERSSON (Chairman): The linear relationship between reactivity and void depth shown in some of your curves is, I suppose, purely accidental and depends on the lattice used.

J.E. LUNDE: Yes, the fact that some curves show linear relationship between void depth and void reactivity in the differential experiment is purely accidental.

EFFECTIVENESS OF A LARGE NUMBER OF CONTROL RODS IN THE SECOND CHARGE OF THE HALDEN BOILING WATER REACTOR

H. SMIDT OLSEN
OECD HALDEN REACTOR PROJECT, NORWAY

Abstract — Résumé — Аннотация — Resumen

EFFECTIVENESS OF A LARGE NUMBER OF CONTROL RODS IN THE SECOND CHARGE OF THE HALDEN BOILING WATER REACTOR. The reactivity worth of various control-rod configurations has been measured in the second fuel charge of the Halden Boiling Heavy Water Reactor (HBWR) under low power conditions. The second fuel charge of HBWR consists of 7-rod UO_2 cluster elements with 1.5% enrichment. A total of 30 control rods is placed in the open positions of the hexagonal fuel-lattice structure. In order to facilitate theoretical comparisons, measurements have been made on symmetrical control-rod configurations only.

The experiment consisted of measuring the critical water level for the clean core and with the different rod configurations inserted to various distances from the bottom of the reactor.

The temperature dependence of the reactivity worth was investigated by performing measurements, using a ring of 6 control rods, at the three different temperatures 34°C, 150°C and 220°C.

Comparisons of the experimentally-determined critical water levels and the calculated critical water levels are presented. The critical water levels are calculated both by a method in which the control rods are homogenized together with fuel and moderator to form a control-rod zone, and also by a heterogeneous method in which the fuel elements and control rods are regarded as line sinks to thermal neutrons and the fuel elements are regarded as line sources of fast neutrons.

EFFICACITÉ DE BARRES DE COMMANDE EN GRAND NOMBRE, DANS LA DEUXIÈME CHARGE DU RÉACTEUR A EAU LOURDE BOUILLANTE DE HALDEN (HBWR). L'auteur a mesuré l'antiréactivité de plusieurs configurations de barres de commande dans la deuxième charge de HBWR dans des conditions de puissance faible. La deuxième charge de ce réacteur est constituée par des cartouches formées de sept barres d'UO_2 enrichi à 1,5% en grappe. Trente barres de commande, au total, ont été disposées dans les places libres de la structure hexagonale du réseau de combustible. Pour faciliter les comparaisons avec les résultats théoriques, les mesures n'ont porté que sur les configurations symétriques de barres de commande.

L'expérience a consisté à mesurer le niveau critique de l'eau dans le cœur non empoisonné, les différentes configurations de barres étant enfoncées à des distances diverses du fond du réacteur.

L'auteur a étudié comment l'antiréactivité varie avec la température en procédant à des mesures sur un groupe circulaire de six barres de commande, aux températures de 34, 150 et 220°C.

Il établit des comparaisons entre les niveaux critiques de l'eau déterminés par l'expérience et ces mêmes niveaux obtenus par calcul. Les niveaux critiques de l'eau sont calculés, d'une part, selon une méthode dans laquelle barres de contrôle, combustible et ralentisseur considérés comme un tout sont homogénéisés pour former une zone de barres de contrôle et, d'autre part, selon une méthode hétérogène dans laquelle les éléments combustibles et les barres de contrôle sont considérés comme des «absorbants» linéaires pour les neutrons thermiques et les éléments combustibles comme des sources linéaires de neutrons rapides.

ЭФФЕКТИВНОСТЬ БОЛЬШОГО КОЛИЧЕСТВА РЕГУЛИРУЮЩИХ СТЕРЖНЕЙ ВО ВТОРОЙ ЗАГРУЗКЕ РЕАКТОРА HBWR. Поглощающая способность регулирующих стержней различной конфигурации была измерена во второй загрузке Халденского кипящего тяжеловодного реактора (HBWR) в условиях работы на малой мощности. Вторая топливная загрузка реактора HBWR состоит из топливных сборок, в каждой из которых по семь стержней из обогащенной до 1,5% UO_2. В незанятые ячейки гексагональной конструкции топливной решетки установлены 30 регулирующих стержней. Для облегчения теоретических сравнений измерены были только симметрические конфигурации регулирующих стержней.

Эксперимент заключался в измерении критического уровня воды для чистой активной зоны с различными конфигурациями стержней, введенных на различные расстояния от основания реактора.

Температурная зависимость компенсирующей способности, выраженной в единицах реактивности, была изучена путем проведения экспериментов с кольцом из шести регулирующих стержней при трех различных температурах (34, 150 и 220°C).

Приводится сравнение экспериментальных и расчетных критических уровней воды. Для расчета уровней использовались как метод, при котором регулирующие стержни гомогенизированы с топливом и замедлителем для создания зоны регулирующих стержней, так и гетерогенный метод, при котором топливные элементы и регулирующие стержни рассматриваются как линейные поглотители тепловых нейтронов, а топливные элементы — как линейные источники быстрых нейтронов.

EFECTIVIDAD DE LAS BARRAS DE CONTROL EN LA SEGUNDA CARGA DEL REACTOR HBWR. El autor determinó la influencia de las barras de control sobre la reactividad, para distintas configuraciones de dichas barras, con la segunda carga de combustible en el reactor de agua pesada hirviente de Halden (HBWR), en régimen de baja potencia. Esa segunda carga de combustible del HBWR consta de haces de siete varillas de UO_2 enriquecido al 1,5%. En total se colocan 30 barras de control en las posiciones abiertas del reticulado hexagonal de combustible. A fin de facilitar las comparaciones teóricas, las determinaciones se llevaron a cabo solamente con configuraciones simétricas de las barras de control.

El experimento consistió en medir el nivel crítico de agua para el cuerpo «limpio», con las barras en diferentes configuraciones e introducidas a distancias variables del fondo del reactor.

Se estudió la manera en que varía, en función de la temperatura, la influencia de las barras sobre la reactividad, efectuando mediciones con seis barras de control dispuestas anularmente a tres temperaturas distintas, a saber, 34°C, 150°C y 220°C.

El autor compara los niveles críticos de agua, determinados experimentalmente, con los valores calculados. Estos últimos se encuentran aplicando un método que se basa en suponer que las barras de control, el combustible y el moderador forman homogéneamente una «zona de barra de control»; y, asimismo, aplicando un método heterogéneo en el cual se considera que los elementos combustibles y las barras de control actúan como sumideros lineales de neutrones térmicos, mientras que los elementos combustibles desempeñan la función de fuentes lineales de neutrones rápidos.

1. INTRODUCTION

The relatively high excess reactivity of a cold fresh power reactor might necessitate control rod installments up to 20 to 30% k_{eff}. In boiling power reactors, the reactivity changes due to temperature, steam voids, fission products and burn-up are considerable, which implies that the excess reactivity which has to be shimmed off may vary strongly with temperature, power level and during the reactor life-time. The most practical and common way to compensate this excess reactivity is to have a number of control rods spread out over the core.

An accurate prediction of the effectiveness of a large number of fully or partially inserted control rods in a reactor is a difficult task. A variety of useful methods of calculation exists, but only meagre experimental material is yet available for verification of the theories.

This paper presents a comparison of the experimentally and theoretically determined effectiveness of some control rod configurations in the Halden Boiling Water Reactor (HBWR). In order to facilitate theoretical comparisons, measurements have been made on symmetrical control rod configurations only. The experiment consisted of measuring the critical water level for the clean core and with different rod configurations inserted to various distances from the bottom of the reactor.

Theoretical comparisons with experimental critical water levels have been made by a method in which the control rods are homogenized together with fuel and moderator to form a control rod zone. The reactivity effect

of this zone is determined by applying a two-group multi-region macroscopic calculation.

This homogeneous method is compared with a heterogeneous method, based upon the theory of Feinberg-Galanin, for geometries fairly similar to those experimentally investigated.

2. EXPERIMENTAL PROCEDURE AND RESULTS

2.1. The second fuel charge of HBWR

The second charge fuel elements of HBWR are of the cluster type and each element consists of seven stringers with UO_2 enriched to 1.5%. The stringers are formed of two identical parts of 83 cm length, separated by 5.3 cm of non-fissionable material. The core consists of 100 fuel elements forming an open hexagonal lattice structure with a lattice pitch of 13 cm and control rods are placed in the open lattice positions to the number of 30. A cross-sectional view of the reactor is shown in Fig. 1.

The control rods are of two types. 24 of the rods have an absorber radius of 3.5 cm, while 6 have a reduced radius of 2.65 cm due to smaller holes in the top lid. The absorber material is a 30% cadmium and 70% silver alloy canned in stainless steel. Each rod has at the lower end a stainless-steel plunger of 21 cm length. Fully inserted control rods are level with the core bottom, while the steel plungers extend down into the 38-cm thick bottom reflector.

2.2. Experimental procedure

The critical water level for the clean core was determined by the approach to criticality method. Water was added in steps to the reactor tank which was loaded with 100 fuel elements. The count rates were taken at each water level with two BF_3-counters located in the bottom reflector.

From the plot of the inverse count rates versus water level and by extrapolation towards infinite count rates, the critical water levels were determined. The addition of water was stopped about 2 cm from the critical water level.

The above mentioned procedure was also followed in order to determine the critical water level for several configurations of control rods inserted into the core. The measurements were carried out at three moderator temperatures :34, 150 and 220°C.

2.3. Experimental results

Table I presents the measured critical water levels obtained for annular zones consisting of 6, 12 and 18 rods. The rods are numbered as shown in Fig. 1 by:

6 rods: 10 - 15
12 rods: 10 - 15, 20, 22, 23, 25, 27, 28
18 rods: 10 - 15, 20 - 29, 32, 37.

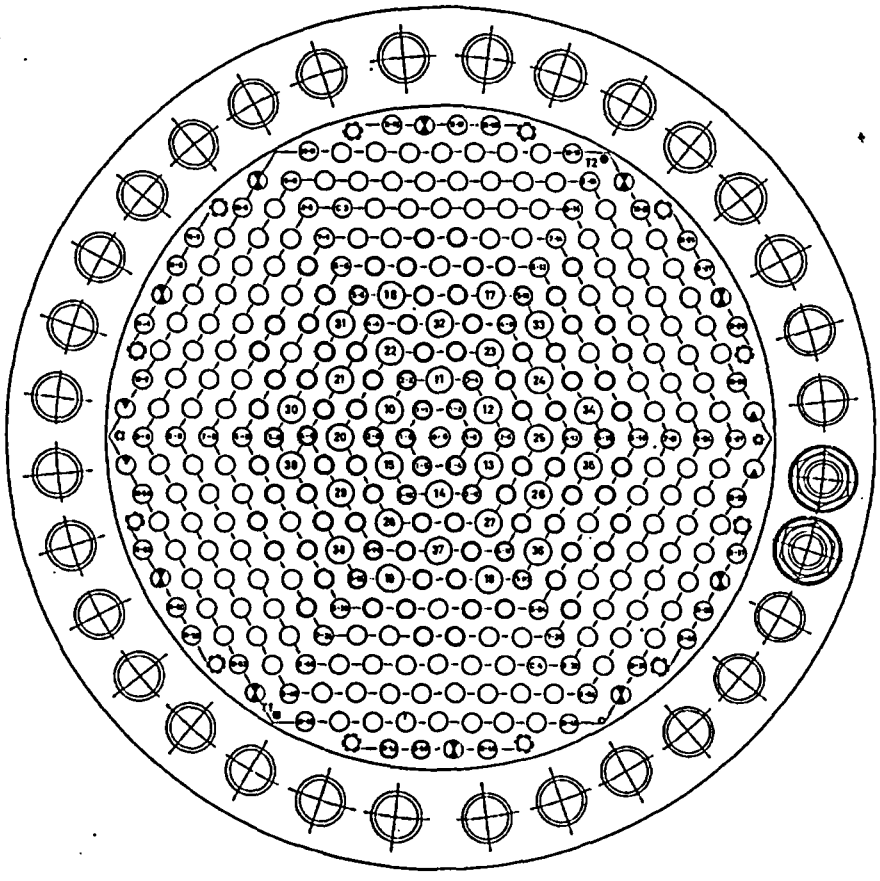

Fig.1

Core loading

o	Pressure meter P14 and P5	1
ⓒ	Nuclear Instr.	2
	Bolts.	32
	Plugged holes for exp. equipment	201
	Control station	30
	Fuel element	102
	Steam out	10
	Condens in	2
	Subcooled water-bottom	2
	Subcooled water-top	12
	Steam pipe drain	2
•	Thermocouples	2

Control rods 10-19 bank 1
Control rods 20-29 bank 2
Control rods 30-39 bank 3
Control rods 20-22-23-25-27-28 are of smaller type.
Control rods 31-35-38 are regulating rods

TABLE I

EXPERIMENTAL AND CALCULATED REACTIVITY-WORTH OF 6, 12 AND 18 RODS

Number of control rods	Insertion Z (cm)	Critical water level H_{cr} (cm)	ρ_{exp} (%)	ρ_{calc} (%)	$\frac{\rho_{calc.}-\rho_{exp.}}{\rho_{exp.}}$	Temperature (°C)
0	clean core	106.4	0	0	0	34
6	80	124.4	7.3	5.61	-0.23	34
6	60	135.8	10.2	8.26	-0.19	34
6	38	140.8	11.1	9.31	-0.16	34
12	92	126.4	7.8	5.23	-0.33	34
12	85	152.6	12.9	8.61	-0.33	34
18	96	150.0	12.5	8.55	-0.32	34
0	clean core	118.3	0	0	0	150
6	100	125.7	3.0	2.66	-0.12	150
6	80	149.7	8.9	7.60	-0.15	150
6	60	172.9	12.0	10.09	-0.16	150
6	38	181.8	12.9	10.73	-0.17	150
0	clean core	132.0	0	0	0	220
6	100	172.5	8.5	6.09	-0.29	220
6	80	215.5	12.1	9.82	-0.19	220

The Z values give the distances between the reactor bottom plate and the lower end of the absorber section of the control rods. The critical water levels are determined with an accuracy of ± 2 mm at 34°C and 150°C. Difficulties in stabilizing the temperature introduced uncertainties of ± 5 mm at 220°C. This corresponds, in all cases, to an uncertainty less than ± 0.2% in k_{eff}. The total uncertainty in the measured reactivity values is ± 7%. This uncertainty is mainly caused by uncertainty in the water level coefficient. Fig. 2 shows the plot of the critical water level against insertion for the 6 rods at 34, 150 and 220°C.

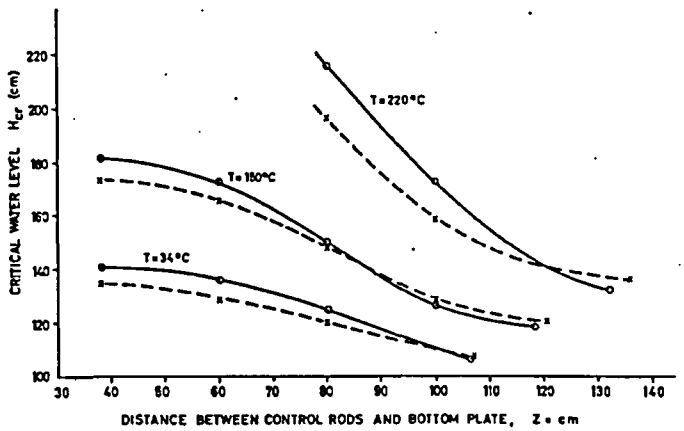

Fig. 2

Critical water level plotted against insertion of the six central control rods

O Experimental
X Calculated

3. METHODS OF CONTROL ROD CALCULATIONS

3.1. The homogeneous method

Comparison between the experimental results and a theoretical approach called the homogeneous method has been made. In the homogeneous calculations the heterogeneous core without control rods is transformed in the usual way into a homogeneous medium which, if infinite in extent, would possess the same mean neutron parameters as the infinite heterogeneous lattice. The two-group homogenized core parameters are calculated applying the Swedish lattice parameter code, Burnup 5 [1].

The introduction of control rods between the fuel elements is taken into account by a homogenization procedure, essentially identical to the one described by CARLVIK et al. [2]. A certain core area is associated to each control rod so as to form a cylindrical control rod cell consisting of the rod in the centre, surrounded by the homogeneous medium with the known average neutron parameters. The equivalent two-group neutron parameters for a homogenized control rod cell are calculated applying diffusion theory. The

boundary conditions at the rod surface are given in terms of the extrapolation lengths, defined according to KUSHNERIUK and McKAY [3] and at the cell boundary by the condition of zero-flux gradient.

The macroscopic calculation of the composite system consisting of a homogenized core, a homogenized control rod zone and homogenized reflectors is carried out applying the computer programme solving the multigroup neutron diffusion equations in the two space dimensions, by HASSITT [4]. An example of one of the geometries used in the macroscopic calculation is given in Fig. 3, showing the core, reflectors and control rod zone when six rods are at a distance of 60 cm from the bottom plate.

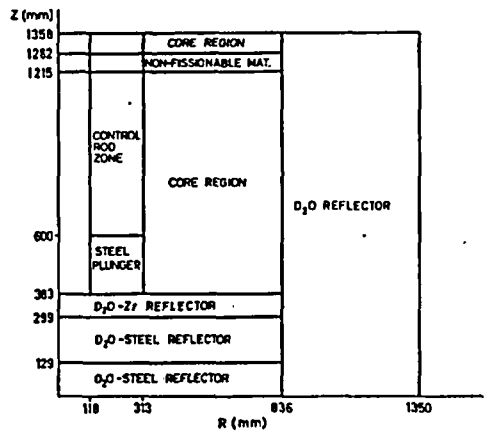

Fig. 3

HBWR core geometry
Six control rods at z = 60 cm

3.2. *The heterogeneous method*

The heterogeneous calculation, applying the source and sink method, was first considered by Feinberg and Galanin. The fuel elements are considered as line sources of fast neutrons and line sinks of thermal neutrons while the control rods are considered as additional line sinks for the thermal neutrons. Two-group diffusion theory is applied. A description of the derivation of the critical condition is given by JONSSON and NÄSLUND [5]. This theory was modified by JONSSON [6] to cover three-dimensional problems, which enables calculations for partly inserted control rods. A computer programme named Hetero 11, coded by NÄSLUND [7], is used for the heterogeneous calculations.

4. COMPARISON OF RESULTS

Calculations of k_{eff} for all core geometries at which the critical water level was measured have been made applying the homogeneous method. A

comparison of the experimental and calculated critical water levels for six rods at the various temperatures is presented in Fig. 2. Table I gives the absolute and the relative discrepancy between the experimental and calculated reactivity values of the rods. (The experimental reactivity value, ρ_{exp}, is obtained by integrating the water level coefficient from the clean core critical water level to the level obtained with control rod inserted.) It is clear that the calculations underestimate the reactivity value of the control rods. The discrepancy shows no clear dependence upon the number of rods or on the rod insertion. For six fully inserted rods the discrepancy is 17% and for 12 or 18 partly inserted rods there is a disagreement as great as 33 per cent.

The heterogeneous method, which explicitly takes into account the heterogeneous nature of the reactor, may give results which are more in agreement with the experimental results. In order to facilitate comparison between the homogeneous and the heterogeneous methods, the reactivity value of partially and fully inserted control rods in a reactor with a somewhat simplified geometry as compared to HBWR, but with the same lattice and reflector constants, has been investigated. Calculations have been made applying both the heterogeneous and the homogeneous methods. The reason for making the comparison of the two methods on an idealized core, as shown in Fig. 4, is that the geometry of HBWR is too complex to be treated by the heterogeneous programme because of the bottom reflectors and the steel plungers at the end of the control rods. The comparison is carried out for annular zones of 6, 12 and 18 rods. Figs. 5, 6 and 7 show the reactivity value as function of insertion for the 6, 12 and 18 rods respectively, all at a temperature of 30°C. Fig. 8 presents the reactivity value versus temperature for six fully inserted rods. Table II gives the result of the calculations. The agreement between the two methods is good except for fully inserted rods.

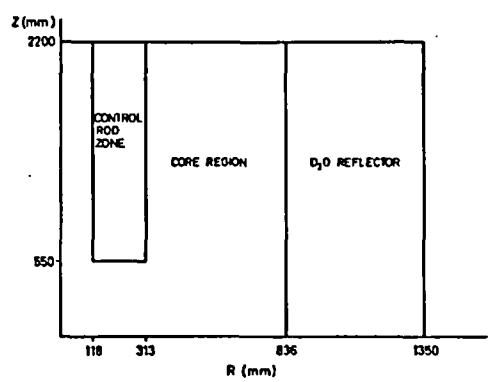

Fig. 4

Simplified core geometry
Six control rods at z = 55 cm

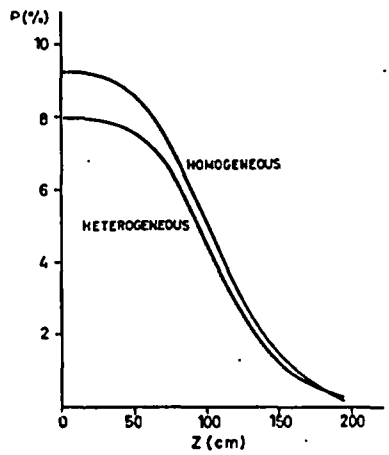

Fig. 5

Reactivity worth plotted against insertion for six rods

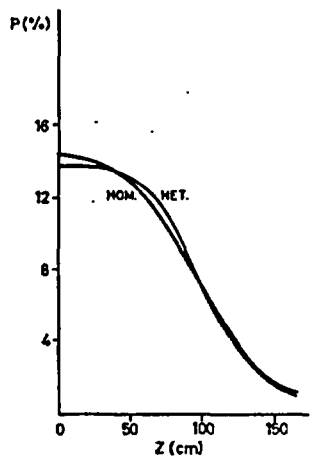

Fig. 6

Reactivity worth plotted against insertion for 12 rods

5. DISCUSSION AND CONCLUSION

The results reveal clearly that the calculations underestimate the reactivity value of the control rods. The reasons for this may be several, but some points which may account for the discrepancy are:

(a) The method of homogenization of the control rod cell,

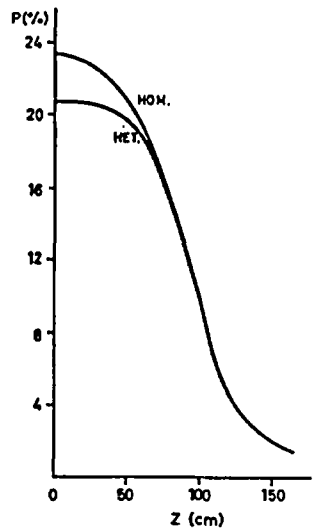

Fig.7

Reactivity worth plotted against insertion for 18 rods

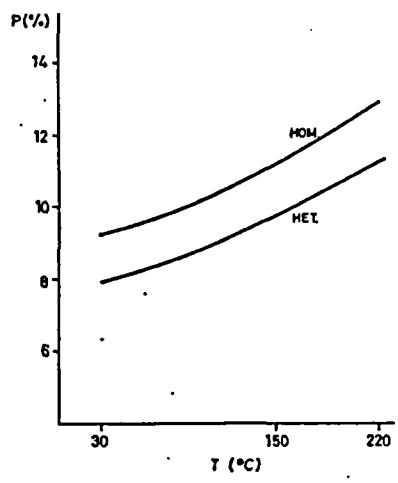

Fig.8

Reactivity worth plotted against temperature for six rods

(b) The size of the homogenized control rod zone, and

(c) Epithermal neutron absorption in the control rods.

(a) The calculated reactivity value of the control rods is directly dependent upon the average homogenized physics parameters of the control rod zone. These parameters are obtained by a two-step homogenization procedure,

TABLE II

COMPARISON OF CONTROL ROD WORTH CALCULATED BY THE HOMOGENEOUS AND THE HETEROGENEOUS METHODS

Number of control rods	Insertion Z (cm)	ρ_{Hom} (%)	ρ_{Het} (%)	$\Delta\rho=(\rho_{Hom}-\rho_{Het})$ (%)	Moderator temperature (°C)
6	0	9.23	7.96	1.27	30
6	25	9.17	7.94	1.23	30
6	55	8.43	7.40	1.03	30
6	110	3.91	3.58	0.33	30
6	165	0.85	0.78	0.07	30
6	195	0.17	0.28	-0.11	30
12	0	14.29	13.65	0.64	30
12	55	12.84	13.08	-0.24	30
12	110	5.12	5.09	0.03	30
12	165	1.06	1.12	-0.06	30
18	0	23.32	20.70	2.61	30
18	55	19.88	19.77	0.12	30
18	110	6.38	6.26	0.12	30
18	165	1.34	1.39	-0.05	30
6	0	11.20	9.74	1.46	150
6	0	12.91	11.29	1.62	220

as described in section 3.1, which may give inadequate characteristics of the control rod zone.

(b) The evaluation of the homogenized neutron parameters is based upon the assumption of an infinite medium. This can of course never be fulfilled, but in the experiment all the control rods were at the interface between the two zones. It is not to be expected that geometries of this type are covered well by the homogenized theory.

(c) The epithermal neutron absorption in the control rods has not been taken into account in the homogenized calculations. Although the epithermal absorption tends to increase the reactivity effect, a rough calculation shows that this would not account for more than approximately 3 to 5% increase in ρ for rods of the HBWR type.

The comparison of the results of the homogeneous and heterogeneous calculations shows good agreement, although the heterogeneous method gives slightly lower values than the homogeneous method in most cases. This is

in agreement with previous two-dimensional calculations [8]. The large discrepancy for the fully inserted rods is, however, unexpected since these cases represent the simplest geometry, where the axial flux distribution may be represented by a pure cosine function. The difference is probably due to the computational methods and not to the theory behind. This is, however, not yet investigated, but a more detailed and extensive analysis of the work presented in this paper will be issued in a forthcoming HPR-report.

From the comparison of the two calculation methods it is obvious that points (a) and (b) above cannot explain the discrepancy between the experiment and the homogeneous calculations. Because, if it had been so, it was to be expected that the heterogeneous calculations would give higher reactivity worths than the homogeneous. Epithermal absorption is, however, not included in the heterogeneous calculation either and these calculations will therefore also underestimate the reactivity worth of the rods according to point (c) above. The discrepancy between the experimental and theoretical results indicates that the control rod effectiveness in a heavy-water power reactor with large excess reactivity cannot be satisfactorily predicted by the computation methods in their present form.

Experiments with groups of control rods of high reactivity worth, in simple core geometries, for instance in a zero-power reactor, will be of great value for the improvement of the calculation methods. Due to the high cost of each control rod and also because each rod adds to the complexity of the plant, more accurate prediction of the total effectiveness of a large number of control rods has a direct implication on the economy of boiling-water reactors.

REFERENCES

[1] AHLSTRÖM, P.E., Calculation of Lattice Parameters as a Function of the Irradiation, Presented to the EAES Symp. Measurements and Calculations of the Influence of Burnup on Reactivity, Risø, Denmark (1961).

[2] CARLVIK, I. et al., Calculations of the Influence of a Large Number of Control Rods on the Reactivity of a Thermal Reactor, Proc. 2nd.UN Int. Conf. PUAE 11 (1958) 532.

[3] KUSHNERIUK, S.A. and McKAY, C., Neutron Density in an Infinite Non-Capturing Medium Surrounding a Long Cylindrical Body which Scatters and Captures Neutrons, AEC Rpt. CRT-566 (1956).

[4] HASSITT, A., A Programme for Solving the Multigroup Neutron Diffusion Equations in Two Space Dimensions on the Ferranti Mercury Computer, U.K.A.E.A. Rpt.AERE T/R 2487 (1958).

[5] JONSSON, A. and NÄSLUND, G., Heterogeneous Two-Group Diffusion Theory for a Finite Cylindrical Reactor, AB Atomenergi Rpt.AE-57 (1961).

[6] JONSSON, A., The Source and Sink Method for a Three-Dimensional System, private communication.

[7] NÄSLUND, G., Description of a Three-Dimensional Heterogeneous Programme, private communication.

[8] SKARDHAMAR, T., Comparison of Control Rod Calculations Using Homoeneous and Heterogeneous Methods, private communication.

DISCUSSION

J. COEHOORN: What was the reactor power during control-rod calibration at moderator temperatures of 220°C and what was the void fraction in the core? If there were no voids in the core, was it possible to calibrate the control rods as a function of the void fraction?

H.S. OLSEN: Calibration of single control rods at power was carried out against a cadmium shutter of known reactivity amplitude. All the measurements reported in the paper were performed at low power levels without any void in the reactor.

C.E. COHN: Could you tell me how you determined the rod-reactivity worths which you reported?

H.S. OLSEN: This was done by integrating the water-level reactivity coefficient from the water level of the clean core to the water level as measured with the control rods inserted.

PULSED-NEUTRON MEASUREMENTS ON A HEAVY-WATER REACTOR AT ZERO ENERGY

M. KÜCHLE

KERNFORSCHUNGSZENTRUM, KARLSRUHE, FEDERAL REPUBLIC OF GERMANY

Abstract — Résumé — Аннотация — Resumen

PULSED-NEUTRON MEASUREMENTS ON A HEAVY-WATER REACTOR AT ZERO ENERGY. During the start-up of the research reactor FR2 reactivity measurments with a pulsed neutron-source have been made. Because of the relatively long lifetime of the neutrons in a D_2O system, a correction for the build-up of delayed neutrons during the prompt neutron decay has been applied.

From measurements of the subcriticality as a function of the water level and extrapolation to the full tank, the excess reactivity of the reactor was obtained. The result agreed well with that of a boron-poisoning technique. A lot of reactivity measurements have been made from which only control-rod calibration curves for different control-rod combinations will be reported here. The information is new. It has not been published or reported elsewhere.

MESURES, A L'AIDE DE NEUTRONS PULSÉS, SUR UN RÉACTEUR A EAU LOURDE, DANS LES CONDITIONS DE PUISSANCE ZÉRO. Pendant le démarrage du réacteur de recherche FR2, on a fait des mesures de la réactivité à l'aide d'une source de neutrons pulsés. Les neutrons ayant une durée de vie relativement longue dans un assemblage à D_2O, on a appliqué un facteur de correction pour tenir compte de l'accumulation de neutrons retardés pendant la décroissance des neutrons instantanés.

On a obtenu l'excédent de réactivité du réacteur à partir de mesures de la sous-criticalité en fonction du niveau d'eau, en faisant une extrapolation correspondant au caisson plein. Le résultat concordait avec celui obtenu par une méthode de l'empoisonnement au bore. L'auteur a fait de nombreuses mesures de la réactivité, mais dans le présent mémoire il ne mentionne que les courbes d'étalonnage des barres de commande pour différentes combinaisons de ces barres. Les données présentées sont nouvelles et n'ont pas encore été publiées ou mentionnées ailleurs.

ИЗМЕРЕНИЯ ИМПУЛЬСНЫХ НЕЙТРОНОВ НА ТЯЖЕЛОВОДНОМ РЕАКТОРЕ ПРИ НУЛЕВОЙ ЭНЕРГИИ. Во время запуска исследовательского реактора FR2 были проведены измерения реактивности с помощью источников импульсных нейтронов. Ввиду сравнительно продолжительного времени жизни нейтронов в системе D_2O применялась поправка на образование запаздывающих нейтронов во время распада мгновенных нейтронов.

В результате измерений подкритичности как функции уровня воды и экстраполяции ее на полный бак была получена величина избыточной реактивности реактора. Результат хорошо согласуется с данными, полученными в результате использования методов определения по степени отравления бором. Проведено большое число измерений, из полученных данных сообщается только о кривых калибрования регулирующих стержней для различных сочетаний регулирующих стержней. Эти данные публикуются впервые.

MEDICIONES REALIZADAS EN UN REACTOR DE AGUA PESADA DE POTENCIA NULA CON FUENTES NEUTRÓNICAS PULSADAS. Durante la puesta en marcha del reactor de investigaciones FR2, el autor efectuó mediciones de la reactividad con una fuente neutrónica pulsada. Debido a la vida relativamente larga de los neutrones en un sistema de D_2O, introdujo una corrección para tener en cuenta la acumulación de neutrones retardados durante la desintegración de los neutrones inmediatos.

Basándose en mediciones de la subcriticidad en función del nivel de agua y extrapolándolas a un tanque lleno, midió el exceso de reactividad de un reactor. Los resultados concuerdan satisfactoriamente con los obtenidos mediante la técnica de envenenamiento por el boro. El autor efectuó una serie de mediciones de la reactividad; en la memoria sólo presenta las curvas de calibración correspondientes a las barras de control para diferentes combinaciones de estas barras. Estos datos son inéditos; no se han publicado ni divulgado en otros trabajos.

1. INTRODUCTION

The pulsed neutron method has already been extensively used for reactivity determinations of reactors [1], but very little has been reported about its application to heavy-water systems. Therefore our experiments in the FR2 might be of interest.

2. THEORY

The principle of the method consists in injecting a short burst of fast neutrons from an accelerator into a subcritical reactor and observing the prompt neutron decay. When the transients from the burst have died away, this decay is exponential in time with a decay constant of

$$\alpha = \frac{\rho + \beta}{\Lambda_p}, \tag{1}$$

where ρ is the negative reactivity measured from delayed critical, β is the delayed neutron fraction and Λ_p is the prompt neutron generation time. From measurements with the critical reactor $\alpha_c = \beta/\Lambda_p$ is obtained, and, assuming that Λ_p is independent of ρ, the reactivity in dollars can be determined from

$$\frac{\rho}{\beta} = \frac{\alpha - \alpha_c}{\alpha_c}. \tag{2}$$

To improve the statistics, not just one burst is injected, but the source is pulsed periodically and the counting rate from a neutron detector is accumulated with a synchronized multi-channel time analyser.

In Eqs. (1) and (2) it is assumed that the decay constants of the delayed neutrons λ_i are very small compared to α so that the delayed neutrons can essentially be treated as a constant background. This holds for a light-water reactor but for heavy-water lattices the inhour equation

$$\alpha = \frac{1}{\Lambda_p}\left[\rho + \beta + \sum_i \frac{\beta_i \lambda_i}{\alpha - \lambda_i}\right] \tag{3}$$

has to be used instead of Eq. (2) [2]. The additional term is largest for $\rho = 0$, being 5% of β in this case.

Moreover, when $|\rho| < 50$ mk a correction has to be applied for the build-up of delayed neutrons during the prompt neutron decay. This effect has been calculated by Fraude giving for the time dependence of the fundamental mode

$$\phi(t) = \text{const.}\ e^{-\alpha t} \cdot F(t, \rho) \tag{4}$$

with

$$F(t, \rho) = \sum_{j=1}^{p+1} \frac{1}{1 + \frac{K_{eff}}{\Lambda p} \sum_{i=1}^{p} \frac{\beta_i \lambda_i}{(\lambda_i - w_j)^2}}\, e^{(\alpha - w_j)t}$$

Here w_j are the roots of the inhour equation and p is the number of delayed neutron groups. The correction term F (t, ρ) depends on ρ and α, making an iteration procedure necessary. First, rough values for ρ and α were taken from the experimental curve; with these values F (t) was calculated and a more precise value for α was obtained from a plot of ϕ(t)/F(t) in a semilogarithmic scale.

Fig. 1 shows as an example a decay curve with and without this correction. Only when the correction has been applied is a good exponential observed. A fit of the uncorrected curve would lead to about a 5% error in ρ.

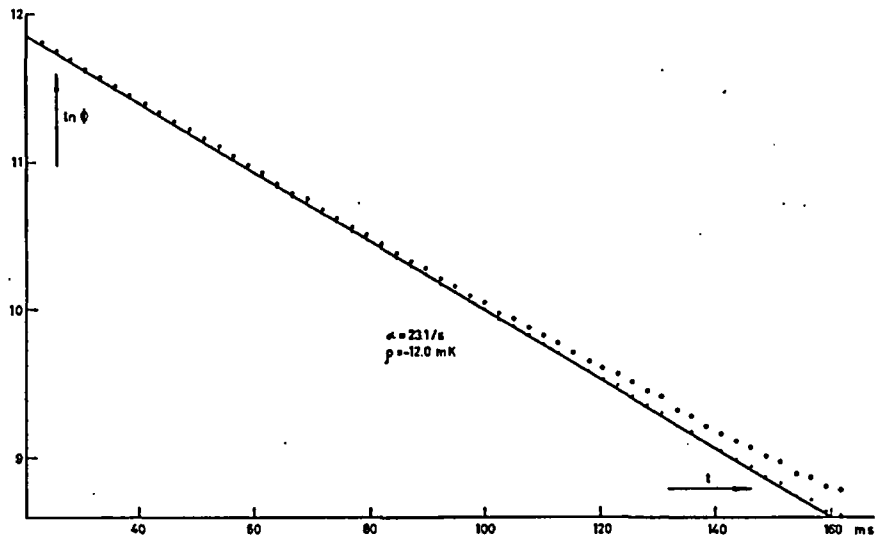

Fig. 1

Time decay of the neutron flux
● with correction for delayed neutrons
O without correction for delayed neutrons

We have so far assumed that the generation time does not change with reactivity. This is true to a first approximation because $\Lambda_p = l_p/K_{eff}$ and the prompt neutron life time l_p changes in the same way as K_{eff} does. If, for instance, K_{eff} is changed by variation of B^2, Λ_p remains constant according to one-group theory and varies only slowly in a two-group approximation. In our experiments, where B^2 was changed by variation of the water level, a correction for the variation of the generation time has been applied. The maximum change of Λ_p was 2,5%.

When K_{eff} is varied by local changings of the absorption cross-section, for instance by insertion of control rods, the effect is still smaller because it enters in lp and K_{eff} very much in the same way. The situation is not very clear yet for large absorptions where the flux distribution is distorted appreciably. Therefore a constant value for Λ_p has beeen used in the evaluation of the measurements with absorbers, arguing that this is correct

for small perturbations, and for far subcritical conditions a high degree of precision is generally not required. To avoid this difficulty another kind of evaluation of pulsed neutron experiments has been proposed [3]. Here the additional information contained in the delayed neutron tails is used.

Little use has been made of this method in our experiments for the following reasons:

(1) For far subcritical conditions the statistics of the delayed neutron tail is very poor and also the delayed neutron harmonics can probably not be neglected; and

(2) There was often a background from delayed photoneutrons from previous runs of the reactor which was much higher than the delayed neutron contribution from the pulse experiment would be.

Eqs. (1) and (2) generally are derived for unreflected systems only. In the case of lattices with reflectors one must be careful in distinguishing between static reactivity, which is normally used in calculations, and dynamic reactivity, as measured in the pulsed experiment. Therefore, FRAUDE [2] has calculated the decay constants of our systems twice, first based on the static eigenfunctions and then with the dynamic eigenfunctions of the system. It turned out that the difference was completely negligible for the normal loading, where the core radius is $R_c = 120$ cm and the radial reflector thickness $d = 35$ cm. But even in a case where $R_c = 55$ cm and $d = 100$ cm, which occurred during the loading of the reactor, the difference in the α-values was only 2.4% for a reactor which was 8 $ subcritical.

3. EXPERIMENTAL ARRANGEMENT

The measurements were made during the start-up of the natural uranium heavy-water research reactor FR2, a description of which was given by WIRTZ et al. [4]. Fig. 2 shows a schematic view of the reactor.

The pulsed experiments were performed with (d, t)-neutrons from a 150 keV pulsed Cockroft-Walton accelerator constructed by EYRICH [5]. The accelerator was installed in front of the reactor and the ion beam had to pass a 4.50-m long, 5-cm diameter tube which was inserted into a horizontal beam hole. The target was mounted at the end of the tube, so that the pulsed neutron source was almost at the centre of the reactor. The neutron burst was produced by pulsing the extraction voltage. A 1-ms pulse width with 1-mA ion current was used, giving about 10^8 neutrons per burst. The repetition rate ranged from 100 ms to 1 s.

A BF_3 neutron counter could be moved inside a 1-in diameter thin-walled aluminium tube going through the vertical axis of the reactor. The signals from the detector were amplified and fed into a 256-channel time analyser which also triggered the accelerator. The time analyser was open only for that fraction of the entire time cycle during which the harmonics had almost died away and the background from the delayed neutrons was not too high. In general the waiting time was about $0.5/\alpha$ and the interval for the measurement $5/\alpha$.

After correcting for dead time, background and build-up of delayed neutrons the results were plotted on a semilogarithmic scale and the true exponential part and α-value were found by visual inspection. The error

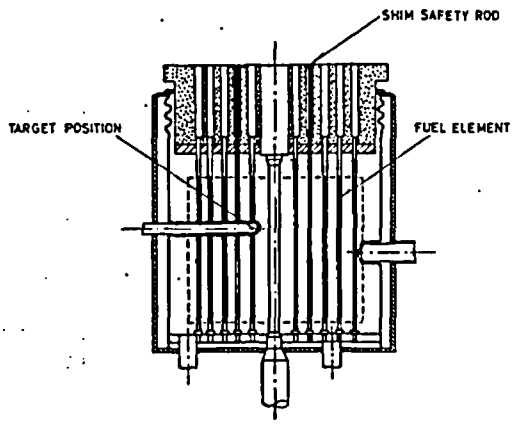

VERTICAL SECTION

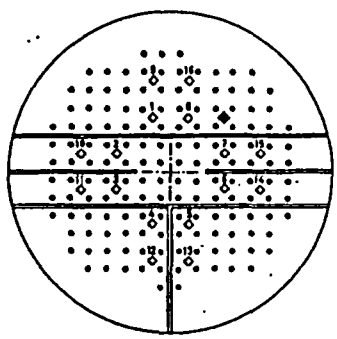

CROSS SECTION

Fig. 2

Reactor FR2
O fuel element,
◇ shim safety rod,
◈ control rod

obtained from this procedure was small compared to other errors. Depending on the harmonics present, the accuracy in α varied from 1 to 2%.

4. MEASUREMENTS

Of the many pulsed reactivity determinations which were performed under various loading conditions, only those which are of more general interest will be reported here.

4.1. The determination of the neutron life time

Apart from its use for the normalization of pulsed experiments, β/l_p is an important reactor parameter. Its determination from pulsed measurements at delayed critical has the difficulty that the running reactor yields a tremendous background of neutrons over which only a small number of decaying neutrons from the pulsed source is superimposed. Therefore the following procedure has been adopted; after the critical control rod position had been determined the reactor was made subcritical until practically all neutrons had died away; the control rod was then taken out to the critical position and the pulsed measurements started immediately. After about 20 bursts the neutron flux was so high that the reactor had to be made subcritical again. The whole procedure was repeated until the statistics were good enough.

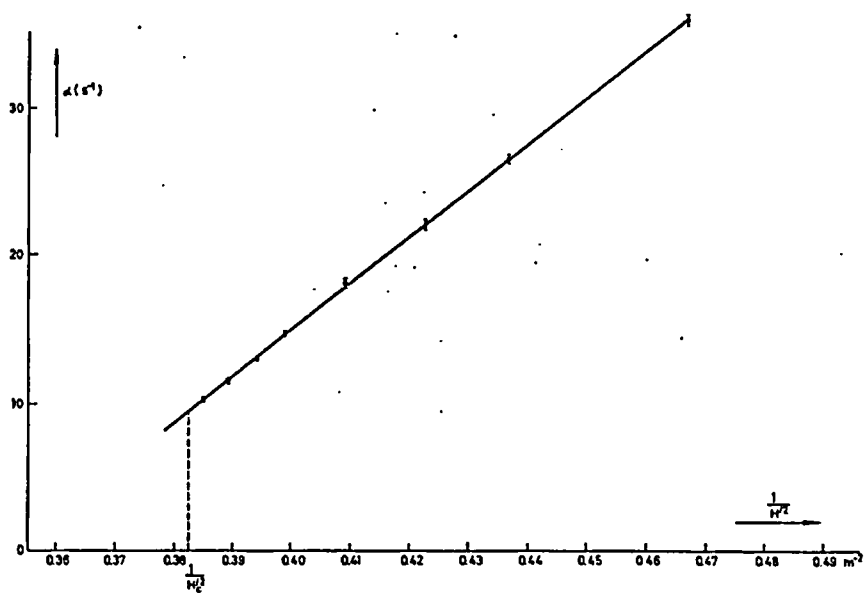

Fig. 3

Determination of α_c

Another possibility consists in measuring α as a function of the water level in a slightly subcritical reactor and extrapolating to the critical water level (Fig. 3). The results of both methods agreed well within the limits of error, giving for the full loading:

$$\alpha_c = 9.5 \pm 0.2 \ [s^{-1}] .$$

From α_c, with the calculated value of $\beta_{eff} = 0.78 \times 10^{-2}$ [6], l_p can be obtained. In Table I the results are compared with the importance weighted lifetime for reflected reactors as calculated by FRAUDE [2]. Whereas

TABLE I

NEUTRON LIFE TIME

R_c (cm)	d (cm)	α_c (s^{-1})	l_p (experim.) (ms)	l_p (theory) (ms)
69.8	85.2	7.7±0.4	1.04±0.06	1.18
97.0	58.0	8.8±0.5	0.94±0.06	0.97
119.1	35.9	9.5±0.2	0.86±0.02	0.88

R_c = core radius d = reflector thickness

there is a large discrepancy in the first case, the agreement is very good for the latter two, especially when we consider that the calculation does not include the effect of the beam holes.

4.2. Determination of the excess reactivity

Another important problem is the precise determination of the excess reactivity of the cold clean reactor, which is the positive reactivity that would exist in the reactor if all control rods were withdrawn. This can be found from pulsed experiments in the subcritical region only by some extrapolation procedure. If, for instance, the shape of the control rod calibration curve has been measured for the critical loading, where the excess reactivity is zero, and the lower part of the calibration curve is measured again at full loading, the excess reactivity can be determined, if we assume that the shape of the curve has not changed. This assumption is not well justified yet and we preferred another method. This was a measurement of the reactivity versus the height H of the D_2O in the reactor tank.

According to one-group diffusion theory a linear relation between reactivity and $1/H^2$ exists which can be easily extrapolated from the subcritical state to the supercritical state. In the two-group approximation the equation reads:

$$\rho = \frac{\pi^2(M^2+2B_r^2\tau L^2)}{K_\infty}\left[\frac{1}{H_c'^2}-\frac{1}{H'^2}\right]+\frac{\pi^4 L^2\tau}{K_\infty}\left[\frac{1}{H_c'^4}-\frac{1}{H'^4}\right], \qquad (5)$$

where B_r^2 is the radial buckling, H and H_c are the water level and the critical water level respectively, $H' = H+2\times0.71\ \lambda_{tr}$ and $H_c' = H_c+2\times0.71\ \lambda_{tr}$. When plotting

$$\rho^*(H') = -\frac{\pi^4 L^2\tau}{K_\infty}\left[\frac{1}{H_c'^4}-\frac{1}{H'^4}\right]$$

versus $1/H'^2$ and extrapolating linearly to the full tank, where $H' = H_0$, the excess reactivity is obtained from:

$$\rho_{ex} = \rho^*(H'_0) + \frac{\pi^4 L^2 \tau}{K_\infty} \left[\frac{1}{H_c'^4} - \frac{1}{H_b'^4}\right].$$

Since the second term is only a small correction, it is sufficient to use rough calculated values for L^2, τ, and K_∞ here.

Eq.(5) is valid for a reactor without vertical reflector and simple boundary conditions. The real situation was more complicated. The fuel did not extend to the bottom of the tank, but ended about 7 cm above the bottom and was followed by structural material for the support of the fuel elements. Moreover, below the bottom there was about 7-cm D_2O which belonged to the cooling system. Therefore a vertical flux map was taken for the reactor with control rods withdrawn and lowered water level. By fitting this curve with a cos-distribution, the effective extrapolation distance was obtained. At the top of the reactor the geometrical situation was somewhat simpler and the reactivity effect of the upper 14 cm of the water level was measured against a calibrated control rod. It was found to be 1.6 mk smaller than would be predicted from the $1/H'^2$ behaviour.

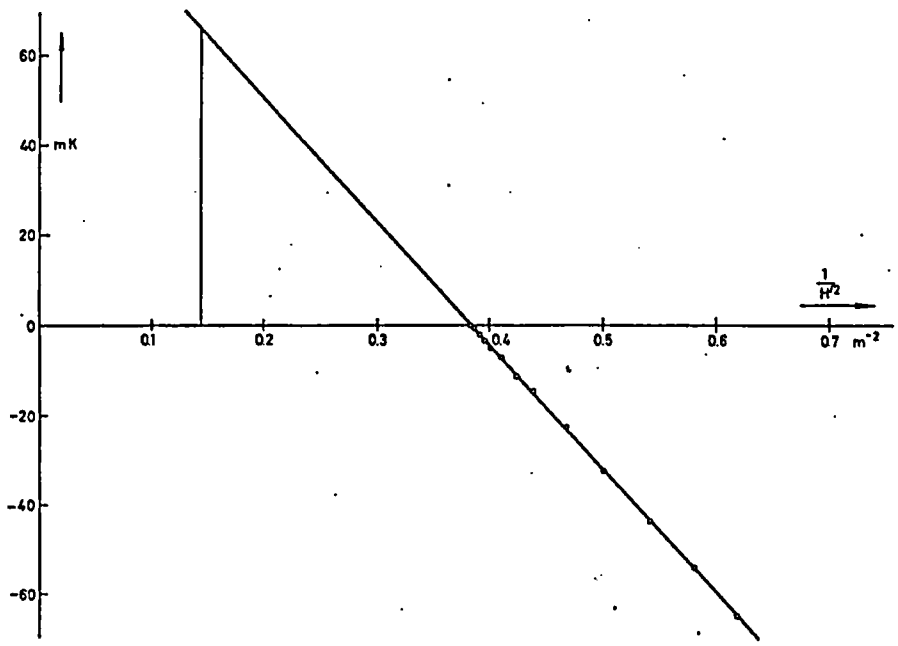

Fig. 4

Determination of excess reactivity

The results of the measurements are given in Fig. 4. Though there are some spaces in the D_2O due to horizontal beam holes, just in this region of the water level the points lie fairly well on a straight line. When the above mentioned correction for the top part has been applied, an excess

reactivity of

$$\rho_{ex} = 66.7 \pm 1.2 \text{ mk}$$

is obtained.

The excess reactivity was determined independently by a boron poisoning technique. The method consists in poisoning the D_2O homogeneously by adding D_3BO_3 until the reactor is just critical with all control rods withdrawn. The reactivity effect of the boron can be calculated.

The details of this measurement have been reported by DIEDERICHS et al. [7]. The result was

$$\rho_{ex} = 67.0 \text{ mk}.$$

The excellent agreement is somewhat fortuitous especially when we take into account the inaccuracy of the assumed β_{eff}, which is not included in the limits of error given above. In principle β_{eff} could be determined from a combination of the two measurements. If this is done one obtains

$$\beta_{eff} = (0.783 \pm 0.018) \times 10^{-2}.$$

Moreover from the slope to the plot $\rho^*(H')$ versus $1/H'^2 \cdot M^2$ can be obtained, because K_∞ is generally known to a much higher accuracy than is M^2. The term $2B_i^2 L^2 \tau$ of Eq. (5) is only a small correction of about 3% in M^2, and can be determined from calculated values. In this way a value of

$$M^2 = (325 + 10) \text{cm}^2$$

was found. A measurement of M^2 was also made, with the boron poisoning technique, giving

$$M^2 = (323 + 13) \text{cm}^2.$$

4.3. Control rod calibration

The FR2 has 16 shim-safety rods, the positioning of which is seen from Fig. 2. Their total reactivity worth is about 20%. The control of the reactor is made with a control rod which has a reactivity effect of about 1 $. The reactivity worth of several shim-safety rod combinations has been measured to study coupling effects. An example is given in Table II. The numbers of the rod positions refer to Fig. 2. One can see that coupling effects are small for symmetrical configurations but appreciable for asymmetric arrangements.

Fig. 5 shows calibration curves, with arbitrary normalization, where 1, 4, or 16 shim-safety rods were moved simultaneously. Included are calculated curves for the case of weak absorption (a) and complete depression of the flux between the rods (b). From the stepwise addition of boron and measurement of the critical rod position the upper part of the calibration curve was obtained again. The agreement with the results from the pulse

TABLE II

REACTIVITY EFFECTS OF GROUPS OF SHIM-SAFETY RODS

Rods inserted	Rod number	ρ (total) (mk)	ρ (per rod) (mk)
2 inner ring	2.6	28.5	14.2
4 inner ring	2, 4, 6, 8	65.2	16.3
8 inner ring	from 1 to 8	125.3	15.7
4 outer ring	9, 11, 13, 15	26.8	6.7
8 outer ring	from 9 to 16	51.9	6.5
4 inner ring all	2, 3, 4, 5 from 1 to 16	40.6	10.1

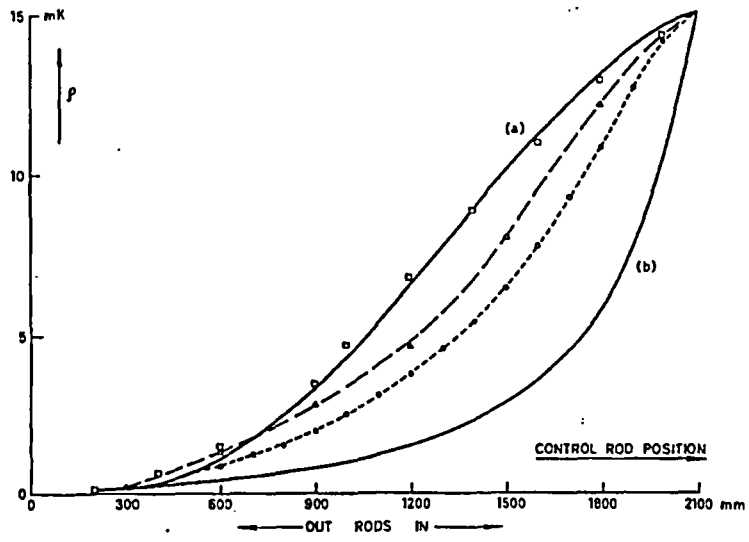

Fig. 5
Control rod calibration curves
——— (a) calculated, weak absorption
——— (b) calculated, complete flux depression between the rods
---O--- 16 rods, —Δ— 4 rods, □ 1 rod

method was very good. The same is true for a comparison between pulse and period measurements.

5. CONCLUSION

The pulsed neutron method has been successfully used for reactivity measurements of a heavy-water reactor at zero energy. With a correction for the build-up of delayed neutrons the reactivity range covered went from $\rho = -0.5\%$ to $\rho = -20\%$. For $|\rho| < 1\%$ period measurements are to be preferred. The optimum region for pulse measurements is around $\rho = -5\%$.

REFERENCES

[1] BECKURTS, K.H., Nucl. Instrum. Meth. 11 (1961) 144.
[2] FRAUDE, A., Nukleonik 4 (1962) 84.
[3] GOZANI, T., Nukleonik 4 (1962) 348.
[4] WIRTZ, K., Proc. 2nd.UN Int. Conf. PUAE 10 (1958) 140.
[5] EYRICH, W., Nukleonik 4 (1962) 167.
[6] WINTZER, D., private communication.
[7] DIEDERICHS, M., GLANNER, H.W., GRÄBNER, H. and WINTZER, D., Die homogene Vergiftung des Reaktors FR2 mit Borsäure während der Nullenergiemessungen, Karlsruhe report KFK 130 (1962).

DISCUSSION

A. WARD: Since you have a reflector, this facility can be described as non-uniform. In view of the difficulties which arise in defining excess reactivity for relatively non-uniform reactors, I am wondering what definition you would use for purposes of calculation or experiment.

M. KÜCHLE: The reflector is very small and so there is no problem from this point of view. The excess reactivity defines the reactivity that would exist if the control rods were withdrawn. Use is made of an extrapolation procedure.

A. WARD: If you were doing a calculation for a reactor which was not critical and you then wanted to adjust some parameter to obtain data for a critical reactor, what parameter would you choose? Would it be the one associated with the multiplication factor in the core only?

M. KÜCHLE: Yes, the multiplication factor in the core only.

A. WARD: Your method is a normal one but use has also been made in the past of adjustments that correspond to adjustments of the multiplication factor or the core constants that go into the multiplication factor in non-multiplying regions.

M. KÜCHLE: Yes, this comes in in the difference between static and dynamic reactivity but the effect is very small. It is even small in the case of a thicker reflector.

C.E. COHN: The problem of defining the reactivity of a multi-region reactor was considered by Avery in his 1958 Geneva Conference paper on the theory of coupled reactors*. If the multiplication factor of each region and the cross-multiplication factors between regions are known, the excess reactivity can be calculated by solving the polynomial equation resulting from the expansion of an n'th-order determinant, where n is the number of regions. My own work, reported in Nuclear Science and Engineering**, and

* AVERY, R., Proc. 2nd UN Int. Conf. PUAE 12 (1958) 182.

** COHN, C.E., "Reflected reactor kinetics", Nucl.Sci.Engng 13 (1962) 12-17.

relating to a simple reflected-reactor model with one multiplying and one non-multiplying region, indicates that if the multiplication factor of the multiplying region, or core, is written as the multiplication factor at critical times a coefficient, which is interpreted as the multiplication factor of the whole reactor, the results obtained are consistent with the predictions of simple one-region kinetics.

F. FEINER: In your paper you mention that you extrapolate the excess reactivity using a two-group model. What extrapolated value for the excess reactivity do you obtain from a one-group treatment of the reactivity versus water-height measurements?

M. KÜCHLE: The one-group approximation would give $\rho = 6.87\%$. With the correction for the two-group theory a value of $\rho = 6.67\%$ is obtained.

A.E. PROFIO: Did you use a tritiated target in your accelerator? If so, did you encounter any difficulties with photoneutrons following the nitrogen-16 activity?

M. KÜCHLE: We did have a tritium target, but we did not make use of the information contained in the delayed neutrons. In any case, the effect of the photoneutrons you mention is probably extremely small.

S.K. WALLACE: I am not clear about the utility of measuring k excess, since the value inferred from experiment is not appropriate to any situation liable to occur during the life of a power reactor. For example, if you want to ensure that there is sufficient reactivity to override poisons and to allow for burn-up, you are in fact envisaging a situation which is quite different from the situation used for the measurement. Another point is that it is not possible to make accurate reactivity tables for different effects and then sum these values.

M. KÜCHLE: We need the value of the excess reactivity to be able to predict critical loadings when different components are inserted into the reactor. These effects do not add up in a linear fashion, but in any case the excess reactivity is the quantity one has to start with.

FLUX-FLATTENING EXPERIMENTS ON A HEAVY-WATER CRITICAL FACILITY

F. ACCINNI AND G. B. ZORZOLI
CISE LABORATORIES, SEGRATE, MILANO, ITALY

Abstract — Résumé — Аннотация — Resumen

FLUX-FLATTENING EXPERIMENTS ON A HEAVY-WATER CRITICAL FACILITY. The work is divided into two parts. The first one deals with thermal flux and cadmium-ratio measurements in a heavy-water critical facility with three different geometries: (a) outer reflected; (b) inner and outer reflected; (c) with a black body inserted into the inner reflector.

The second part makes a comparison between experimental results and theoretical calculations, pointing out the possibility to achieve core thermal flux flattening, without high reactivity losses and changes in core neutron spectrum, by means of a black body inserted into the inner reflector.

EXPÉRIENCES D'APLATISSEMENT DU FLUX DANS LES ASSEMBLAGES CRITIQUES A EAU LOURDE. L'étude est divisée en deux parties. La première concerne les mesures du flux de neutrons thermiques et du rapport cadmique, qui ont été faites dans un assemblage critique à eau lourde pour les trois géométries ci-après: a) réflecteur externe; b) réflecteurs externe et interne; c) corps noir incorporé au réflecteur interne.

Dans la deuxième partie, les auteurs procèdent à une comparaison entre les résultats expérimentaux et les calculs théoriques et montrent qu'il est possible d'aplatir le flux de neutrons thermiques du cœur, sans pertes importantes de réactivité ni variations du spectre neutronique du cœur, en se servant d'un corps noir incorporé au réflecteur interne.

ОПЫТЫ ПО ВЫРАВНИВАНИЮ ПОТОКА НА ТЯЖЕЛОВОДНЫХ КРИТИЧЕСКИХ УСТАНОВКАХ. Работа состоит из двух частей. В первой части рассказывается об измерениях потоков тепловых нейтронов и кадмиевого отношения в тяжеловодной критической установке с тремя различными геометриями: а) с наружным отражателем; б) с внутренним и наружным отражателями; в) с черным телом, вставленным во внутренний отражатель.

Во второй части экспериментальные результаты сравниваются с теоретическими расчетами; при этом отмечается возможность достижения выравнивания потоков тепловых нейтронов в активной зоне без больших потерь реактивности и изменений спектра нейтронов активной зоны с помощью черного тела, помещенного во внутренний рефлектор.

EXPERIMENTOS DE NIVELACIÓN DEL FLUJO EN CONJUNTOS CRÍTICOS DE AGUA PESADA. La memoria se divide en dos partes. La primera trata de mediciones del flujo térmico y de la razón de cadmio en un conjunto crítico de agua pesada con tres geometrías diferentes: a) con reflector exterior, b) con reflectores interior y exterior, c) con un cuerpo negro introducido en el reflector interior.

La segunda parte de la memoria compara los resultados experimentales con los valores calculados, destacando que es posible nivelar el flujo térmico en el cuerpo del reactor por medio de un cuerpo negro insertado en el reflector interior, sin que se produzca una disminución pronunciada de la reactividad ni una alteración del espectro neutrónico.

1. INTRODUCTION

The work is divided into two parts. The first one deals with thermal flux and cadmium ratio measurements in a heavy-water critical facility with three different geometries: (a) outer reflector; (b) inner and outer reflector; and (c) with a black body inserted into the inner reflector. The second part makes a comparison between experimental results and theoretical calculations, pointing out the possibility of achieving core thermal flux

flattening without high reactivity losses and changes in core neutron spectrum, by means of a black body inserted into the inner reflector.

One of the goals in power reactor design is the achievement of a high power shape factor, so as to get fairly balanced fuel utilization.

Instead of following one of the standard solutions for such a problem [1], at CISE it was thought interesting to improve the radial power shape by means of the combined effects of an inner reflector of small dimensions (i. e. by withdrawing a few central elements from a constant lattice pitch core) and of a black body inserted into that reflector.

In fact the former improves the flux shape in the whole core except the zone adjacent to itself, where the well-known flux peaking happens, whereas the latter - when of proper size - can cut such flux peaking.

Preliminary calculations showed that a fairly good improvement in the radial shape factor (from 0.74 to 0.85) could be achieved in the case of a heavy-water-moderated pressure-tube reactor, having a core diameter of about 500 cm and an outer graphite reflector, simply by withdrawing the four central fuel elements and adding a cadmium tube 7 cm in diameter and 1 mm thick, which actually behaves like a nearly perfect black body, because fast neutrons crossing it from outside are mostly slowed down by the inner reflector (Fig. 1), and therefore absorbed by the cadmium while escaping from the inner moderating region.

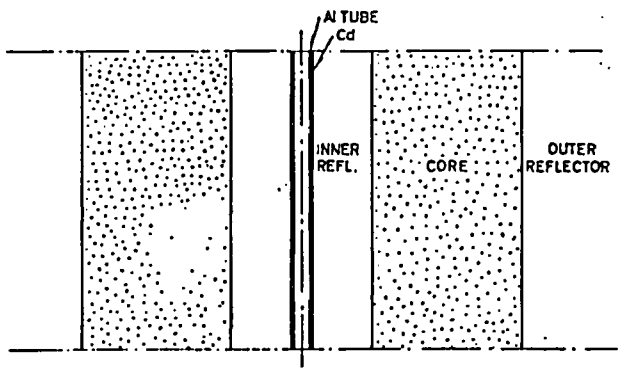

Fig. 1

Reactor section

Moreover, since the number of withdrawn fuel elements is pretty low and the black body acts in a non-multiplying region, the reactivity loss is particularly small (in the above-mentioned case arount 500 pcm).

Such calculations were performed by means of the WANDA code [2] in its version for the ELEA 6001 digital computer (named WANDEL). It is a one-dimensional code, here used in its two-group version, accounting for the transverse (axial) leakage by adding in both groups to the absorption cross-section term the quantity DB_z^2, where D is the proper diffusion coefficient and B_z^2 is the transverse buckling.

The inner reflector is square, as is the lattice geometry, and therefore, because of the one-dimensional feature of WANDA, it is replaced by a circular one having the same cross-section area; in addition, one is also forced to apply diffusion theory inside the cadmium tube. The latter problem was solved by attributing cadmium with a fictitious thermal diffusion coefficient and absorption cross-section, evaluated after WACHSPRESS' theory [3] for a strongly absorbing slab, modified to account for the cylindrical geometry involved here.

Thus it looked worthwhile to check the accuracy of the above-mentioned procedure and chiefly:

(a) How accurate was the code evaluation of the reactivity changes due to the withdrawal of fuel elements and to the insertion of the cadmium tube; and

(b) How accurately the code predicted the neutron flux spatial behaviour and the radial shape factor.

The measurements described below were aimed solely at obtaining the information needed to answer items (a) and (b).

2. DESCRIPTION OF THE EXPERIMENTAL ARRANGEMENT

The RB zero-power critical assembly, installed at the Institute of Nuclear Sciences Boris Kidrič, was used for the experiments. The RB assembly, described in more detail in [4], essentially consists of an aluminium tank, 199.86 cm inner diameter by 1 cm thick by 210 cm high, placed upon a metal frame so that the closest scattering surface (floor and walls) is 4 m away from the tank.

An upper and lower grid plate hold the fuel elements and criticality is achieved by varying the heavy-water level inside the tank. No outer reflector is available, so that the assembly is actually axially unreflected and the side reflection varies according to the extent of the fuel charge.

The fuel elements used during the experiment were of the type shown in Fig. 2: the fuel is made up of 2% enriched, Al clad, uranium metal, and all the other structural components are made of aluminium.

Preliminary calculation, by means of COCCO BILL, a criticality calculation code [5], showed that suitable configurations to be investigated ought to have moderator-to-fuel ratios corresponding to square lattice pitches around 11 cm. Therefore, since grid plates pierced for a 8-cm square lattice pitch were available, fuel elements were placed diagonally, as shown in Fig. 3, so as to have a 11.31-cm lattice pitch.

The consequent disposition of fuel elements did not allow much degree of freedom in selecting the configurations to be investigated. Therefore, in addition to the reference configuration made up of 56 elements, the following configurations were also studied:

(a) The two elements closest to the reactor centre withdrawn, i.e. with an inner reflector of equivalent radius R = 9.06 cm;

(b) The six central elements withdrawn (but four elements added at the core outer boundary, so as to get 54 elements as in case (a), i.e. with an inner reflector of equivalent radius R = 15.6 cm.

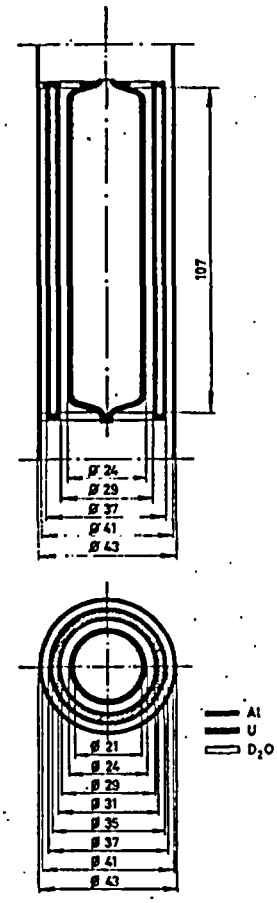

Fig. 2

Fuel element cross-section

Cases (a) and (b) were studied also with a central absorber made up of an aluminium tube, 1 mm thick, having 0.7 mm outer Cd cladding.

Two different aluminium tubes were used, 3 cm and 4 cm outer diam. In case (a) only the 4-cm tube was used, mainly because of lack of time.

Some preliminary considerations derive immediately from the very qualitative survey of the configurations shown in Fig. 3. First of all, the circularization of the inner reflector is rough indeed. Secondly, the total number of fuel elements is in any case very little; therefore also the assumption of a core equivalent radius is doubtful and even the core homogenization cannot hold very well. Last but not least, the dimensions involved are rather limited and diffusion approximation is somewhat questionable.

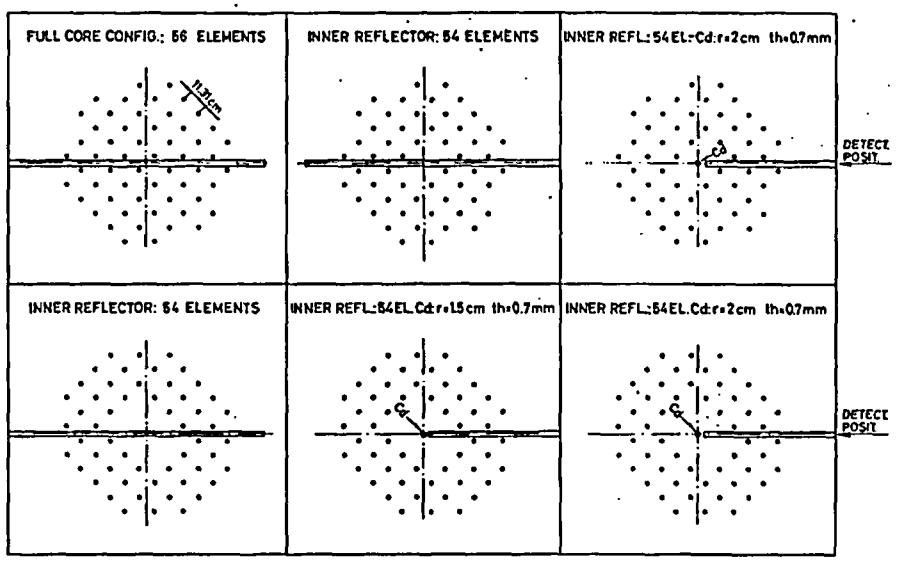

Fig. 3

Experimental configurations

In conclusion, such experimental conditions are to be considered as a limiting case; any discrepancy between calculated data and experimental results should consequently be taken as a maximum, which substantially overestimates the corresponding case for a large power reactor.

3. EXPERIMENTAL PROCEDURE AND RESULTS

Flux measurements were performed by means of gold detectors 1 cm in diameter and 0.002 mm thick, equivalent to a surface density of 3.776 mg/cm^2.

Gold detectors were placed upon a thin Al plate, at a relative distance of 16 cm. The plate was inserted into the reactor along a diameter for radial measurements, as shown in Fig. 3, covering the fuel diameter when the Cd tube was not present and half a diameter approximately with Cd tube. Axial distribution measurements were performed by inserting the Al plate along the central reactor axis.

Two sets of measurements were performed with bare and Cd-covered detectors. Each irradiation was about 20 minutes long, with neutron fluxes around 10^8 n cm^{-2} s^{-1}. Each detector was counted under two different G-M beta counters. The final result, corrected for detector efficiency, background and dead time losses, is the average value of the two results collected by the two counters, for the plate inserted along half a diameter only; when the measurement covered the full diameter, since detectors were positioned two by two at centre-symmetrical points, the results represent average values of the four results corresponding to the two symmetrical detectors under the two different G-M counters.

As far as axial measurements are concerned, the average of the two G-M counts was taken.

The cadmium ratio R_{Cd} between bare and Cd covered detectors is related to Westcott's epithermal index "r" through the following expression

$$R_{Cd} = \frac{gG_{th} + rsG_r}{rsG_rF + \frac{r}{K}\sqrt{\frac{T}{T_0}}G_r}, \tag{1}$$

where g, r, s are defined according to WESTCOTT's notation [6], 1/K is a coefficient, also defined by WESTCOTT [6], to account for 1/v epicadmium activation, G_{th} and G_r are the thermal and epithermal self-shielding factors respectively, F is the cadmium transparence for resonance neutrons, T is the neutron temperature and $T_0 = 293.58°K$.

From Eq. (1) the following expression for r is derived:

$$r = \frac{gG_{th}}{R_{Cd}\left[sG_r\left(F - \frac{1}{R_{Cd}}\right) + \frac{G_r}{K}\sqrt{\frac{T}{T_0}}\right]} \tag{2}$$

In the actual experimental arrangement it was

$1/K = 0.467$ (derived from [6])
$F = 0.967$ (derived from [7])
$G_{th} = 0.97$ (derived from [7])
$G_r = 1$ (derived from [8])
$T \approx T_0$.

Therefore,

$$r = \frac{0.05671}{R_{Cd} - 1.006}. \tag{3}$$

Since, moreover [6],

$$r = f\frac{\sqrt{\pi\mu}}{4}, \tag{4}$$

where f is the epithermal fraction of the total neutron density and $\mu = 3.681$ is the cut-off energy of the 1/E neutron spectrum in KT units [9], combining Eqs. (3) and (4) gives

$$f = \frac{0.0667}{R_{Cd} - 1.006} \tag{5}$$

and therefore, since

$$\frac{\phi_e}{\phi_M} = \frac{f}{1-f}\frac{\bar{v}_e}{\bar{v}_M} \tag{6}$$

(where ϕ_M and ϕ_e are the thermal and epithermal neutron flux, $\bar{v}_M$ and $\bar{v}_e$ the mean thermal and epithermal neutron velocity respectively), combining

Eqs. (5) and (6) gives in each point the ratio of epithermal to thermal flux as a function of R_{Cd}.

Then, if n is the total neutron density, as the bare activation is proportional to

$$[n(1-f)+nf](gG_{th}+rsG_r) = \left[\frac{\phi_M}{\vartheta_M}+\frac{\phi_e}{\vartheta_e}\right](gG_{th}+rsG_r), \qquad (7)$$

the system of (6) and (7) allows the evaluation of both ϕ_M and ϕ_e.

Figs. 4 through 9 show the derived thermal and epithermal radial flux distributions in the six configurations tested.

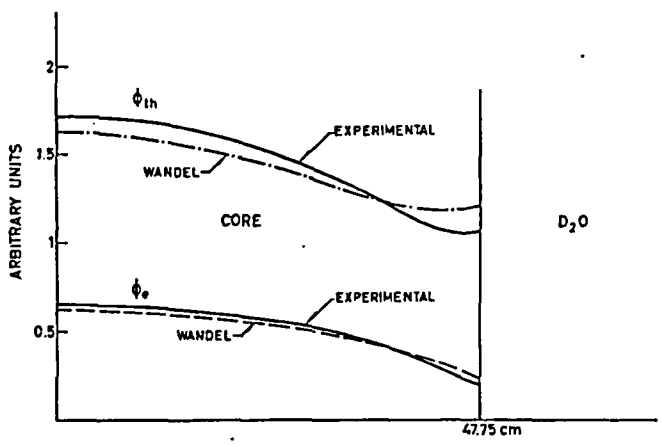

Fig. 4

Full configuration
56 elements
Critical level D_2O: 111.59 cm
Temperature: 20°C

Fig. 10 shows the axial flux distribution measured in the full configuration and that with an inner reflector corresponding to six withdrawn elements only.

Since in both cases, i.e. with a measurement performed in the core lattice and in the heavy water, the extrapolated length is 1.76 cm, this value was assumed in all the numerical calculations (see section 5).

Figs. 11 and 12 show the behaviour of R_{Cd} as a function of the reactor radius; it is worth pointing out how a careful choice of the inner reflector and of the inner Cd tube can leave the neutron spectrum unchanged, with respect to the full core configuration; this is of some importance for the long-term fuel isotope evolution in a power reactor.

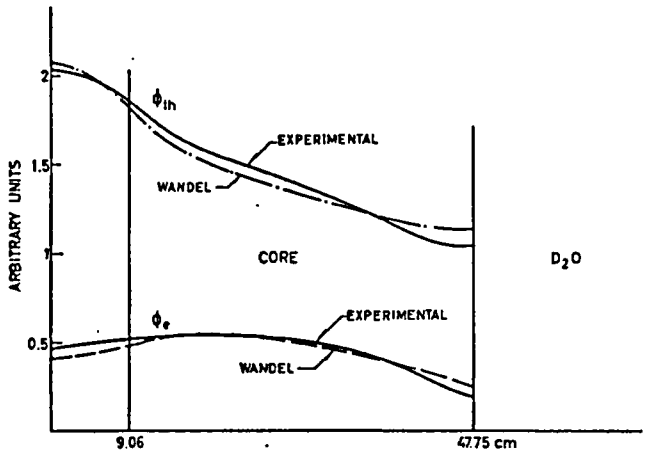

Fig. 5

Configuration without two central elements
54 elements
Critical level D_2O: 114.95 cm
Temperature: 22.33°C

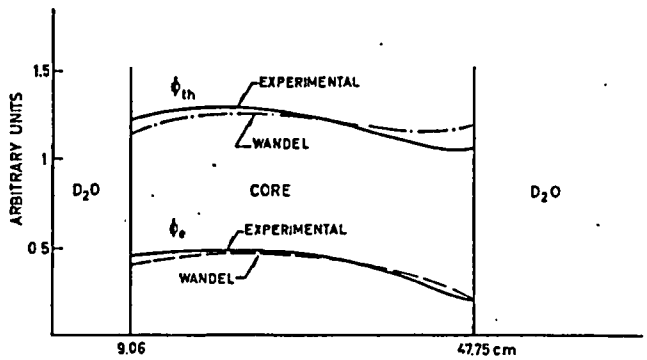

Fig. 6

Configuration without two central elements

Central absorber diameter: 41 mm
54 elements
Critical level D_2O: 137.5 cm
Temperature: 20°C

4. FINE FLUX MEASUREMENTS

As well as macroscopic flux distribution, fine flux measurements for each configuration were performed across the reactor cell closest to the

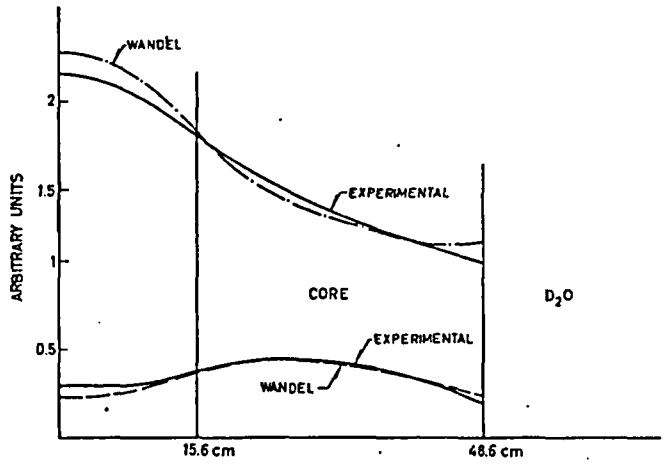

Fig. 7

Configuration without six central elements
54 elements
Critical D_2O: 119.77 cm
Temperature: 20.78°C

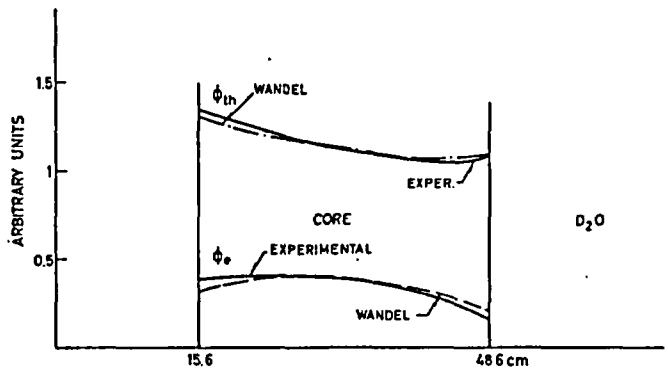

Fig. 8

Configuration without six central elements
Central absorber diameter: 31 mm
54 elements
Critical level D_2O: 139.3 cm
Temperature: 20.65°C

centre, as shown in Figs. 14 to 19, along the direction connecting the centre of the element to the reactor centre.

Dysprosium metal discs, 0.2 mm thick and 2 mm in diameter, were used as detectors. Detectors were separated by means of small Perspex

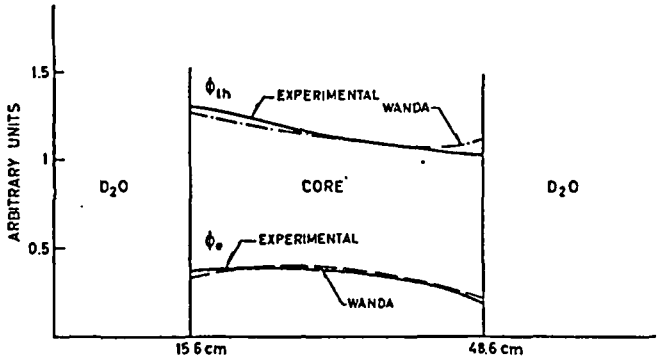

Fig. 9

Configuration without six central elements
Central absorber diameter: 41 mm
54 elements
Critical level D_2O: 144.63 cm
Temperature: 20.8°C

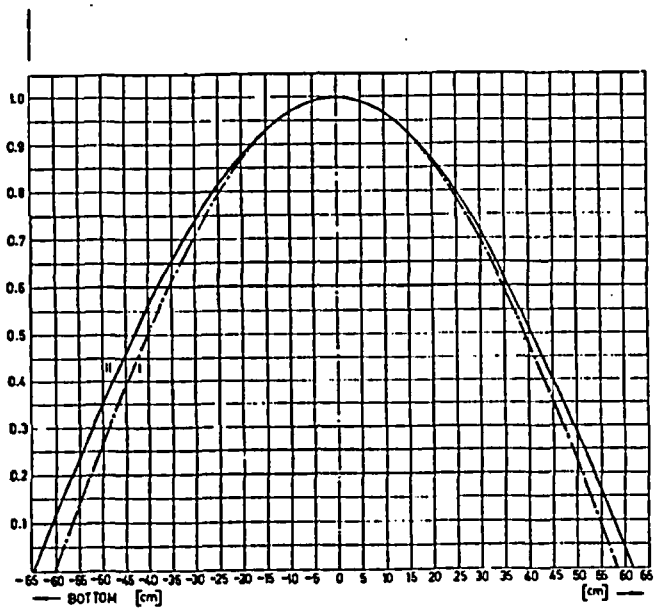

Fig. 10

Radial flux distribution

Curve I
Full configuration; 56 elements
Critical level: 111.75 cm; temperature: 20.6°C

Curve II
Configuration without six central elements; 54 elements
Critical level: 119.99 cm; temperature: 20.6°C

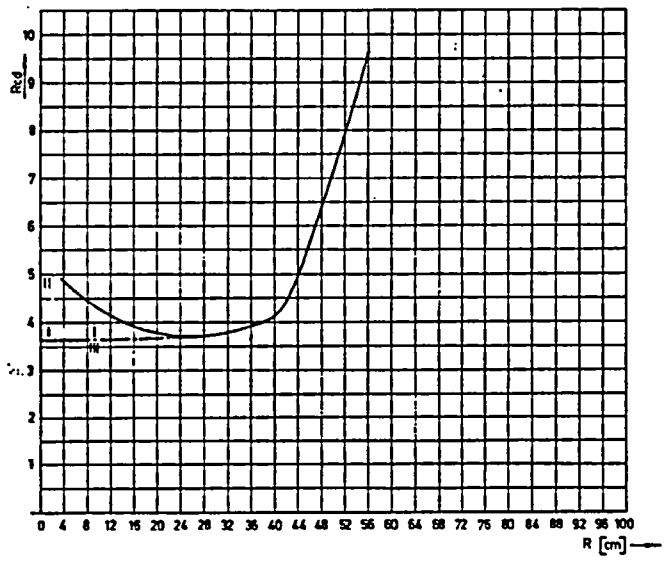

Fig. 11

Cadmium ratio - radial distribution

Curve I
Full configuration; 56 elements

Curve II
Configuration without two central elements; 54 elements

Curve III
Configuration without two central elements
Absorber diameter: 40 mm; 54 elements

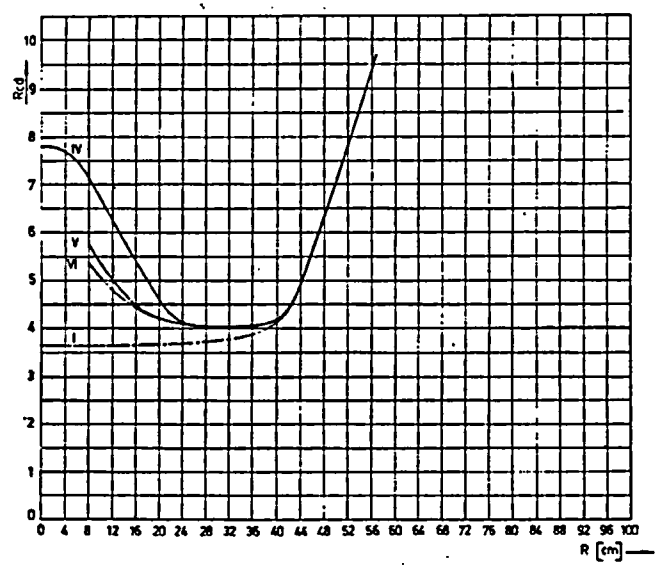

Fig. 12

Cadmium ratio - radial distribution

Curve I
Full configuration; 56 elements

Curve IV
Configuration without six central elements; 54 elements

Curve V
Configuration without six central elements
Absorber diameter: 30 mm

Curve VI
Configuration without six central elements
Absorber diameter: 40 mm

cylinders having the same diameter; the whole arrangement was inserted into an Al tube, 0.2 mm thick, which was placed into the fuel element, as shown in Fig. 13. The length of the Al tube was such that the detectors covered the full cell length.

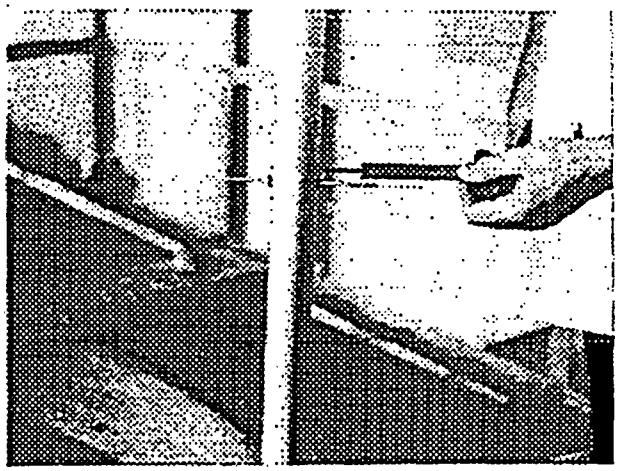

Fig. 13
Arrangement of detectors for fine flux measurements

Each irradiation took about five minutes with a flux of $\sim 10^8$ n cm^{-2} s^{-1}. The beta activity of the detectors was counted for about two minutes under four G-M counters, rotating each detector under all the counting chains.

For the full core configuration the thermal neutron distribution, corresponding to the total measured neutron density, was deduced as follows: one has

$$\frac{R}{v_0 \sigma_0} = (n_e + n_M)\left\{ gG_{th} + \frac{\sqrt{\pi\mu}}{4} sf \right\}$$

$$= n_e \left(gG_{th} + \frac{\sqrt{\pi\mu}}{4} s \right) + n_M g G_{th}$$

$$= n_e \left\{ gG_{th} \left(1 + \frac{1-f}{f} \right) + \frac{\sqrt{\pi\mu}}{4} s \right\}$$

$$= n_e \frac{\sqrt{\pi\mu}}{4} \left\{ \frac{gG_{th}}{r} + s \right\}.$$

Since n_e can be taken as constant throughout the cell, one can obtain n_e by measuring the value of the epithermal index r.

The upper curve of Fig. 14 shows the fine flux distribution once the epithermal contribution has been subtracted and a correction has been made to account for the macroscopic flux gradient. As one can see, such a distribution actually exhibits the same behaviour as the one deduced from the

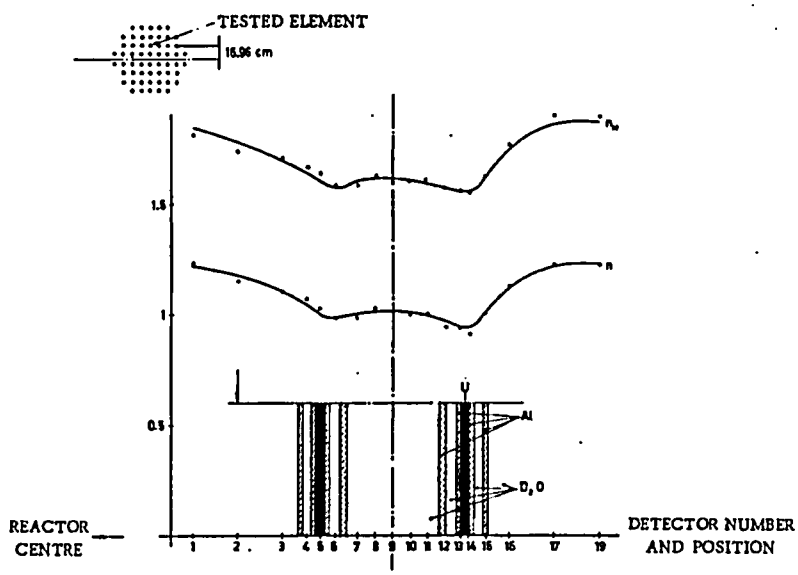

Fig. 14

Full configuration

total collected counts, and therefore the above-mentioned correction was not performed in all the other cases, whose distributions are shown in Figs. 15 to 19.

An interesting result is derived from a qualitative comparison among the different flux distributions. The use of an inner reflector substantially increases the macroscopic flux gradient, wheras the additional insertion of a proper Cd tube leads to a gradient approximately equal to the one present for the full core configuration. Of course, since the uranium thickness is here rather limited, the effect of the change in flux gradient is not very high in the fuel itself, but if one considers that in a power reactor the cell region occupied by the fuel is much larger, one can conclude that, as for the case of the neutron spectrum, it is possible to design a combination of inner reflector and black absorber which would not affect the neutron behaviour inside the reactor cells.

5. COMPARISON OF NUMERICAL DATA AND EXPERIMENTAL RESULTS

As mentioned in section 1 theoretical calculations were performed by means of two computer codes named COCCO BILL and WANDEL.

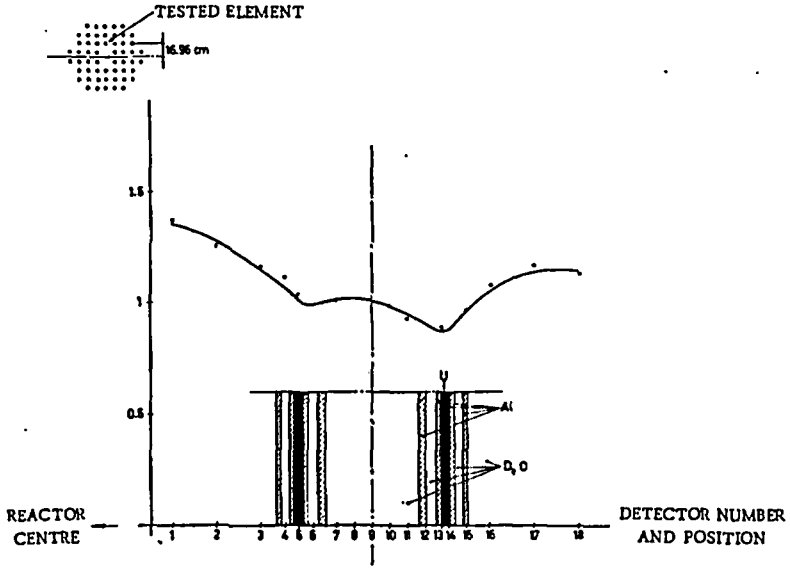

Fig. 15

Inner reflector
(Two elements withdrawn)

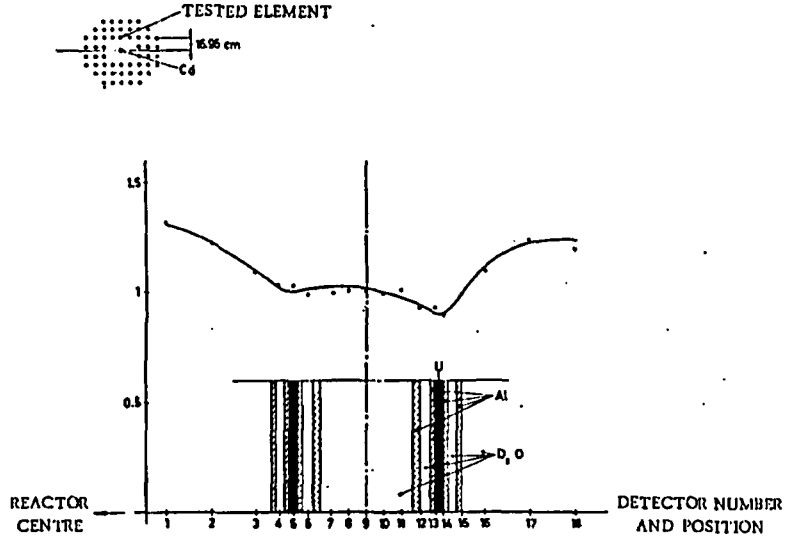

Fig. 16

Inner reflector
(Two elements withdrawn)
Cd; R = 2 cm th = 0.7 mm

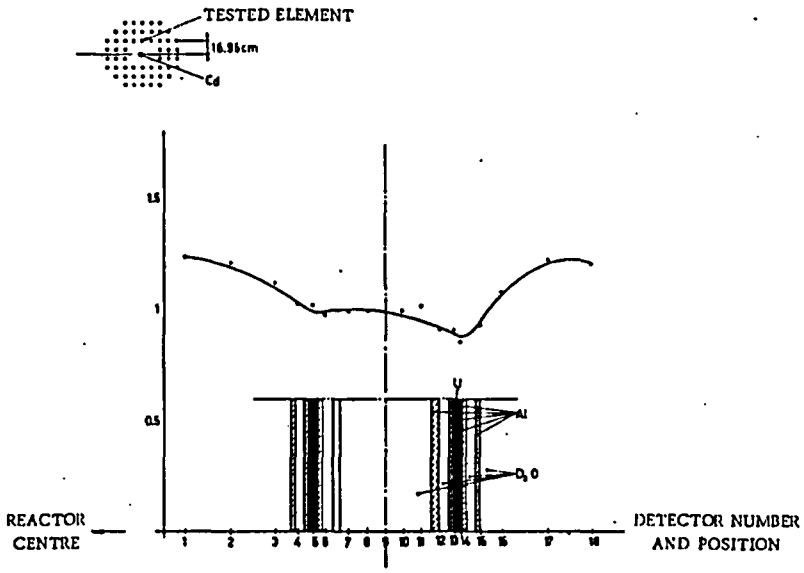

Fig. 17

Inner reflector
(Six elements withdrawn)

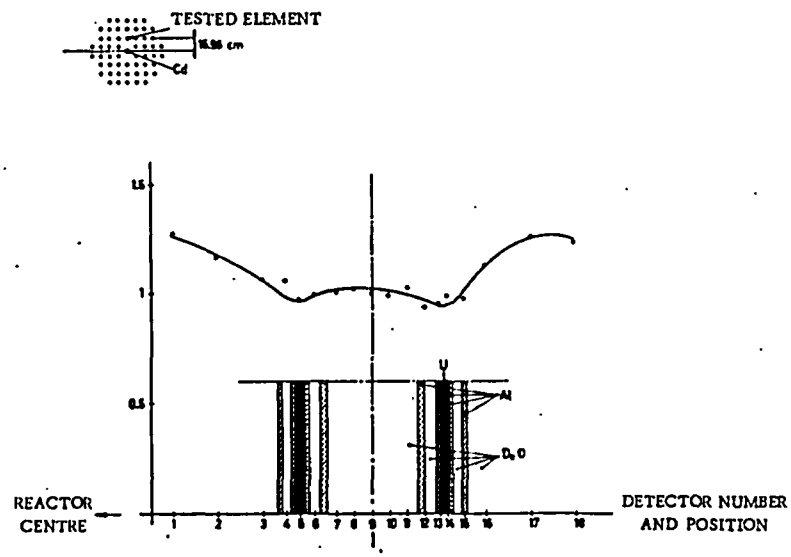

Fig. 18

Inner reflector
(Six elements withdrawn)
Cd ; R = 1.5 cm th = 0.7 mm

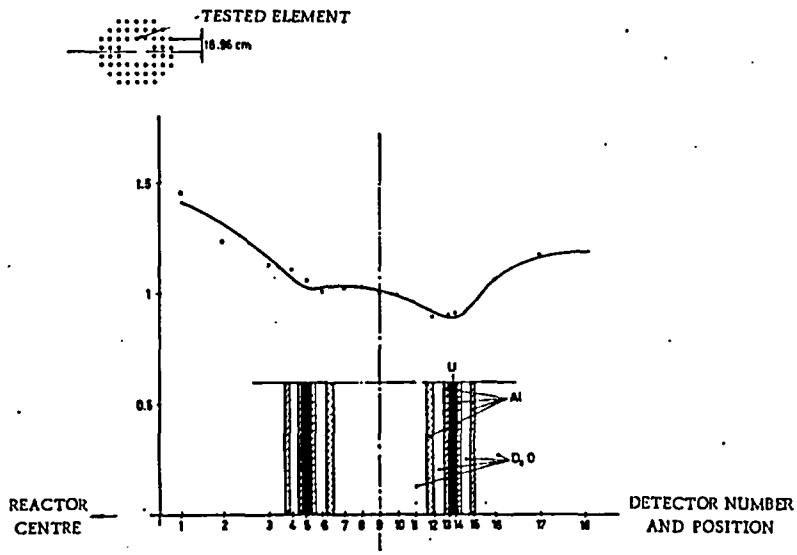

Fig. 19

Inner reflector
(Six elements withdrawn)
Cd; R = 2 cm th = 0.7 mm

For a given cell configuration COCCO BILL evaluates the corresponding parameters according to a three-group model. The three groups are so divided:

(a) Group 1 goes from 0.1 MeV to 2 MeV, i.e. covering the fission energy range;
(b) Group 2 goes from the epithermal cut-off energy to 0.1 MeV; and
(c) Group 3 covers the thermal energy range.

The parameters that COCCO BILL calculates are the following:

D_i : diffusion coefficient ($i = 1, 2, 3$)
Σ_{ri} : cell removal cross-section ($i = 1, 2$)
Σ_i : cell absorption cross-section ($i = 2, 3$)
$\nu\Sigma_{fi}$: average cell fission neutron source per unit flux ($i = 2$)
f : thermal utilization factor
p : resonance escape probability
ϵ : fast fission factor, as defined by CARLVIK and PERSHAGEN [10] i.e. accounting for all fission and capture events above 0.1 MeV
η : thermal fission factor

Such data for the same configuration used during the experiment are listed in Table I.

WANDEL, however, is used in its two-group form:

$$D_1\nabla^2\phi_1 - (\Sigma_{r1} + \Sigma_1 + D_1B_z^2)\phi_1 + \epsilon\eta f\Sigma_2\phi_2 = 0$$

$$D_2\nabla^2\phi_2 - (\Sigma_2 + D_2B_z^2)\phi_2 + \Sigma_{r1}\phi_1 = 0$$

TABLE I

CALCULATED CELL PARAMETERS

Energy group	D (cm)	Σ_r (cm^{-1})	Σ (cm^{-1})	$\nu\Sigma_f$ (cm^{-1})	f	ϵ	η	p
1	1.5548	0.04446	-	-	-	1.0078	-	-
2	1.1240	0.01227	0.0009236	0.001390	-	-	-	0.9257
3	0.8362	-	0.007759	-	0.9473	-	1.7243	-

where group 1 goes from the epithermal cut-off energy up to 2 MeV and group 2 covers the thermal energy range. All the symbols have the same meaning as those listed as COCCO BILL outputs; in addition λ is the eigenvalue to which the code converges when the system is critical, and B_z^2 is the axial buckling which, multiplied by the proper diffusion coefficient, gives an integral value of the axial leakage effect to be introduced into the radial flux calculation.

In order to fit COCCO BILL outputs to WANDEL inputs, the following relationships were used (simple asterisk refers to WANDEL inputs):

$$\frac{1}{\Sigma_{r1}^{**}} = \frac{1}{\Sigma_{r1}} + \frac{1}{\Sigma_{r2}}$$

$$D_1^* = (L_1^2 + L_2^2)\Sigma_{r1}^{**}$$

$$\Sigma_1^* = \Sigma_2 \frac{\Delta u_2}{\Delta u_2 + \Delta u_3} + (1 - p)\Sigma_{r1}^{**}$$

$$\Sigma_{r1}^* = p\Sigma_{r1}^{**}$$

The axial buckling for each configuration to be investigated was chosen as equal to the actual experimental critical height plus twice the extrapolation length, as deduced from the measured axial distributions (see section 3).

Radial dimensions were derived from the actual ones by reducing them to the equivalent cylindrical ones. Of course the external reactor radius was taken equal to the geometrical radius plus the extrapolation length, as experimentally derived.

Therefore if the theoretical approximations represent the physical phenomena correctly, the eigenvalue λ should come out equal to unity. Table II lists the calculated eigenvalues, each referred to the proper moderator temperature. As one can see, they are all substantially different from unity clustering around 1.04. Since the cell parameters derived from COCCO BILL were in a very good agreement with Russian data for the given fuel element, and for large reactors WANDEL gives a much better approximation,

TABLE II

THEORETICAL AND EXPERIMENTAL RESULTS

Configuration of	λ_{calc}	$\delta\lambda$	$\Delta\lambda$	Error (%)	F_{exp}	F_{th}
Fig. 4	1.0493				0.774 ±0.012	0.810
Fig. 5	1.0503	+0.0010	0.0079	+13.2	0.715 ±0.011	0.716
Fig. 6	1.0430	-0.0063	0.0652	-9.7	0.916 ±0.014	0.957
Fig. 7	1.0496	+0.0003	0.0237	+1.3	0.752 ±0.010	0.711
Fig. 8	1.0399	-0.0094	0.0729	-11.9	0.831 ±0.012	0.856
Fig. 9	1.0414	-0.0079	0.0799	-9.9	0.859 ±0.013	0.884

as pointed out in section 2 the discrepancy is that expected because of the peculiar geometry of the experimental facility. What is important is the fact that all the eigenvalues are rather close to each other, therefore ensuring that differential effects in reactivity due to inner reflector and black body insertion are pretty well accounted for by the criteria used to get WANDEL inputs. The maximum variation $\delta\lambda$ in the eigenvalues with respect to the full core case corresponds in fact to 940 pcm.

Moreover, if the same calculations are performed for all the configurations having the same height of the full core configuration, it is possible to know the changes in λ (named $\Delta\lambda$ in Table II) and to evaluate percentage errors all but one clustering around 10%. This error is not uncommon, since it is related to calculations of a black body worth, and, in the case of Fig. 5, to an inner reflector highly non-symmetrical; in fact, when six elements are withdrawn (Fig. 7), the better symmetry leads to a very low error.

As far as radial flux distributions, and particularly thermal flux behaviours, are concerned, the calculated flux shape factors F_{th} exhibit a deviation from the experimental ones F_{exp} never higher than 0.041.

That is mostly due to the inaccuracy by which WANDEL accounts for the peak effect at the boundary between core and outer reflector, which, in a small configuration, affects the thermal flux shape over the whole core; on the contrary such an effect is less important in a large power reactor. Moreover, the statistical uncertainty in the measured detector activities leads to an uncertainty in the experimental shape factors of about 1%, whereas the accuracy by which WANDEL evaluates the single mesh points in the flux distribution is believed to be (with the chosen convergence limit of 1×10^{-4} assumed here) of the order of 1%.

Consequently the discrepancy between measured and calculated shape factors is to be considered rather satisfactory and anyway well inside the hot-spot factors generally used in designing large power reactors.

6. CONCLUSIONS

The experiments here described can give enough confidence in the use of an inner reflector coupled with a cadmium tube to flatten the thermal flux inside the power reactor. In fact a proper choice of either can keep in the core the same neutron energy distribution without modifying the fine flux distribution in the fuel elements closest to the inner reflector.

With a shape factor of 0.85, which is easily achievable in a power reactor, without a substantial loss in reactivity, one is granted that the long-term fuel isotope evolution is nearly the same in all the fuel element, and, when different, exhibits a trend towards an additional flux flattening, whereas in the case of variable lattice pitch the trend is the opposite one, and in the case of different enrichment fuel regions one is compelled to a more complex fuel cycle (with the solution here proposed it may be very convenient, for reasons of economy, to choose a batch cycle solution).

ACKNOWLEDGEMENTS

The authors wish to thank Prof. M. Silvestri for his kind suggestions and helpful criticisms; they are also deeply grateful to Nenad Raisič and Hranislav Markovič of the Institute of Nuclear Sciences, Boris Kidrič, Vinča, Belgrade, for their continuous co-operation and assistance during the performing of the experiments, along with the operating crew of the RB Reactor.

Thanks are also due to the management of the Institute of Nuclear Sciences Boris Kidrič for making its facilities available free of any charge.

REFERENCES

[1] JANKOWSKI, F.J., Power flattening in sodium graphite reactor cores, USAEC RPT. NAA/SR 6403 (1961).

[2] MARLOWE, O.J. et al., WANDA, a one dimensional few group diffusion equation code for the IBM 704, USAEC Rpt. WAPD/TM 28 (1956).

[3] WACHSPRESS, E.L., Thin regions in diffusion theory calculations, Nucl. Sci. Engng 3 (1958) 186.

[4] POPOVIČ, D., A bare critical assembly of natural uranium and heavy water, Proc. 2nd.UN Int. Conf. PUAE 12 (1958) 392.

[5] BONALUMI, R. and ZORZOLI, G.B., COCCO BILL, a criticality calculation code (revised edition) CISE Rpt. 94 (1963).

[6] WESTCOTT, C.H. et al., Effective cross sections and cadmium ratios for the neutron spectra of thermal reactors, Proc. 2nd.UN Int. Conf. PUAE 16 (1958) 70.

[7] WESTCOTT, C.H. et al., Reactor Physics Constants, USAEC Rpt. ANL 5800 (1958) 487.

[8] BIGHAM, C.B., CHIDLEY, B.G. and TURNER, R.B., Experimental effective fission cross sections and neutron spectra in a uranium fuel rod, Part II, AEC Rpt. AECL 1350 (1961).

[9] WESTCOTT, C.H., Effective cross section values for well-moderated thermal reactor spectra, AEC Rpt. AECL 1101 (1960).

[10] CARLVIK, I. and PERSHAGEN, B., The fast fission effect in a cylindrical fuel element, A.B. Atomenergi Rpt. AE 21 (1959).

DISCUSSION

F. FEINER: How do you compare flux shape calculations with measured activations?

G.B. ZORZOLI: The procedure was as follows. Experimental determinations were made of activation with bare and Cd-covered gold. From these two values we derived what we called the experimental epithermal or fast flux and the thermal flux. By means of the two-group version of WANDA we then derived theoretical values for the fast and thermal flux and made a comparison. This is explained in the paper.

F. FEINER: What was the thickness of the gold?

G.B. ZORZOLI: The surface density was 3.776 mg/cm^2 and the thickness 0.002 mm. Moreover, in the calculation we evaluated both the thermal and the epithermal self-shielding effect of the detectors. The values were 0.97 and 1 respectively.

F. FEINER: Experimentally then, you were really determining the thermal flux?

G.B. ZORZOLI: Yes, I was referring to the thermal flux. The epithermal flux was used for the sake of comparison because we were interested in evaluating the possibility of a high power shape factor. In this kind of reactor the thermal flux is the most important one.

C.F. HØJERUP: You quoted a value of 0.85 for the shape factor of this reactor. Was that the total or only the radial shape factor?

G.B. ZORZOLI: The radial shape factor.

C.F. HØJERUP: I take it that this high value resulted not only from the central reflector and black body but also from the presence of a thick outer reflector.

G.B. ZORZOLI: Yes.

C.F. HØJERUP: What was the radial shape factor before the introduction of the central reflector and absorber?

G.B. ZORZOLI: The previous radial shape factor was 0.74.

SYMPOSIUM ON
EXPONENTIAL AND CRITICAL EXPERIMENTS

HELD AT AMSTERDAM, 2-6 SEPTEMBER 1963

CHAIRMEN OF SESSIONS

Session 1	A. WARD	Atomic Energy of Canada Ltd., Chalk River, Ontario
Session 2	D. BRETON	Centre d'études nucléaires de Saclay
Session 3	C.G. CAMPBELL	Atomic Energy Establishment, Winfrith, Dorchester, Dorset
Session 4	J. PELSER	Reactor Centrum Nederland, Petten
Session 5	W.C. REDMAN	Argonne National Laboratory, Argonne, Illinois
Session 6	R. PERSSON	AB Atomenergi, Studsvik, Nyköping
Session 7	V.A. KUZNETSOV	Physical Institute of Obninsk
Session 8	N. RAIŠIĆ	Boris Kidrič Institute for Nuclear Sciences, Belgrade
Session 9	U. FARINELLI	Centro di Studi Nucleari della Casaccia, Rome

SECRETARIAT OF THE SYMPOSIUM

Scientific Secretaries:	J.W. WEBSTER	Division of Reactors, IAEA
	A. MERTON	Division of Reactors, IAEA
Editor:	A. HAMENDE	Division of Scientific and Technical Information, IAEA
Records Officer:	L. LIEBERMAN	Division of Languages, IAEA
Administrative Secretary:	P. GHELARDONI	Division of Scientific and Technical Information, IAEA